Addis Ababa University
(Since 1950)

HYDROGEOLOGICAL SYSTEM ANALYSIS OF ALLYDEGI PLAIN AND ITS SURROUNDINGS USING GEOCHEMICAL MODELING AND ISOTOPE TECHNIQUES

A THESIS SUBMITTED TO THE SCHOOL OF PLANETARY AND EARTH SCIENCES IN PARTIAL FULFILLMENTS OF THE REQUIREMENTS FOR THE DEGREE OF MASTER OF SCIENCE IN HYDROGEOLOGY

BY

EPHREM TADESSE

June, 2013
Addis Ababa

HYDROGEOLOGICAL SYSTEM ANALYSIS OF ALLYDEGI PLAIN AND ITS SURROUNDINGS USING GEOCHEMICAL MODELING AND ISOTOPE TECHNIQUES

By

Ephrem Tadesse Tagegne

A THESIS SUBMITTED TO THE SCHOOL OF PLANETARY AND EARTH SCIENCES IN PARTIAL FULFILLMENTS OF THE REQUIREMENTS FOR THE DEGREE OF MASTER OF SCIENCE IN HYDROGEOLOGY

SCHOOL OF EARTH SICENCES
COLLEGE OF NATURAL SCIENCE
ADDIS ABABA UNIVERSITY

June, 2013
Addis Ababa

Addis Ababa University

College of Natural science

School of Planetary and Earth Sciences

Hydrogeological System Analysis of Allydegi Plain and its Surroundings Using Geochemical Modeling and Isotope Techniques

By
Ephrem Tadesse Tagegne

Approved by Board of Examiners:

Suryabhagavan K.V.(Ph.D) ______________________

(Chairman)

Seifu Kebede (Ph.D) _______________________

(Advisor)

Engida Zemedagegnehu (Ms.C) _______________________

(Co-Advisor)

Tenalem Ayenew (Prof.) ______________________

(Examiner)

Asfawossen Asrat (Ph.D) ______________________

(Examiner)

Acknowledgement

Before all, I would like to praise God, for being with me from the very beginning of my carrier up to the end of the thesis work.

I would like to thank Dr. Seifu Kebede, my advisor and instructor, for his unreserved advice, and kind provision of all required materials. I would like to thank Mr. Engida Z/Agegnehu, my co-advisor, for his advice, follow up, facilitation of the post-gradute study and for everything.

I am also grateful to Water Works Design and Supervision Enterprise (WWDSE) giving me a financial support to successfully accomplish my research work and education, Ministry of Water and Energy, Geological Survey of Ethiopia (GSOE) and National Meteorological Services Agency for providing me the necessary data.

My appreciation and thanks is also to my office collogues: Tilahun Azagege, Muauz Amare, Yoseph Tamirat, Seife Negash, Bizuneh Bekele, Asfaw Aymeku, Ewnetu Bedane for their brotherly support and W/t Tsega for her sisterly support to safely accomplish my work.

I am indebted to the contribution of my wife Sosina G/micheal for her support and editing my thesis and finally, I would like to express my grateful thanks and appreciation to all my families and relatives for their heartfelt encouragement, best wishes and support.

Abstract

Allydegi plain and its surrounding, which is located in the middle Awash river basin of the Main Ethiopian Rift has lack of water supply problems. Hydrogeochemistry and isotope techniques were used to study the groundwater system of the area. Tertiary and Quaternary volcanic rocks with recent alluvial and elluvial sediments are major geologic units. Fractured and weathered volcanic rocks and unconsolidated sediment aquifers are the key aquifers.

Hydrochemical study result reveals that the area is characterized by four major water types. Water group of Ca-Mg-HCO_3 and Na-Ca-HCO_3 types are characterized by recharge area waters. Na-HCO_3 type waters are an evolved water types from highland and escarpments of Ca-Mg-HCO_3 and Na-Ca-HCO_3 water types located in the center of the study area whereas highly concentrated Na-HCO_3-Cl and/or Na-HCO3-SO_4 type waters are characteristics of discharge area water types. The result of inverse geochemical modeling depicts that dissolution of silicate minerals, calcite, anhydrite and halite minerals, cation exchange, precipitation and/or weathering of clay minerals with a consumption of CO_2(g) as a heat from deeper source through fractures control the groundwater chemistry of the area. Beside these, from the correlation of $\delta^{18}O$ as a function of chloride content of the groundwater implies that rigorous evaporation and dissolution can be discriminated as salinity sources without ignoring the impact of Beseka Lake after draining in to Awash river. The estimated groundwater recharge of the area using CMB method is 98.11mm/yr and the roughly estimated ground water flow velocity using stable isotope monitoring results is about $5.6x10^{-3}$ m/sec.

Stable isotopes study result illustrates that the ground water system is recharged from the combination of direct recharge from precipitation, from highlands that bounds the study area through fractures and from Awash river. Isotope monitoring result of Boreholes in Allydegi plain and Awash river also testifies that Awash river recharges the Allydegi plain. The hydrochemical and water level monitoring of reservoir and borehole at dam axis shows that the source of leakage at the left abutment is from reservoir rather than the groundwater system.

Acronyms

AAU	Addis Ababa University
AHC	Agglomerative Hierarchical Clustering
APGWRAP	Allydegi Plain Groundwater Resource Assessment Project
@	At
CMB	Chloride Mass Balance
DEM	Digital Elevation Model
EC	Electrical Conductivity
FAO	Food and Agricultural Organization
GMWL	Global Meteoric Water Line
GNIP	Global Networking of Isotopes in Precipitation
GSOE	Geological Survey of Ethiopian
HDW:	Hand Dug Well
HCA:	Hierarchical Cluster Analysis
IAEA	International Atomic Energy Agency
IGM	Inverse Geochemical Modeling
ITCZ	Inter Tropical Convergence Zone
LMWL	Local Meteoric Water line
m.a.s.l	meter above sea level
MCM	Million cubic metre
MER:	Main Ethiopian Rift
MOWE:	Ministry of Water and Energy
NNE-SSW:	North North East- South South West
NW-SE:	North West –South East
RA:	Residual Alkalinity
SWL:	Static Water Level
TDI	Total Dissolved Ion
TDS:	Total Disolved Solids
TGD	Tendaho–Ghob'ad Discontinuity
TU	Tritium Unit
VSMOW	Viena Standard Mean Oceanic Water
WFB	Wonji Fault Belt
WHO:	World Health Organization
WWDE:	Water Well Drilling Enterprise
WWDSE:	Water Works Design and Supervion Enterprise

Table of Contents

Annexes

List of Figures

List of Tables

1. Introduction

1.1 Background

Water, also known as blue gold, is vital to human life and to the survival of water related biodiversity and natural ecosystems. Ethiopia, like many African countries, is still far from achieving the safe drinking water and adequate sanitation. Allydegi plain and its surrounding, which is located in the complex volcanic center of the Ethiopian rift valley, is one of the areas with water supply problems. Due to shortage of surface water, groundwater is the only resource supply for human, domestic and agricultural consumption.

Groundwater is closely interrelated with other components of the environment. Any changes in atmospheric precipitation without doubt cause changes in the groundwater system, resource and quality, the reverse is also true (Wakgari, 2010).

Hydrogeochemistry and isotope tracers were used in order to investigate the groundwater flow system and estimate the groundwater residence time (Mahlknecht et al., 2006). Isotope methods when introduced in to catchment hydrology is a complementary tool to conventional hydrologic and hydregeologic methods for addressing questions of where water goes when it rains, what pathways it takes to the stream and how long water resides in the catchment (Mc Donnell, 2003).

Groundwater resource assessment in areas like Allydegi plain and its surroundings has multidimensional importance from economic and environmental point of view. In view of groundwater resource assessment and potential evaluation for the intended purpose, the assessment should include hydrogeochemical and environmental isotope approaches. To utilize groundwater for the above mentioned purpose; the occurrence, localization, quantity, sustainability and quality are among the major requirements. To study the hydrogeological system of the area, it is important to know its hydrogeochemical and isotope hydrologic characteristics.

1.2 Statement of the Problem and Relevance of the Study

Previous works tell that understanding of the groundwater resource of Allydegi plain is increasing since 1972 to date. The geological system of Main Ethiopian Rift is much complex that the functioning of groundwater with the limited data source is not adequate to understand the hydrogeological system of the area. Most of the studies conducted within and surroundings of Allydegi plain have a data gap to determine, for instance source and mechanism of groundwater recharge, Interaction between Awash river and groundwater, spatial variation of water quality, source of salinity, ground water connection with modern day rainfall,…..etc. The main limitations to do these are lack of properly monitored hydrochemical and environmental isotope data, properly managed borehole data and lack of hydrochemical and isotope data from varying depths are the least once.

To supplement the previous works and to upgrade the knowledge of the hydrogeological system of the Allydegi plain, Water Works Design and Supervision Enterprise is under contract with Ministry of Water and Energy working for study and development of ground water resource for domestic as well as irrigation purpose to achieve one of the goal of the country's five-year development and transformation plan.

So, this research work is intended to solve the problems mentioned above; hydrogeochemical modeling and isotope techniques will be applied to understand the hydrogeological system of Allydegi plain in relation with Awash river with the help of geological, hydrological and hydrogeological findings.

1.3 Objectives

1.3.1. General Objective

The main objective of this thesis is to provide conceptual hydrogeochemical model of the area. Along with geological, hydrological and hydrogeological findings of the project, hydrogeochemical models and Isotope techniques will be applied to prove the prevailing facts and to identify recharge area, flow direction, Interaction between Awash River and the aquifer of the Allyidegi plain, spatial and depth ward hydrogeochemical variation and evolution to characterize different aquifer systems in the study area.

1.3.2. Specific Objectives

The specific objectives of the research work are expected to address the following ideas:-

- To evaluate the source and mechanism of ground water recharge, discharge, groundwater flow direction, recharge rate and evolution of the study area.
- To determine the major process for the origin of salinity.
- To determine the relative age of the groundwater.
- To assess the Awash river-ground water interaction of Allydegi plain.
- To investigate groundwater connection to modern day infiltration from rainfall.
- To investigate the role of evaporative fractionation prior to recharge.
- To compute groundwater flow velocities along selected flow line.
- To assess the leakage source of Kesem Dam
- To provide conceptual hydrogeochemical model of the area.

1.4 Previous Works and Related Literatures

Previous works executed so far in the area are:-

Asfaw Aymeku (2006). Hydrogeology of the Allydegi Plain and its Environs (Middle Awash Valley, Afar Region), Unpublished Msc.thesis, Addis baba University.

He summarizes that Allydegi plain has got a deep groundwater flow system whose groundwater level varies northwards over the plain. Fractured basalts and ignimbrites interbeded with old outwash gravel and volcanic sand is the major aquifer units of the area. Groundwater recharge to the plain is mostly possible from precipitation of eastern mountain range and indirect percolation of Awash River.

Bizuneh Bekele (2011). Hydrochemical and isotopic characteristics of the groundwater system of Allydegi plain, unpublished M.sc.Thesis, Addis Ababa University.

He concluded that there is an interaction of Awash river with the groundwater of Allydegi plain that lie within few kilometer distance from Awash river during rainy season only and the recent meteoric water contribution to the groundwater reserve of Allydegi plain is very limited. Subsurface inflow or percolation along the slope from southern, southeastern and eastern highlands are found to be the major recharge mechanism for the Allydegi plain.

D.T. Currey (1973). Geomorphic, geologic and groundwater studies in the Awash Valley, hydrogeological consultant, FAO.

He pointed out that the water resource within Allydegi plain is extensive in area as well as in volume and Awash River water infiltrates directly in to the aquifer of Allydegi plain.

D.T.Currey (1973). Earth Resources Technology Satellite-I usage and additional groundwater studies in the Awash valley, hydrogeological consultant, FAO.

This report describes the groundwater resource of Allydegi plain using Earth Resource technology satellite imagery-I to delineate and record the irrigation areas in the Awash valley and finally the conclusion is that the groundwater resource of the area is extensive.

EVDSA, H. (1989). Master Plan for the Development of Surface Water Resources in the Awash Basin, Final report.

This report summarizes that recharge to Allydegi plain is from the escarpment slopes and through direct infiltration from precipitation. The adjacent awash valley section acts as a sink. Additionally the report concludes that exploitation or irrigation from the area would not be feasible.

Ketema Tadesse & Heroic Ferdinand (1983).Groundwater Resource of Allydegi plain

The Study describes hydrogeological study of the Allydegi plain in the middle awash valley for an area of 1950km^2 between Awash and Gewane towns. They summarize that groundwater is transmitted from the surrounding alluvium and volcanics to the Awash river. The chemical quality of the area is within the standards for Irrigation purpose. However for domestic purpose a high value of floride has been recorded which is hazardous to health.

Mezmure Haile Meskel (1983). Hydrogeology of South Afar and Adjacent areas supported by interpretation of Landsat imagery, Unpublished Msc.thesis, International Institute for Areal Survey and Earth Sciences (ITC) Enschede, The Netherlands.

The study focused on a hydrogeological system of a closed basin that only considers surface water inflow from the southern part and precipitation as input components. Evapotranspiration is the only output considered. The study concentrated on various aspects of input and output relations and analyses different aspects, such as climate, hydrology, geology, geomorphology and vegetation. The water balance of eleven sub- basins is calculated in different ways on a monthly and yearly basis. The report stated that in all the methods, the order of magnitude of the water that is stored in to the whole area is about 55mm/yr. beside that this study also used and statistically analyzed hydrochemical data of 139 water samples.

Seifu kebede, et al. (2010). Ground waters of the central Ethiopian rift: diagnostic trends in trace elements, $\delta^{18}O$ and trace elements, Hydrogeology Journal.

He concluded that the main recharge of the aquifers of the central Ethiopian rift originates from mountain blocks through fractures without evidence for evaporation prior to recharge and the progressive trends in trace element composition along the groundwater flow path reveals continuous groundwater flow from the plateau using an integrated approach of major element, trace element and environmental isotopes.

Stephen E. Grasb et al. (1999). The influence of water-rock interaction on the chemistry of thermal springs in western Canada.

The authors evaluated the influence of water-rock interaction on the chemistry of thermal spring waters using thermodynamic model. A comparison of mineral stability with water compositions suggests that the activities of major cations are controlled by equilibrium reactions with common rock forming minerals and alteration product. Calculations indicate that in low alkalinity thermal springs, HCO_3^- is derived from either dissolution of carbonate minerals or oxidized organic matter. However, for high alkalinity springs (>100 mg/l) HCO_3^- is dominantly derived from carbonate dissolution.

Tenalem Ayenew (2007). The distribution and hydrogeological controls of fluoride in the ground water of central Ethiopian rift and adjacent highlands, Hydrogeology Journal.

The study result shows that extreme spatial variations in Fluoride concentration is often associated with active and sub-active regional thermal fields and acidic volcanics within high temperature rift floor, interactions of Fluoride rich alkaline lakes with the surrounding groundwater and Meteoric waters recharging volcanic aquifers become enriched with respect to Fluoride along the groundwater flow path from highland recharge areas to rift discharge areas. He also pointed out that Variations in Fluoride can also be related to changes in calcium concentration resulting from dissolution of calcium minerals and mixing with waters of different chemical composition originated from variable hydrogeological environment across the rift valley and its concentration significantly declines from the rift towards the highlands with the exception of scattered points associated with thermal springs confined in local volcanic centers.

Tenalem Ayenew et al. (2008). Environmental isotopes and hydrochemical study applied to surface water and groundwater interaction in the Awash River basin, Hydrogeology Journal.

They pointed out that towards the rift the ionic concentration and isotopic enrichment (δ^2H & $\delta^{18}O$) increases along the groundwater flow paths and controlled by axial Rift faults. In addition to this they addressed that the ground water flow converges to the seismically active volcano-tectonic depressions with internal drainage & to the Awash River and the dominant source of recharge for central and lower awash valleys is channel losses from the awash river which is indicated by river discharge records and conventional hydrogeological survey.

Wakgari Furi (2010). Fluoride enrichment mechanism and geospatial distribution in the volcanic aquifer of Middle Awash, Northern MER, Journal, France.

He summarizes that there are two distinct aquifer systems linked to geology and physiographic location. The Ca-alkaline rocks like Basalt, Ignimbrite and trachybasalt form aquifers in the mountain regions where as Na-alkaline rocks which include scoria, pumice, tuff and volcanoclasts in the rift floor. Groundwater circulating in the highland areas is slightly mineralized where as in the rift floor highly mineralized and contain high load of fluoride much higher than the permitted standard. He concluded that river hydrograph, hydrochemistry, environmental isotope, two-dimensional tomography and Numerical groundwater flow modeling are in good agreement showing fast percolation of rainfall and strong interaction between surface water and groundwater in the form of losing and gaining.

WWDSE (2009). Allydegi plain groundwater resource evaluation hydrogeological report.

The report summarized that the Allydegi plain is classified in to two groundwater bearing formations after the findings of test wells drilled for hydrogeological investigation of the area. These are unconsolidated sediment aquifer and fractured volcanic aquifer, of these the unconsolidated aquifer has highly productive than fractured volcanic. The report also incorporates that Allydegi plain receives its recharge mainly from direct infiltration of rainfall followed by indirect recharge from Awash River and then from subsurface percolation from highlands of adjacent slopes.

2. Methodology, Materials and Tools

2.1 Methodology

To meet the objectives of the research work, the following methodologies were applied

I) Pre-Field work

- Review of previous works which include geological and hydrogeological reports and maps, well completion reports, researches done in the similar geological settings; collection and organization of secondary water points data like, characteristics, geochemical (major ions) and environmental isotopes (^{2}H, ^{18}O and ^{3}H) data of water points like dug wells, boreholes, rivers, springs and lakes from different sources
- Compilation and organization of monthly monitoring hydrochemical and environmental isotope result of five wells in the Allydegi plain and Awash river, discharge record data for Awash river at different localities and its tributaries which were used to understand the relationship between awash river and groundwater.
- Collection and organization of climatological data and different borehole lithological data from previously drilled wells from WWDSE database.

II) Field work

- Field work to fill data gap by sampling the representative water points along the traverses made and during well development at different depth in Allydegi plain for both physico-chemical and environmental isotope analysis with in-situ measured parameters like P^{H}, temperature, EC and water level of accessible wells to know the interconnection between different aquifer systems. Based on this twenty water samples (8 deep wells, 2 shallow wells, 8 river samples, 1 hot springs and 1 small hot lake) have been collected.
- Collection of well completion reports and water chemistry of different water points from Afar region water resource and energy office.
- Observation and description of geologic units, structures, grain size and geomorphology.

III) Post-Field work

- Chloride Mass Balance method to estimate and relate the groundwater recharge rate of the area with rates calculated by other methods
- Classification of chemical data (HCA) based on their similar characteristics using STATISTICA 8 version software in to six- clusters followed by analysis of the water type using Aquachem 4.0 software and to help selection of dataset for schematization of geochemical evolution and one of Aquachem 4.0 program (Phreeqc) for inverse geochemical modeling;
- Interpretation of the above data based on the geochemical principles, inverse geochemical modeling and isotope hydrology to support the geochemical findings.
- Report writing by integrating all the gathered information (Knowledge)

2.2 Materials and Tools

The materials used during the research work include:

- Geological and hydrogeological map
- DEM, GARMIN GPS-72, EC meter, P^H meter and bottles for collection of representative water samples.
- Computer software's like Global mapper-11, ArcGIS-9.3, Aquachem-4, and STATISTICA-8, surfer-10, AutoCAD 2007, and PHREEQC interactive-2.8.

3. Description of the study area

3.1 Location and Accessibility

The study area, Allydegi plain and its surrounding, is located in the middle awash valley of Main Ethiopian Rift (MER) about 300 km east of Addis Ababa along the road from Addis Ababa to Djibouti through Awash-7 Asphaltic road with an approximate coordinates in between 543688-to-717026UTME and 961849-to-1132211UTMN and has an area of about 19,139 km^2 (Figure 3.1).

The plain is characterized by an elongated shape, oriented nearly south-north direction and having a total length more than 70 km and width an average of 25 km. The Allydege plain occupies not less than 1400 km^2, i.e. from which 930 km^2 is alluvial plain and about 470 km^2 is alluvial fan. In general, the study area is bordering in the North West by Blue Nile basin drains towards west ward from northern highlands, Asebot and Afdem mountains in the east and wabishebele basin in the south east drains towards eastwards.

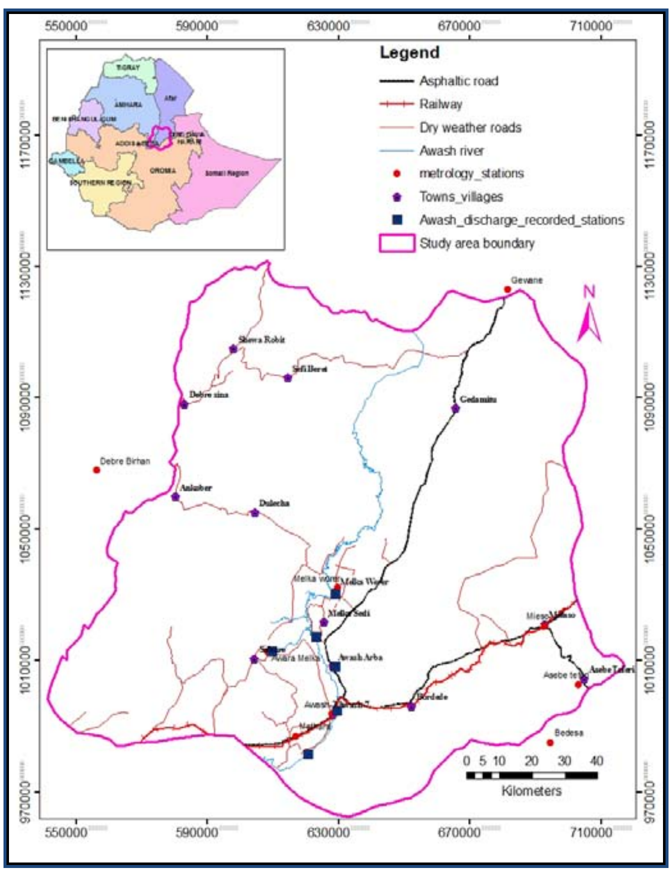

Figure 3.1: Location map of the study area

3.2 Physiography and Drainage pattern

3.2.1 Physiography

The area is part of the central Ethiopia plateau and western most part of the rift margin and floor of the Main Ethiopian rift (MER). On the basis of morphology and drainage type, the area is divided into the following physiographic divisions: Plateau, Escarpment and Rift floor (Figure 3.2). The physiography and drainage patterns of the area were summarized from observation during field work(WWDSE, 2011 and GSOE, 2010).

The plateau occupies the western and north western part of the area that includes Ankober and Debre-sina localities. It is largely characterized by flat lying topography (up lifted 2600m.a.s.l.) with some undulating ridge chains and valleys. The flat lying topography is mostly represented by the Tertiary basalts and Quaternary sediments with sporadic small hills formed by trachyte and erosion remnant of ignimbrites. The undulating ridges are represented by Tarmaber-Megezez basalts.

The escarpment includes the rugged terrain in the range of 1200- to- 2600 m a.s.l. This forms a very steep morphology with a series of normal faults running in the N-S and E-W directions. The western escarpment starts from the East of Debre Sina and Ankober joins Kesem River and mostly represented by ignimbrite-rhyolyte with minor intercalated basalts. The eastern and south eastern part of the study area escarpments represented by Quaternary basalts and some trachyte domes.

The rift floor is the lowest physiographic region in the study area (730-1200 m a.s.l.). It is characterized by flat lying plain with isolated hills (cinder and scoria cones) and elongated ridge chains. The flat laying plain mostly represented by Quaternary sediments whiles the isolated hills, for instance Dofan hills, represented by Quaternary basalt and trachybasalts. The elongated ridge chains are mostly developed on the Quaternary basalts and sometimes on the ignimbrites.

In general, the geomorphology of the area is primarily controlled by en-echelon arrays of normal fault systems, the last phase of faulting in the middle Awash valley known as Wonji Fault Belt (GSOE,2010). This fault belt resulted in the formation of two major grabens in the area, the Allydegi and Awash valley. A series of horst and graben structures are found west of the Allydegi Plain (Figure 3.2).The horst between the Allydegi and the Awash valleys is made up of lava-gravel sequence, has numerous small fault displacement along its length. The Allydegi graben has been filled with outwash gravels, eroded by Awash River (its older course), infilled with alluvium, which has then partially covered by fan deposits along the eastern margin. The alluvium of the plain consists of large areas of black soils. North-North East running volcanic centres like Gumbi, Asebot, Meiso, Afedm, Dijilu and Dofen form a high standing geomorphology in the area. The entire water catchments form part of the Eastern and North Western Ethiopian Highlands.

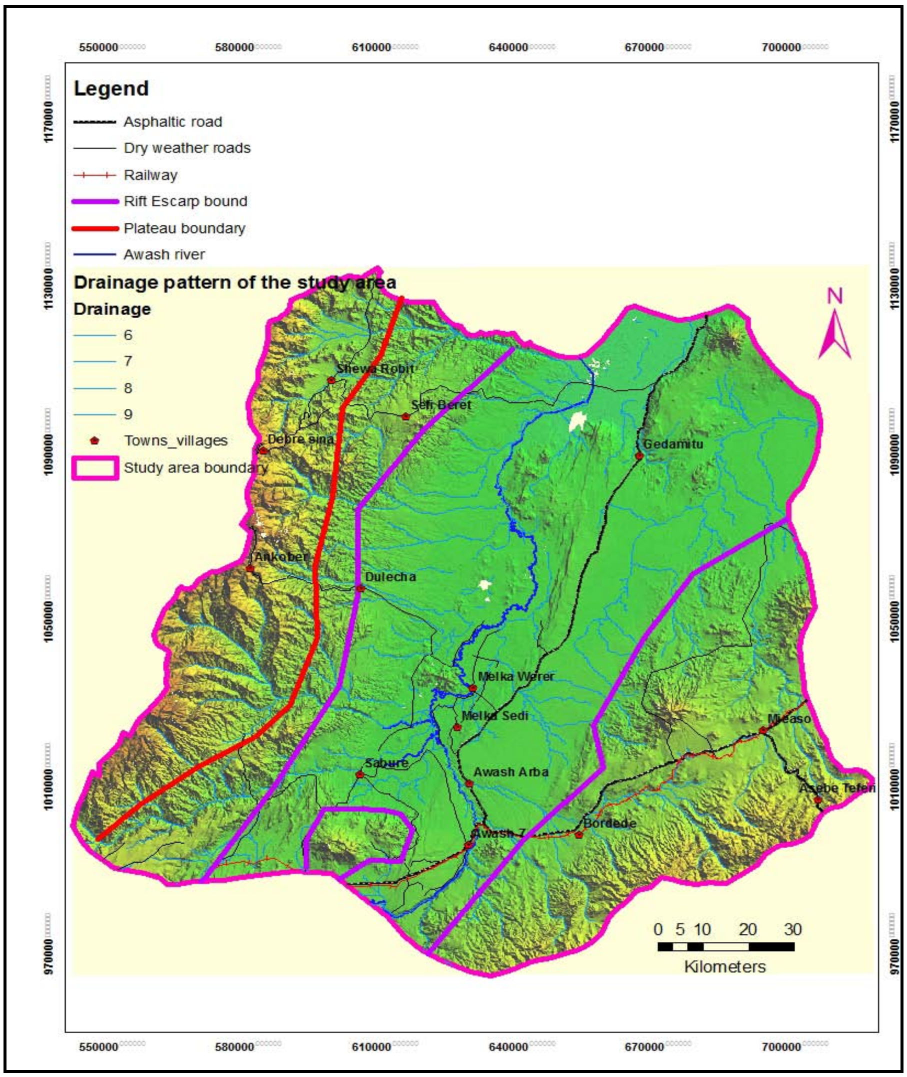

Figure 3.2: DEM showing physiography and drainage pattern of the study area

3.2.2 Drainage

Drainage systems are controlled by climate, topography, land cover, and geology including tectonic structures of the area. In area where the underlying geology is impervious, and topography is steep, dense drainage systems could develop whereas area with porous materials and flat topography produce low drainage density as large volume of water is lost to subsurface through porous materials. The climatic and hydrologic characteristics of the middle Awash basin generally produce a discontinuous stream flow regime in most of the watersheds.

The drainage pattern in the plateau and escarpment areas developed over the steep mountains follow topographic slopes and there is no integrity among tributaries but streams form separate flow in the same direction where as in the rift floor spread drainage system characterized by lack of well developed drainage pattern. Streams that drain in highlands tend to disappear up on reaching the rift porous and permeable volcanic deposits.

The main river, Awash river course follows the steep northerly and northeasterly structures of the underlying volcanic rocks, the WFB forming parallel drainage pattern but the channels of many of the smaller streams are controlled by bedrock grain, hence forms dendritic drainage pattern (Figure 3.2). In general, the drainage pattern of the study area is characterized by dendritic, parallel and sub paralle.

3.3 Climate

The climate of the study area comes under the influence of the Inter Tropical Convergence Zone (ITCZ). This zone of low pressure marks the convergence of dry tropical easterlies and the moist equatorial easterlies. The seasonal rainfall distribution within the project area results from the annual migration of the ITCZ. The ITCZ starts its advance across the project area from south in March bringing small spring rains. From June to September the ITCZ moves rapidly from north part of the country to the project area bringing summer rain. Along with the ITCZ the orography has significant effect for the formation of rain in the project area. The ITCZ returns southwards during September and october, restoring a drier, easterly air stream which prevail until the ITCZ resumes its northward migration in March (HALCROW, 1988/1989).

Rain is the most common form of precipitation in the study area. Precipitation in the study area is recorded by gauges at different stations. In the study are rainfall records are available from nine stations (Annex-I).

Comparison of the monthly rainfall at various stations which differ in the amount of rainfall they receive can be done using the rainfall coefficient (C_{rf}) concept. i.e.

$$\boxed{C_{rf} = P\ (M)/1/12*P(Y)}$$

Where, P (M) =Mean monthly precipitation

P(Y) =Mean annual precipitation

Based on this concept and mean monthly rain fall analysis graph (Figure 3.3), a rain month is defined as the one with a rainfall coefficient exceeding 0.6, whereas a rainfall coefficient below 0.6 defines a dry month (Tenalem Ayenew and Tamiru Alemayehu, 2001). According to the above reasons, the rain season is usually preceded in March until mid may by converging northeast and southeast winds that produce a brief period of light rains (from Indian Ocean). These rains are followed by a short period of hot dry weather in May and toward the middle of June, violent thunderstorms occur almost daily and heavy rain occurs in months of mid June, July, August and mid-September (from Atlantic Ocean) while the rest of the months are generally dry.

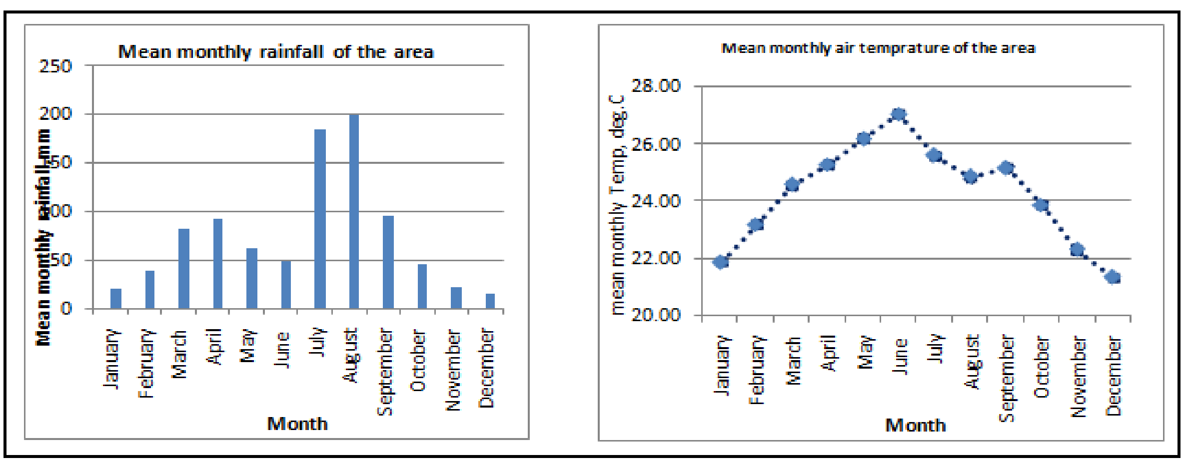

Figure 3.3: Mean monthly rainfall and air temperature pattern of the area.

3.3.1. Arial Depth of Precipitation

The study area is characterized by flat, rugged and elevated topography with sparsely distributed stations to measure the rainfall. In mountainous areas, orographic effect can create vastly different microclimates over small distances; significant precipitation can fall on one side of a ridge but little on the other. In such regions isohytal method of calculating areal depth of precipitation is most applicable than theissen and Arithmetic average methods.Isohytal method provides good results, because it allows the influence of physiographic parameters like Altitude, slope and exposure to rain bearing winds to be taken into account (Fetter, 1994).

Based on the facts mentioned above, isohytal map (Figure 3.4) was created using ArcGIS 9.3 computer code by locating on a base map all rainfall stations, rainfall amount and then draw isohyets(lines of equal rainfall) by proportioning the distances between adjacent gauges according to differences in catch and then estimate the mean precipitation for the area corresponding to each isohyets and fraction of catchment area under each isohyets, Finally multiply by the mean precipitation for that area and sum to get the catchment average (Table 3.1). Thus the annual mean rainfall for the area is 649.4mm.

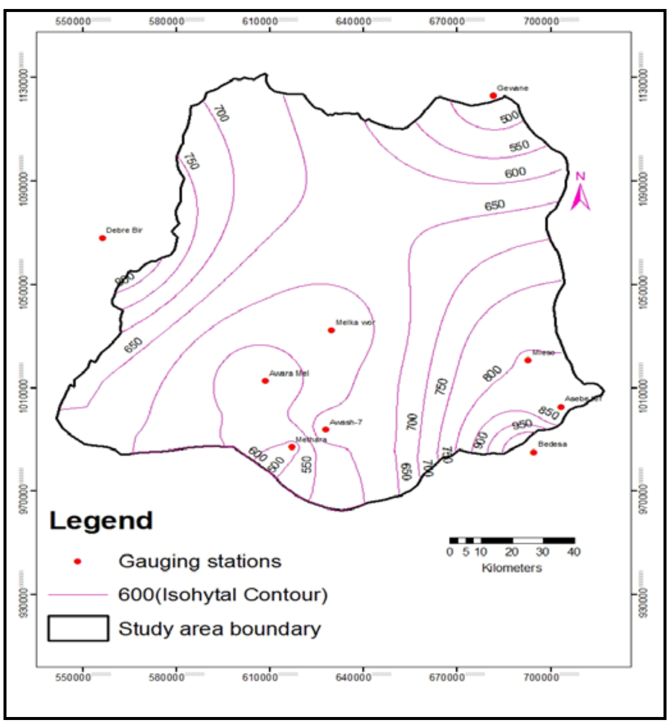

Figure 3.4: Annual isohytal rainfall map of the area

Table 3.1: Areal depth of precipitation calculated using the isohytal method

Rainfall range(mm)	Average value of Isohyets(mm)	Area between Isohyets (km^2)	Weighted area	Weighted rainfall(mm)
<500	500	171.52	0.009	4.48
500-to-550	525	1632.43	0.085	44.78
550-to-600	575	3442.84	0.180	103.43
600-to-650	625	5846.37	0.305	190.92
650-to-700	675	3602.09	0.188	127.04
700-to-750	725	1975.43	0.103	74.83
750-to-800	775	1352.71	0.071	54.78
800-to-850	825	845.48	0.044	36.44
850-to-900	875	154.66	0.008	7.07
900-to-950	925	79.8	0.004	3.86
>950	950	35.71	0.002	1.77
Total		**19,139.04**	**1.000**	**649.40**

The mean monthly temperature of the study area ranges from 17.7^{0}C (Bedessa) to 32.9^{0}C (Gewane). The relationship between mean annual temperature and elevation (Figure 3.5) shows that the highest temperature observed at the lowest elevation (i.e. at Gewane). The increase of temperature value towards the lowland area reveals that the dryness of the land. The mean maximum monthly temperature of 32.9 ^{0}C observed in June at Gewane and in December mean minimum monthly temperate of 17.7 ^{0}C at Bedessa. The mean annual temperature of the project area is about 25^{0}C.

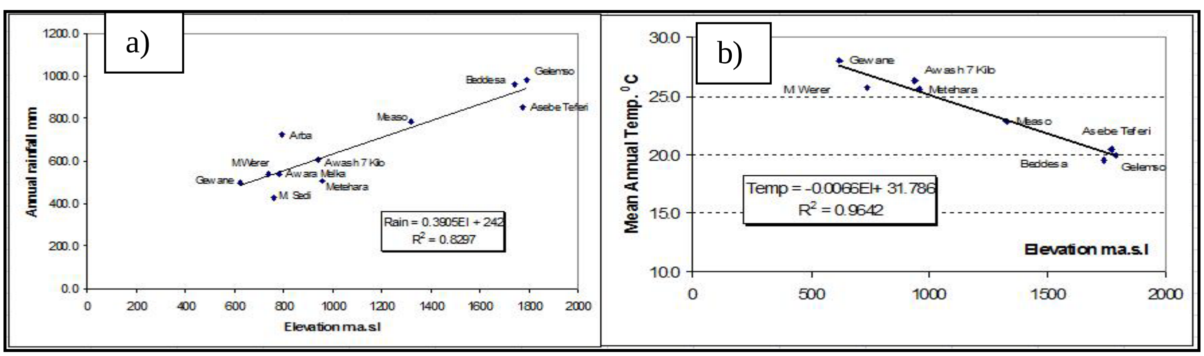

Figure 3.5: (a) Annual rainfall and (b) Temperature vs. altitude relation of the area

The summary of the sun radiation duration reveals that it is lower during the wet season (June-September), while during the dry season the highest sunshine observed in the month May. Spatially, the highest sunshine duration observed on low lands with the maximum record of 10 hours. An average sunshine duration for the study area comprises about 8.2 hours.

The maximum wind speed recorded at the area is in the rainy months of June, July August. Highest wind speed, i.e. more than 2 m/s is observed in Gewane area. Topographically the strength of the wind speed increases towards the lowland and it is vice versa at the higher elevation. Relative humidity is medium to high (> 50%) during the wet season and medium-to-low for the rest of the year. Maximum evaporation observed in June at Gewane about 475 mm and the minimum is recorded in month of August at Metehara about 180 mm. The spatial variation of evaporation is generally related to altitude and inversely proportional to rainfall.

3.4 Hydrology

The Awash river drains the northern part of the rift valley in Ethiopia which lies at an altitude of around 2500 m.a.s.l in the plateau to the west of Addis Ababa around Ginchi town. It first flows east draining Becho plains and joined by several major and minor tributaries which descend in to the rift valley. The river then turns gradually northwards flows to a lower gradient along the base of western and eastern highlands. Several major and minor tributaries enter the Awash River in the study area from highlands, like Kesem and kebena through deep gorges. After receiving a substantial flow on the way and terminates in a series of lakes and the principal of which is lake Abe at an altitude of around 250 m.a.s.l. According to Adane bekele (1999), the total length of Awash river to its termination to this lake is about 1200km giving the total catchment area of 111,211km^2 with western and eastern catchment area 63,852km^2 and 47,359km^2 respectively.

The study area is part of Awash river basin which lies in the middle Awash river valley. Awash river in the area has gauged at four stations along the main river and at two location in its tributaries. It is the main river in the study area that flow toward northeast following the main rifting axis and its discharge is measured at several places along its course at (Methara, Awash-7, Melka-sedi, Melka-werer and Gewane).

Due to it is controlled in between Melka-sedi and Melka-werer for irrigation,discharge recoded from Awash River was not used in this study. Whereas recorded discharge from tributaries like Kesem @ Awara melka, Mieso and Awash-Arba Analysis of long term daily stream discharge records show that most of the streams are flashing types that exists only during the short rainy seasons. Between summer rainfall events, the rivers exhibit continuous flow to the Awash River from residual watershed but flows are entirely dry during the dry seasons. However, Flow data analysis (Annex-II) has shown that mean annual flow of Awash river @ Awash-7 is much larger than Awash river at Meleka -Sedi in the route of about 30km. Examination of the existing hydrological data of Awash with catchment area at Awash-7 (19,111 km^2) and Awash at Melka-sedi (21,520 km^2) demonstrate a deficit of an average about 314MCM/year of water. From the study of hydrology and in situ observation of the river bed character(Basalt), Allydegi plain and surrounding aquifer is recharged by Awash River through fractures of the volcanic rocks.

Based on the Darcinal approach the mean annual rechargeable water into the Allydegi plain is more than 112.42MCM/year. It is computed separately for Awash river, Volcanics and direct precipitation (WWDSE, 2011).

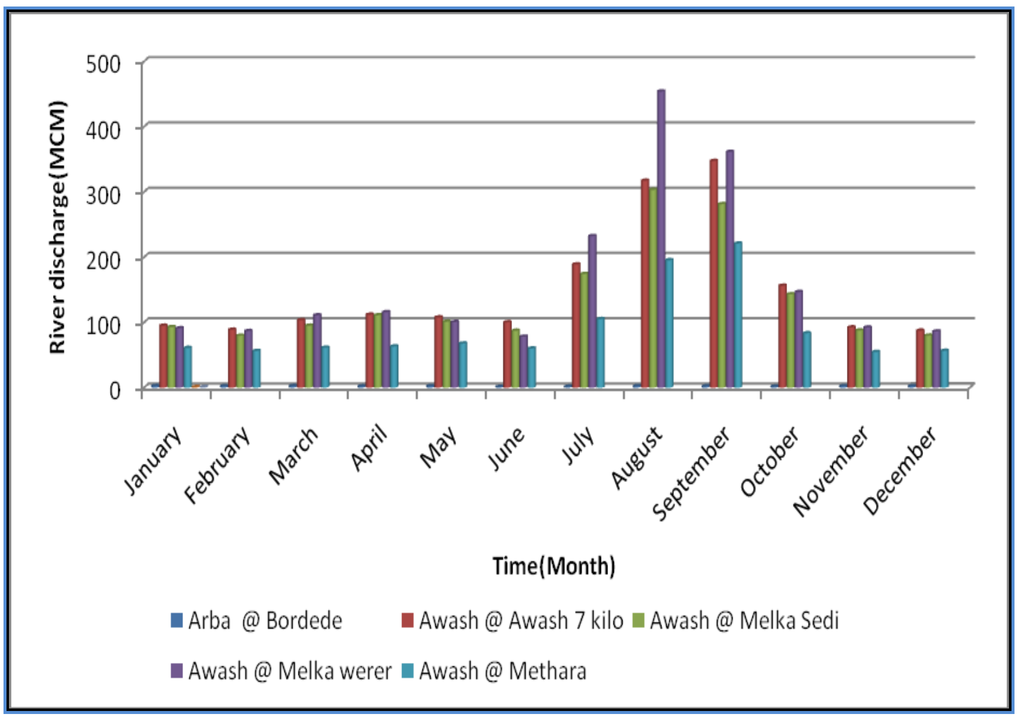

Figure 3.6: Average mean monthly Awash river discharge at different locations

3.5 Geology and Hydrogeology

3.5.1 Geology

The major geological formations and tectonic features of the research area were adopted from Allydegi Groundwater Resource Assessment Project Report (WWDSE,2011) and Geology of Debrebrhan area (GSOE,2010). The geo-structural findings are summarized as shown below.

3.5.1.1 Regional Geology

Four major physiographic regions are recognized in Ethiopia which reflects the geological and tectonic processes that have undergone in the past and currently active and ongoing as well which are believed to continue in the future. These four major physiographic regions in Ethiopia are North-Western and South-Eastern plateaus, the main Ethiopian rift (MER) and Afar depression. The Ethiopian plateau is underlain at depth by Precambrian rocks of the Afro-Arabian shield. The Precambrian basement is covered for the most part by glacial and marine sediments of permian to paleogen period and volcanic rocks of tertiary and quaternary age with related sediments.

The Precambrian basement exposures are found in the north (Tigray), in the west along the Sudan border (Gojam, Wollega, Illubabor, and Kefa), in the south (Sidamo and Bale) and in the east (Harerghe). The Precambrian rocks of Ethiopia are consisting of high-grade gneiss, metamorphosed volcano sedimentary rocks and associated ultramafic bodies and intrusives ranging from mafic to granitic composition.

The Mesozoic era transgression and regression event depositions of sediments, like Adigrat sandstone, which rests uncomfortably on the crystalline basement rock, Abay beds composed of gypsum and shale units, Antalo Limestone which conformably overly the Abay beds, Amba Aradam sandstone.

The flood basalts, forming the Ethiopian plateau, erupted apparently in short time interval (<5Ma) with the greatest eruption rates during 31 to 28 Ma. In the northwestern Ethiopian plateau, the flood basalt is further subdivided into three main magma types, distinguished by their contrasting geochemical signatures.

This plume-related uplift caused deep-seated faults within the Ethiopian lithosphere, leading to the initiation of the Afar Depression at ~24Ma and the Main Ethiopian Rift (MER), followed by shield-volcano-building episodes (central volcano) start around 26 to 22Ma in the northwestern Ethiopian plateau ~23Ma. The Shield volcanics get progressively younger (15 to 13Ma) towards the SE in central-Ethiopia. The Tertiary volcanic successions are mainly consisting of Ashange basalts (49-to-46 Ma), Aiba basalts (34-to-30 Ma), Alaji rhyolites and basalts (30-to-26 Ma), Tarmaber basalts(25-to-13 Ma) and Balchi rhyolites (8-to-2 Ma).

Subsequent volcanism was restricted in MER (rift margin and axial zone) and Afar Depression. The initial stage of the formation of the rift system dates back to early Tertiary (Upper Eocene) where initial uplift of the Afro Arabian dome took place centered on the Afar triple junction. The MER has been classified into structurally diverse Southern, Central and Northern MER segments accompanied by episodic bimodal magmatism. Extension in southern Ethiopia began at ~25-20 Ma whereas volcanism started in the early Miocene (20-21Ma) as a result of a northward propagation of the Turkana rifting process.

Significant rift opening occurred in the Central MER during the Pliocene (5-3 Ma) with the eruption of voluminous ignimbritic covers (Nazret sequence) exposed both on the rift shoulders and on the rift floor. In Pleistocene to recent, the last stage of MER formation is characterized by the localization of volcanism restricted to the axial extensional zone or the Wonji Fault Belt and to the axial ranges of Afar.

The WFB is arranged in an “en-echelon” fashion and it is typified by Dino ignimbrite (oldest), Pantelleritic center (Aluto, Boset, Fantale, Dofan etc.) and sub recent fissural “aa” basalts (Mohr, 1967). The sub recent fissural “aa” basalts are controlled by extensional fractures. Although the post-rift volcanism has been concentrated mainly along the axial zone of MER.

3.5.1.2 Local Geology

The crustal extension, which gave rise to the Ethiopian Rift system, also created lines of weakness for volcanic activity. The volcanic activity in the Allydegi surface water catchments area concentrated along these lines of weakness or faults. Not only volcanism that is associated with the fault zones but also series of graben structures occurs in the Southern Afar where alluvial deposits are accumulated. The Allydege plain and Awash valley are contained in a graben structure, which has been partially in-filled with alluvial deposits derived from the near by volcanic terrains. The study area consists of Cenozoic volcanic rocks of Tertiary and Quaternary age of which Tertiary volcanic rocks mainly exposed on the plateau and along the NE-SW trending rift margin. They are represented by thick succession of fissural Kesem basalt, Seladengay-Debre Birhan-Gorgo ignimbrite with sporadically distributed trachyte, rhyolite and thin beds of Tertiary sediments, overlain by central type Tarmaber-Megezez basalt. The Quaternary volcanic rocks are mostly widespread within the rift-floor and mainly consist of central to fissural type ignimbrite and basalt.

According to the geological studies conducted so far by (WWDSE, 2011) and (GSOE, 2009) the Cenozoic volcanic rocks and superficial deposit formations discussed below from older to younger in age.

A) Tertiary Volcanic Rocks

The Tertiary volcanic rocks are the earliest volcanic rocks in the area that occur along the plateau bordering the rift, which were erupted from fissures due to extensional tectonic activity. The rocks consist of thick succession of aphanitic basalts and ignimbrites which are overlain by central volcano (plagioclase phyric basalts). Within the Tertiary volcanic rocks, thin beds of volcanoclastic sediments (Tertiary sediments) are also found.

Kesem basalt (Pkb): is found at the lower stratigraphic sections of Kesem drainage basin. It is strongly fractured, irregularly to columnarly jointed, spheroidically weathered, aphanitic to porphyritic in texture and forms very steep cliffs. The Kesem basalt consists of dominantly aphanitic basalt intercalated with plagioclase phyric basalts and thin beds of ignimbrite.

Seladingay-Debrebirhan-Gorgo ignimbrite (Pdig): has a sharp contact with the overlying Tarmaber-Megezez basalt and underlying Kesem basalts. It comprises ignimbrite, rhyolite, Tertiary sediment, tuffaceous sediment, aphanitic basalt, agglomerate and ash. The ignimbrite forms gentle to steep cliffs, elongated ridges and sporadically distributed isolated Hills with columnar joint, vertical joints, and fractures. It contains rock fragments of rhyolite and basalt ranging up to 2cm in diameter and elongated fibrous glass shards (fiamme).

Alajae Formation (Na1): Alajae basalt is mildly alkaline to mildly sub alkaline in chemistry, is dominantly aphyric fissural flood basalt with interlayering of rhyolitic lava flows, ignimbrite and rarely trachyte. Generally the basalt is very fine grained, also locally vesiculated and contain olivine phenocryst. A columnar jointing and strong unsystematic fracturing can be encountered. The lithologies in this formation are affected by NE-SW and NW-SE trending faults.

Tarmaber-megezez basalt (Ntb): is dominantly exposed on the western part of plateau which forms a series of linear ridges and high mountains. It includes aphanitic to porphyritic basalts. It is characterized by different phases of basaltic flows separated by randomly exposed reddish palaeosols and reddish brown scoriaceous basalts. It is dominantly represented by plagioclase phyric varieties (plagioclase phyric and olivine-plagioclase phyric basalts) together with minor olivine phyric, pyroxene phyric, plagioclase-pyroxene-olivine phyric and aphanitic basalts.

Anchor basalt (N1n): This unit is regarded as a product of an early rifting stage and defines the margin of eastern escarpment in the area. It is Mio-upper Miocene in age. It outcrops in the east central surface water catchments area. It's grey to dark grey; fine to microcrystalline in texture, fractured and faulted. Fractures and veins in these rocks are in filled with quartz and calcite. The Anchor basalt is transitional in chemistry. The pyroclastic rocks intercalated with the basalt are largely ignimbrite, characterized by homogenous appearance with little sorting of ash particles.

Arba Guracha silicics, rhyolitic lavas and ignimbrites (N1r): This unit overlies on top of the Alajae basalts, along the eastern margin of the rift. It represents several interlayers of basaltic rocks, rhyolites and ignimbrites.

Rhyolitic volcanic centers (Nry): It represents rhyolitic domes and volcanic centers of the study area (Asebot, Afdem, Gumbi, Meiso, etc). Sharp standing hills, vertical joints with various attitudes are general characteristics.

Ignimbrite Sheet (Nig): It is termed as Dino Ignimbrite. Ignimbrite sheet covers an extensive area around Awash-7 Kilo and Gumbi volcanic center and characterized by flows of compact fiamme, in places intercalated with aphyric Afar stratoid basalt and unwelded pyroclastics. The ignimbrite sheet follows valleys and form lower grounds. The ignimbrite lacked internal stratification. At a section, it grades into fine ash deposit consisting of large angular lithic-clasts randomly scattered in matrix of low-density pumice and ash.

Rhyolitic Ignimbrite (Nrig): The Rhyolitic ignimbrite forms a NNE – SSW running horsts (Berita and Bilen Ridges*)* between the Allydegi plain and Awash valley.

Afar Stratoid Basalt Lower (N1ab): This unit outcrops in the southern central part of the area, in the east around Hardim and low grounds of Asebot Mountain which forms low-lying hills. The Afar lower stratoid basalt is equal in age to that of the rhyolitic volcanic centers (Nry). This unit is massive to vesicular, affected by dominant horizontal jointing and unsystematic dipping joints. This unit is fissural type and interbeded with ignimbrites viewed in Awash Bridge at Awash-7 Kilo. It is greatly affected by major and minor tectonics with thickness might reach up to 70m.

Afar Stratoid Basalt Upper (N2ab): The unit forms both high and low lying hills, unconformably overly the lower Stratoid Afar basalt. The Afar stratoid basalt upper is Pleistocene – sub recent in age. The basalt is massive to strongly vesiculated. The vesicles range from open to being filled by calcite and silica.

B) Quaternary Volcanic Rocks and Superficial deposits

Recent Basic Lava (Qb1): This unit occurs on top of upper Afar stratoid basalt, out crops in Dijilu Shield Volcano in the north and around Dofen Stratovolcano in the south west. The basalt is scoraceous and forms both flows and cones mostly cut by minor faults.

Pahoehe Lava (Qb2): It is a very rough surfaced basic lava flow, out crops in the north, and north east of the study area. It occurs in the vicinity of the scoraceous lava and is the product of both fissural to cone eruptions.

Outwash Gravel (Qog): Outwash gravel in the area represents Pleistocene deposits derived from breakdown products of basaltic and acidic materials from the elevated areas, which have been transported towards the centre of the basin to form extensive outwash, gravel plain. The gravel outwash covers extensive areas around cliff faces of Arba River and the surrounding localities, eastern valley sides of Melka-Sedi and Amibara. The outwash gravel contains lenses of clay beds.

Alluvial Fan (Qaf): The alluvial fan in the area represent a compositionally immature sediments consisting of gravel, sand and silty layer, showing fining direction to the west. Extensive area east of the Allydegi plain, downstream pointes from Asebot volcanic centers contains a fan area of enhanced sedimentation, points where laterally confined flow expands.

Quaternary Slope Deposits (Qsd): represent breakdown materials of the elevated areas, consists of mainly sand and gravels - the clasts in the gravel are basaltic and ignimbrite material, seems to be transported from the nearby horsts. The gravel size varies from 10mm-10cm in diameter. The gravel shapes differ from angular to sub-rounded indicating a proximal source. The finer materials are sands and small amount of silt. These slope deposits are transported along minor stream courses of the region and deposited on the gravel terrace. In some location the material is interbedded with the alluvium, especially at the edge of the flood plain traces.

Quaternary Elluvium Deposit (Qed): Quaternary elluvium in the area consists of brown and black clays, sand and silty materials including the lacustrine sediments. The brown sand, brown silt and clays may represent pre-lake sediment, might have been derived from acidic sequences in the area. The Black clays are confined to a former river system and show cracking and are a product of the breakdown of the basaltic rocks of the region.

3.5.1.3 Tectonic Structure

The geological structures occurring in the area which are mapped include Normal faults, beddings and joints. These structural elements within the study area are identified by the combination of results from interpretations of land sat imagery, Digital Elevation Model (DEM) analysis and field observations. Block faulting, fissuring and tilting of various rock units in the area mainly affected the stratoid basalts which are probably occurred in the Pleistocene (WWDSE,2011).

A) Fault Systems

Five sets of Normal fault trends are recognized in the study area. Of these, the most prominent and observable once are discussed.

NW- Fault system: It is the oldest fault system in the area, affected the Alajae formation, the Anchor basalt and Arba Guracha silicics, rhyolitic lavas and ignimbrites in the eastern surface catchments. These faults have extended history, are of crustal scale in nature, served as a conduit for the extensive volcanic formations in the area and their age may go up to early Palaeozoic, but becomes reactivated later with a main tectonic event in the region.

NE - SW (Nazareth trend) Fault system: The Nazareth fault system defines the eastern margins of Ethiopian Rift and terminates around Afdem Area. They are northeast trending, steep west dipping; segmented fault system and associated with the volcanic rocks of the same age (Nazareth Group, Anchor basalt) in the area. The fault system is articulated and segmented but the overall direction strikes about NE-SW.

The Wonji Fault Belt System: A major fault system occurring densely in the area. It is very young and is conduits for most of the volcanic rocks. This Pleistocene recent faulting, generally trends NNE. The fault system extends from within the Ethiopian Rift Valley to curvilinear Tendaho–Ghob'ad discontinuity (TGD) structure in central Afar against which it terminates The Wonji fault belt consists of open fissures and normal faults and is usually curvilinear. This episode of faulting created horsts and graben within broad fault zones in the region. Extension along the Wonji fault belt is marked by normal faulting, open fissures, and fissure-fed basalt flows. The Wonji fault belt is segmented, collectively; the individual segments in the Wonji fault belt display an en echelon, right-stepping array.

B) Bedding

Bedding is a primary structure noted in both volcanic rocks and in gravel layers. This structure in the rocks has been produced by changes in the pattern of basic volcanic flow or changes in sediment composition in case of pyroclastics and gravel layer. The bedding in the gravel layer and pyroclastic rocks are generally horizontal, which is observed in Arba River bank, upstream from the Bridge.

C) Jointing

Almost all of the volcanic rocks in the area have been affected by jointing. These joints vary from having planar to curved surfaces. The stratoid basalts are the most joint affected rock units in the area and jointing is less in density on acidic rocks (rhyolite and ignimbrite).The joints affecting the rocks in the area have any attitude vertical, horizontal and some are inclined. Closely spaced horizontal joints are particularly observable in the stratoid basaltic rocks. Well developed columnar jointing occurs in the Alajae basalt.

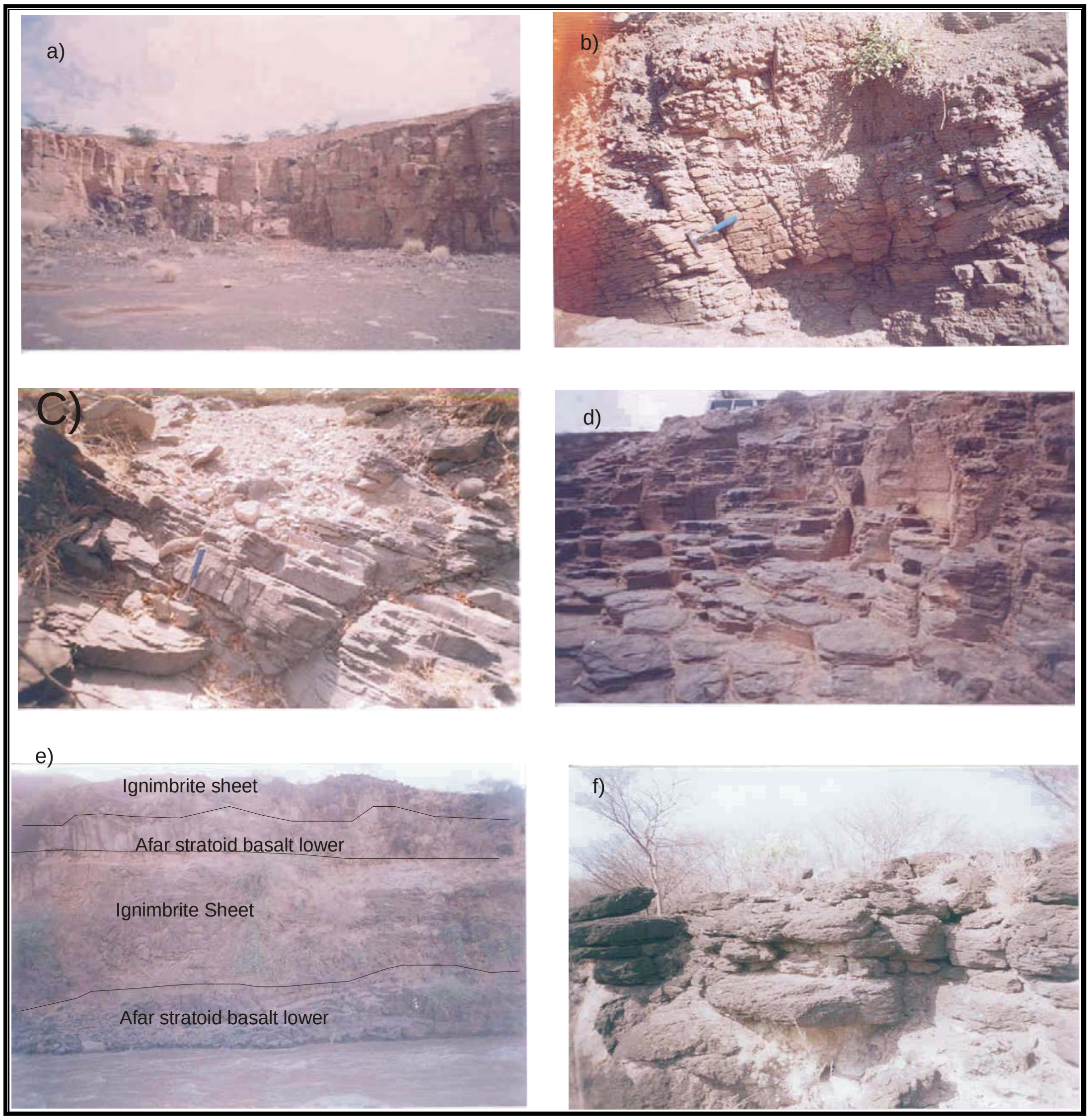

Figure 3. 7: a, b, c, d and e) various system of jointing in the Afar stratoid basalt and (f) Horizontal jointing in rhyolitic ignimbrite (Adopted from WWDSE, 2011).

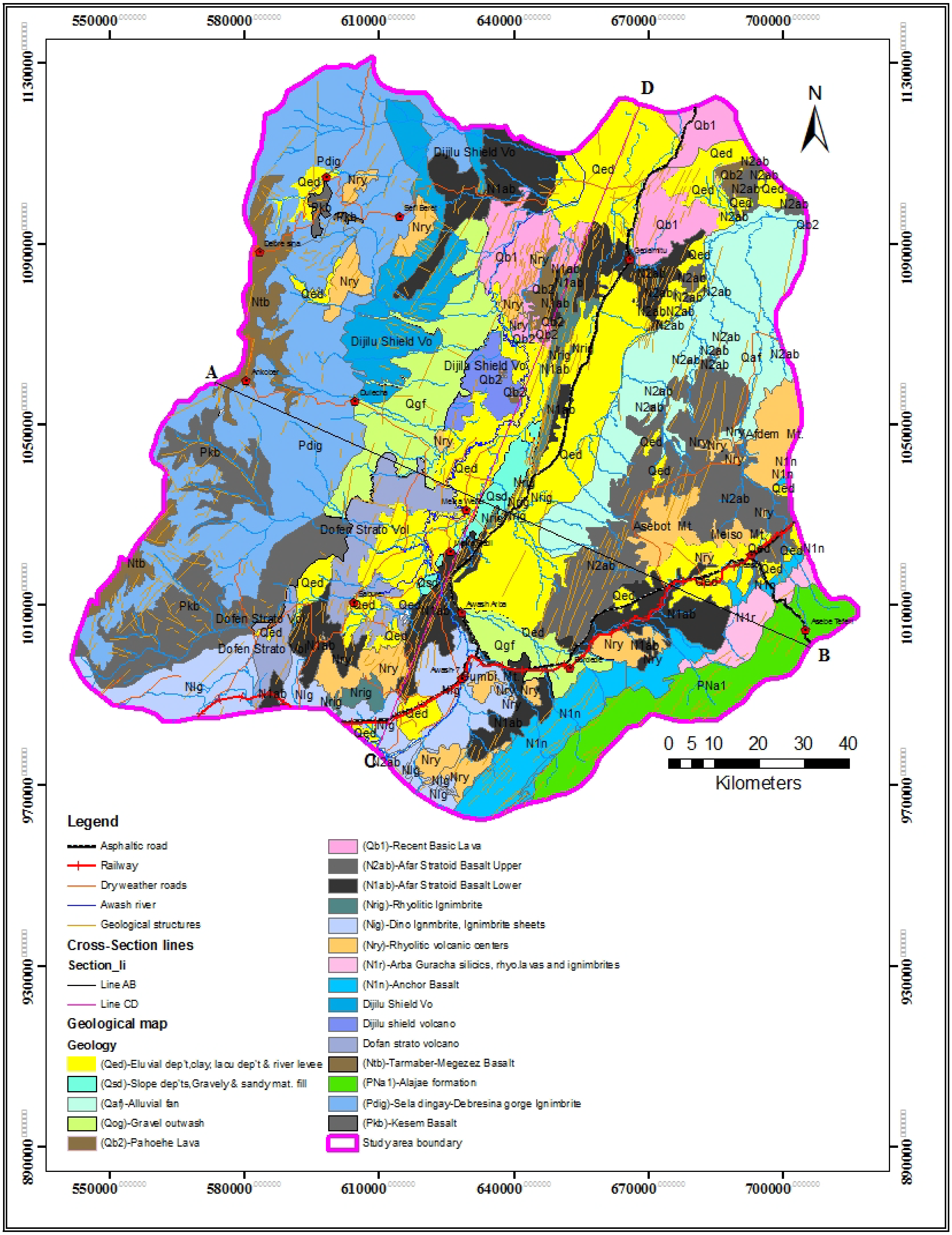

Figure 3.8: Geological map of the study area (Created from a combination of Debrebrhan Sheet (GSOE, 2010) & AGWRAP (WWDSE, 2011))

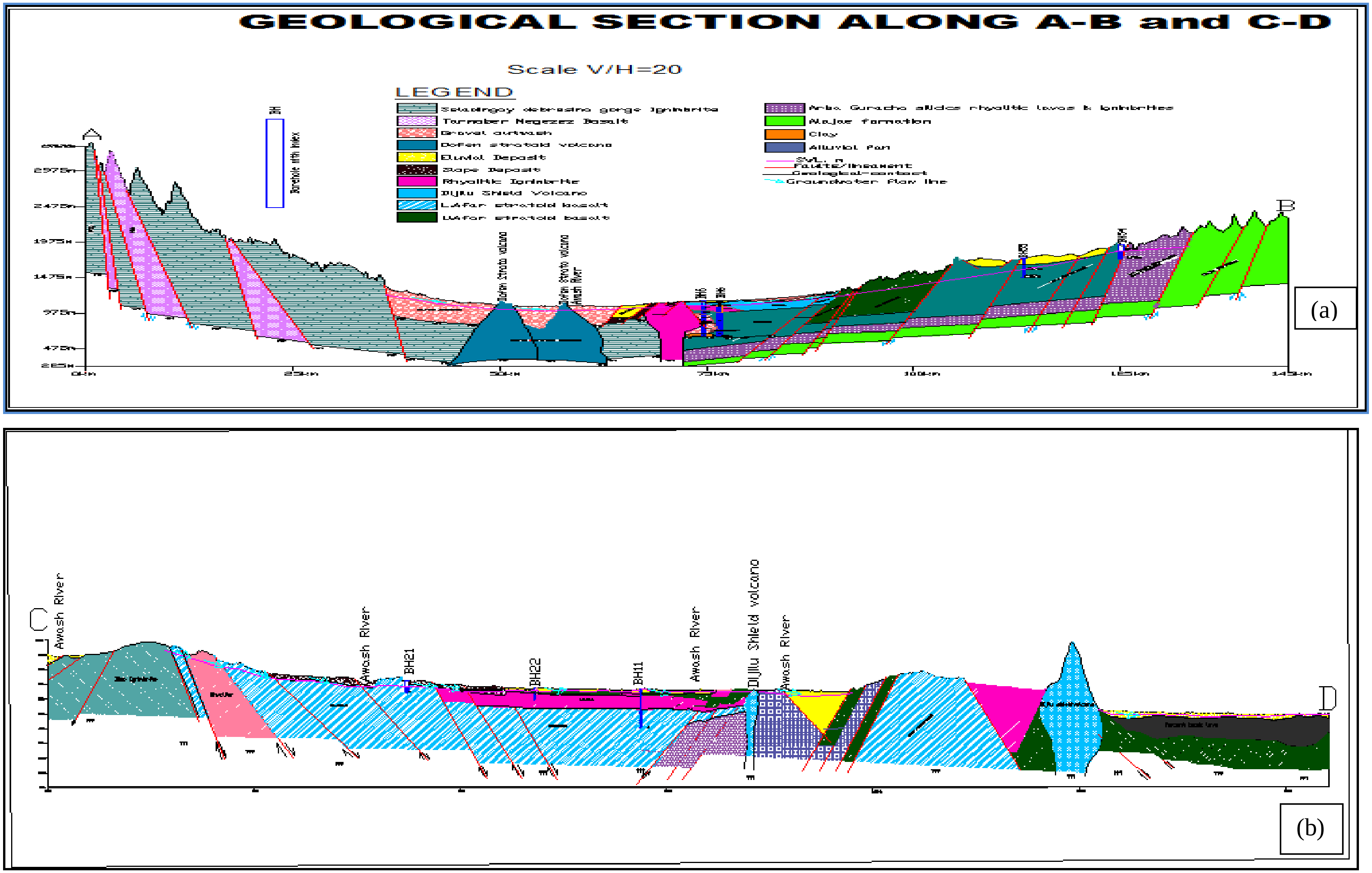

Figure 3 9 Geological Section along (a) A-B and (b) C-D direction respectively

3.5.2. Hydrogeology of Allydegi plain

Hydrogeological setting of the Allydegi plain is summarized based on the review of Allydegi plain ground water resource Assessment project report (WWDSE,2011). Beside this, publications, drilling logs, field observation during drilling supervision of water wells, existing geological and hydrogeological maps. The major hydrogeological findings include:

- The hydrogeological condition of the area is depending on geomorphology, lithology and tectonic structures of the volcanic and alluvial formations of the area.
- Two groundwater-bearing formations (aquifer systems) have been identified. These are highly productive unconsolidated sediment aquifer with inter-granular permeability and Medium to Highly productive volcanic aquifer with fracture permeability.
- The general groundwater flow direction is towards north ward direction. However, local ground water flow direction similar to that of surface water flow direction in the southern and south-eastern volcanic aquifers of the study area.
- The area is characterized by three ground water divides. In the south eastern margin of the plain (Asebot area) which is NNW-SSE trend, directed from Bordede up to Awash Arba village along NW-SE direction and from Melka-sedi village towards in the NNE direction.

3.5.2.1 Aquifer systems

A. Unconsolidated sediment aquifer System

It covers an extensive area in the western Allydegi plain, immediate east and west of the Awash river. They also include lacustrine and river transported units of the Melka-worer and Melka-sedi areas.The lithological log of boreholes drilled in the Awash valley, the quaternary unconsolidated sediments consist of intercalating layers of boulder, gravel, sand, silty sand, silt, silty-clay and clay. The modes of origin of these sediments are elluvium deposits, slope deposits (break down materials of the nearby elevated Ignimbrite horsts), lacustrine and Alluvial.

Clay layers are interbedded throughout the section of the alluvial fill and these fine materials could be water logged due to their low permeability. It is obvious that this unit generally acts as good impervious layer and restricts horizontal and vertical movement of the groundwater. However, since the thicknesses of the coarser sediments are thicker than the impervious clay layers, the impact of the confining clays on the yield of the well is not pronounced.

From geophysical investigations and well logs drilled in the area, the thickness of the sediment aquifer in the western Allydegi ranges from tens of meters to more than 200meters. The most important aquifers which enable good ground water movement so as to yield economical amount of water withdrawal are the coarser materials (mainly sandy & gravely materials) that lay at different levels. The local ground water in this area receives continuous surface water recharge from the surplus water of the irrigation ditch. This is also one of the paramount factors for the area's higher ground water potential.

Hydrogeologically it could be considered that this aquifer decreases in thickness from central western part towards the northern, southern and eastern flank of the valley. The variation in thickness may be attributed either to asymmetry in subsurface elevation of the bedrock or due to variations in rates of erosion and deposition. The static water level ranges from 5m to 13 meters with an average of 8m and yield of the wells ranging from 6 l/sec up to 50 l/se which in turn averages of 17 l/sec. It reveals also higher values of transmissivity which ranges from 119 m^2/day –to- 587 m^2/day and an average of 245 m^2/day. The specific capacity of bore holes varies from 0.59 to 3.5 l/s/m with average value of 1.9 l/s/m.

The water quality is generally fresh and the electrical conductivity (EC) varies from 519-to- 3010µS/cm and total dissolved solids (TDS) from 324 to 1936 mg/l. The high EC and TDS in this formation are mainly due to unprotected hand dug wells which are vulnerable to contamination. Relatively high fluoride concentration of groundwater from boreholes in this aquifer is associated with the disintegration of the parent rocks from which the alluvium derives (WWDSE, 2011).

B. Volcanic aquifer System

This aquifer system outcrops in the Central and in the Southeastern part of Allydegi plain. However, it is also encountered beneath the eastern and southern surficial sediments. The main lithologies under this category are the Afar stratoid basalt, the Ignimbrites, Scoraceous basalt and tuff.

The weathering, fracture and fault openings in this area are one of the major groundwater conduits of the plain. Their significance as recharge zone also varies with local intensity of fracture and joint openings that allow groundwater movement and storage, where the drainage pattern follow these geological structures. In addition Bilen spring (lake) which emerges from the northwestern volcanic rocks also feed the ground water of the area through the permeable fractures.

From the well logs, basalts of this unit are identified by its close association with the ignimbrite and are highly productive aquifer; this may be related to its in-depth fracturing and faulting. In the area, especially the basalts and the ignimbrites are highly jointed, fractured and weathered.

The secondary permeability formed by fracture and joint openings is usually the cause for the significance of the volcanic rock as ground water source. However at places this secondary permeability is filled by clay materials and secondary minerals formed due to chemical Weathering and this could highly reduce the overall permeability of the volcanic rocks in general. This type of reduced permeability is observed in the eastern and southern part of the plain.

Hydrogeological characteristics of this unit can be summarized as the average depth to ground water level of this unit is 79m with minimum 39m and maximum 150m. The yield of the wells ranges from 4 l/sec up to 50 l/sec which average of 12 l/sec. Moreover, they reflect also low to higher values of transmissivity which ranges from 4 m^2/day up to 6030m^2/day of average 580 m^2/day. Specific capacity of bore holes varies from 0.11 to 44.6 l/s/m with average 4.8 l/s/m. In general the water qualities of volcanic rock aquifers reveal relatively lower conductivity, total dissolved solids and fluoride concentration (WWDSE, 2011).

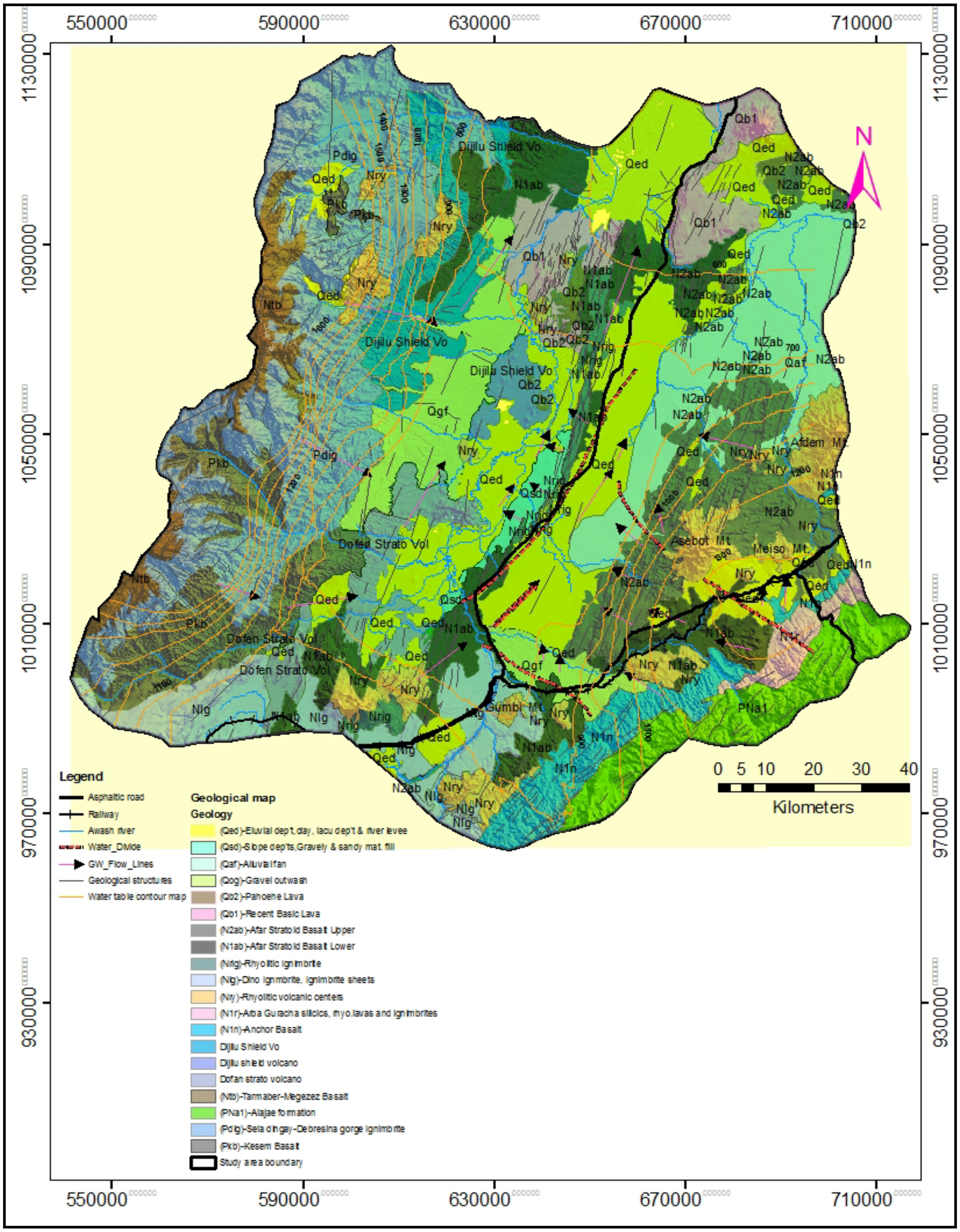

Figure 3.10: Potentiometric map incorporated with geology of the area

(Adopted from WWDSE, 2011)

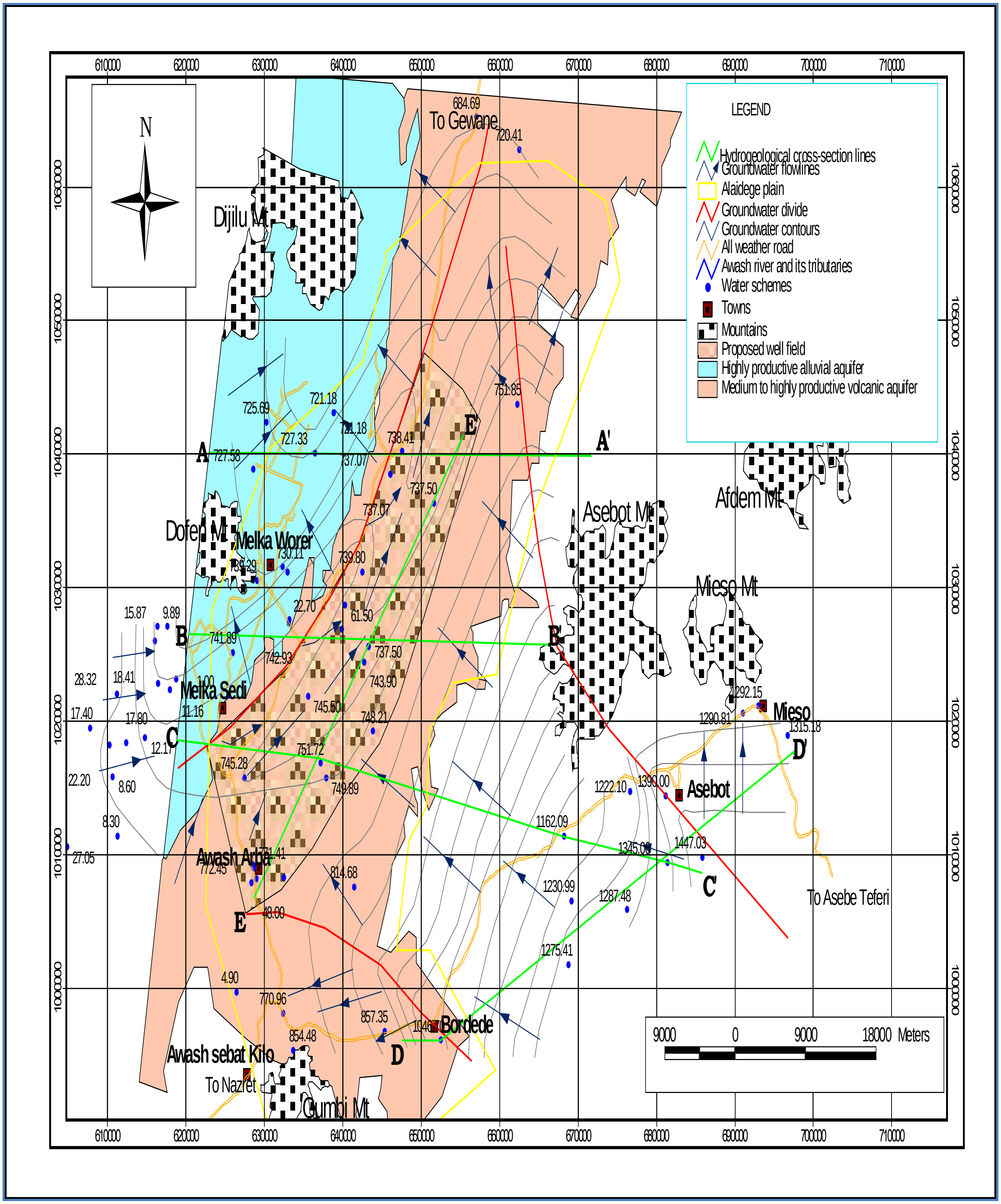

Figure 3.11: Hydrogeological map of Allydegi plain(Adopted from WWDSE,2011)

4. Hydrogeochemistry

4.1 General

Water from oceanic and to a lesser extent from land surface of continents is evaporated, forming clouds that are blown into the continent, where they gradually condense and rain out. On hitting the ground, part of the rain is turned into runoff, flowing back into the ocean, part is returned to the atmosphere by evapotranspiration, and the rest infiltrates and joins groundwater reservoirs, ultimately returning to the ocean as well (Marcel, 2004). The composition of groundwater is the result of net effect of a series of antecedent chemical reactions or processes that have dissolved material from another phase, have altered previously dissolved components, and have eliminated them from solution by precipitation or other processes. The processes to which solutes are taken up or precipitated and the amounts present in solution are controlled by factors, like climate, geological activities, and biochemical effects. Composition of atmospheric precipitation, Sources of solutes in the atmosphere and Anthropogenic activities (Hem, 1985).

Therefore, chemical composition of groundwater and surface water is applied to construct the hydrogeological processes including flow paths and provide information about the recharge system and rate, origin of salinity, mode of groundwater movement and its interaction with the host rocks and the river.

4.2 Data Availability and Quality

4.2.1 Data Availability

After review and collection of existing chemical data of boreholes, springs, river and a lake from different organizations, field work was carried out to fill the data gap. During the field work in-situ measurement of EC, P^H and temperature were made to account the physico-chemical change that could take place together with observation of some major structures of geological and hydrogeological importance. Water samples collection for chemical (twelve) and environmental isotope (twenty one) analysis were carried out from different localities to represent the study area. Water samples were collected and nalyzed for the parameters like, major cations (Na^+, K^+, Ca^{2+} and Mg^{2+}) major Anions (Cl^-, F^-, NO_3^-, CO_3^-, HCO_3^{2-} , SO_4^{2-}) and TDS, EC, pH, total hardness and alkalinity by flame atomic absorption spectrometry and ionic chromatography respectively in MOWE laboratory. Besides, water samples of boreholes during well development and pumping test were collected and analyzed for the above mentioned ions and Awash river at Melka-sedi with five selected representative boreholes in Allydegi plain were monitored for their isotopic behavior since August, 2012 on monthly basis.

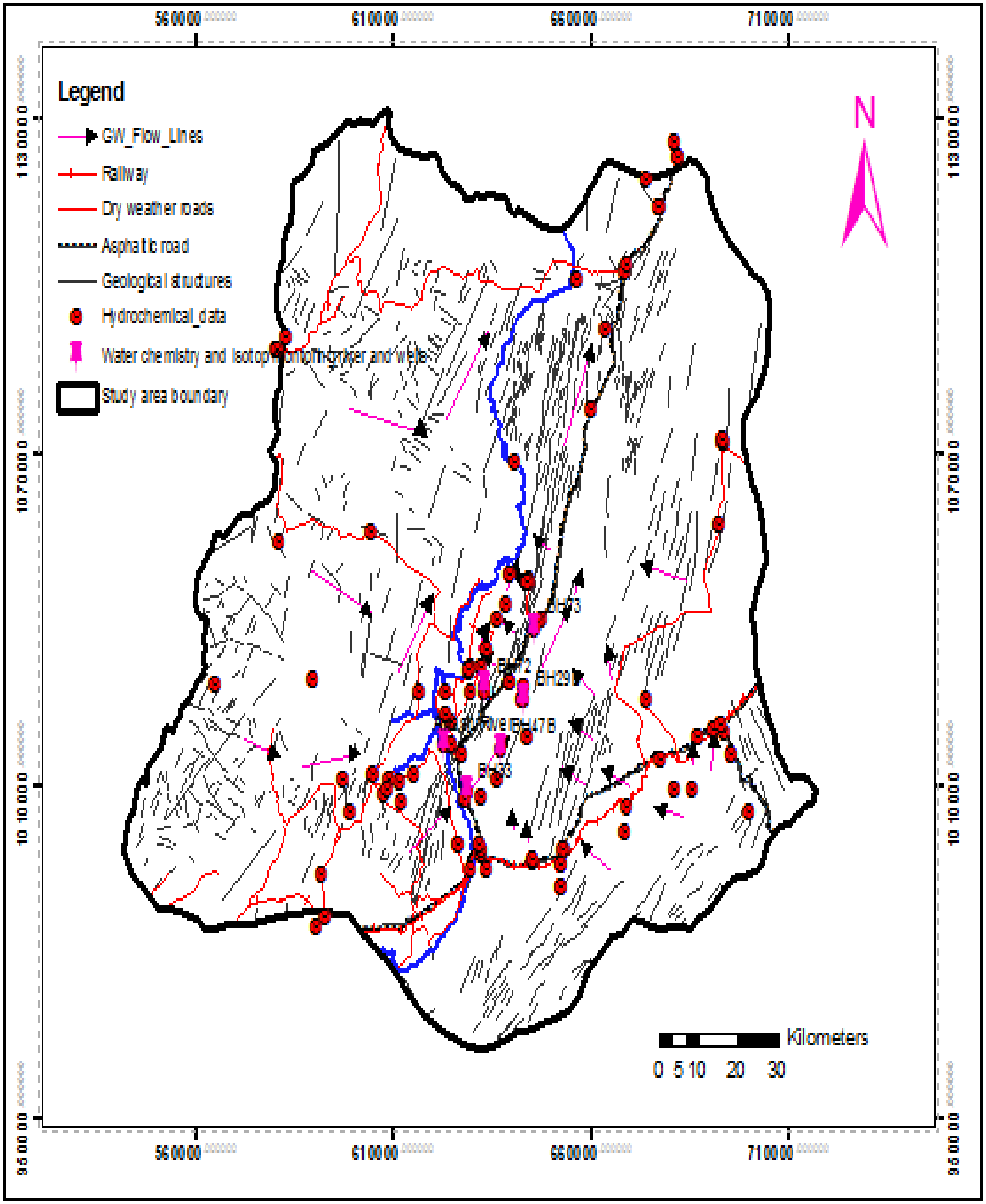

Figure 4.1: Hydrochemical data availability map

4.2.2 Data Quality

The collected Hydrochemical data has to be checked before using for interpretations of hydrochemical studies. All solutions must be electrically neutral. In other words, in a given volume of water sample that has been analyzed for inorganic constituents, the sum of all the cations (meq/l) nearly equal to the sum of all the anions (meq/l). If the analysis reveals the presence of cations and anions in solution, an equation for the electroneutrality condition may be written as:

$$\boxed{\text{Electroneutrality} = \frac{\Sigma\text{Cations} - \Sigma\text{anions}}{\Sigma\text{Cations} + \Sigma\text{anions}} * 100}$$

When the results of a water analysis are plugged into the above equation, it should prove to be close to equality. If the two sides of this equation differ by more than a few percent, either the analysis is erroneous or one or more significant ions were omitted from the analysis. Thus, after charge balance (electroneutrality) calculation, those hydrochemical analysis results with charge balance error less than 5% is regarded as acceptable however, in very dilute or saline water, up to 10% error may be considered as acceptable due to the errors introduced in measuring major ions in dilute groundwater or in the multiple dilution require for analysis of Concentrated groundwater (Fetter, 2001). Thus, the chemical data with charge balance error greater than 10% and those missing any one of the four major cations and anions were discarded. In this study therefore, 95.13% of the data falls in the acceptable 5% criterion and the remaining 4.87% falls in the range of 5-to-10% criterion (Figure 4.2).

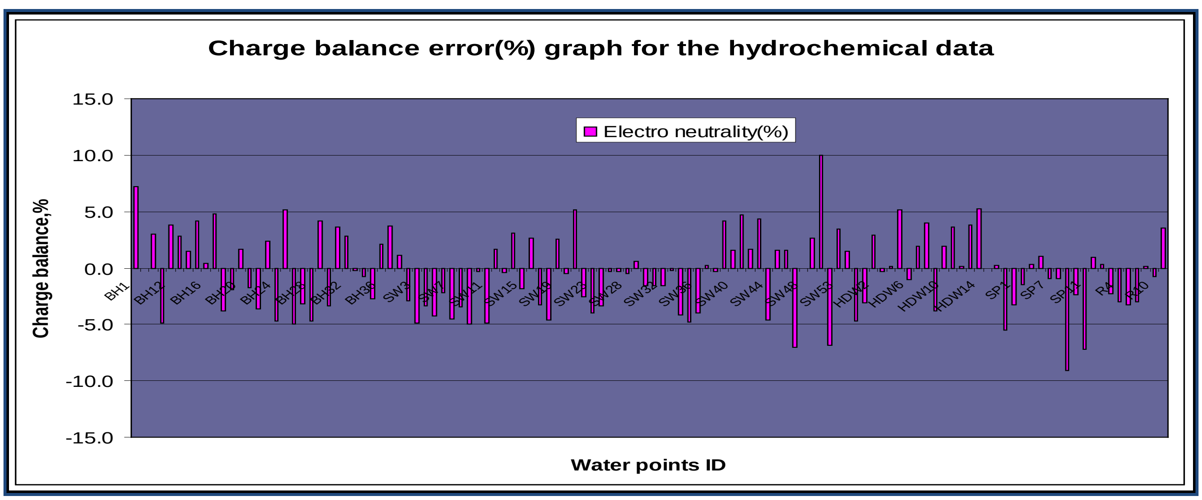

Figure 4.2: Charge balance error graph of hydrochemical data

4.3 Sampling Methods and Physical Parameters

During field work of water sample collection, initially sample bottles wash out three times before taking sample and collected while keeping pumping of the water well. An attempt was made to collect water sample from deep wells from different depths to study the characteristics of aquifers at different depth using groundwater sampler. However, due to the lighter nature of the sampler not to go downwards to the target depth, collection of water sample was carried out at two wells from the static water level only (Figure 4.3).Surface water samples (river, streams and lake) were collected.

Figure 4.3: Photo showing water sample collection from deep well using groundwater sampler

When groundwater removed from its natural environment to the surface temperature, P^H, EC and alkalinity of water undergo changes due to aeration, oxidation and degassing or absorption of atmospheric carbon dioxide (CO_2). This reaction process cause other activities such as, degassing of CO_2 could make precipitation of carbonates and oxidation of some element (Hem, 1989). In order to reduce such problems field water based parameters should preferably be measured immediately since they will changes rapidly after sampling. In this investigation, PH, Temperature, and EC were measured in-situ during field work (Table 4.1).

Table 4.1: Field measured parameters of water

Locality	Source	Water point ID	UTM,E	UTM,N	Elev, masl	Depth, m	SWL ,m	EC, µS/cm	Temp, °.C	P^H
Dudub	Bore hole	BH1	626352	999668	829	100	-	1340	22.8	7.51
Doho	River	R9	618753	1013701	721	0	0	1787	30.5	7.16
Kesem @sabure	River	R6	604977	1012010	767	0	0	616	25.3	7.44
Feres Gubi	Hand dug well	HDW2	605000	1011993	733	10	-	780	28.3	3.31
Marinto	Hand dug well	HDW1	616633	1027149	746	18	11	996	47.2	8.69
Oda Keneneti	Bore hole	BH9	685050	1016620	1285	100	-	997	26.4	7.63
Hugub	Bore hole	BH8	620256	1040033	743	12	10	680	28	7.96
Dulecha	River	R7	604387	1056001	1030	0	0	336	29.4	7.58
Dulecha bahiri	Bore hole	BH2	605661	1055260	1020	105	-	501	29.7	7.42
Awash-7	Awash river	R3	629816	995323	823	0	0	866	22.2	8.27
Awash river @ melka worer	Awash river	R4	629087	1031083	762	0	0	1346	26.3	7.58
Blen	lake(Blen)	L1	644249	1046847	761	0	0	910	42.4	7.8
Blen	Blen spring	SP1	645204	1048781	769	0	0	870	42.7	7.2
Kedadar	Awash river @gewane	R5	656736	1101336	575	0	0	1160	26.4	7.27
Around Gedamitu	Borehole	BH5	657056	1065134	820	282	147.1 5	865	22	7.67
Awash river before beseka lake drains	river	R2	590626	984632	1013	0	0	788	22.6	7.38
Awash river at the starting point	river	R1	417558	988965	2085	0	0	830	25	7.19

4.4 Characteristics of Hydrochemical Variables

The physical characteristics considered in the present study are color, turbidity, temperature, odor, taste, EC and p^H. The water quality analysis result showed that almost all of the water samples analyzed are colorless, odorless, non-turbid and tasteless. The descriptive statistical value of the physico-chemical analysis of the groundwater and surface waters of the area is indicated below.

Table 4.2: Descriptive statistics of hydrochemical data of the area

(Where EC in µS/cm, T in °C and others in mg/l)

	Descriptive Statistics for the entire Hydrochemical data									
Variable	Valid N	Mean	Median	Minimum	Maximum	Variance	Std.Dev.	Coef.Var.	Skewness	Kurtosis
TDS	116	708.54	576.00	54.000	2956.0	218937	467.91	66.04	1.9143	5.048
T	96	32.78	32.40	15.000	50.0	45	6.72	20.49	-0.1599	0.621
PH	114	7.77	7.71	6.800	8.8	0	0.47	6.01	0.3790	-0.542
Na	115	198.05	147.00	1.300	1020.0	35984	189.70	95.78	1.9169	4.179
K	112	11.43	9.70	0.300	69.0	79	8.87	77.64	2.8346	15.325
Ca	114	37.37	27.30	2.520	209.3	1219	34.91	93.42	2.0307	5.563
Mg	114	9.96	8.16	0.400	45.1	67	8.17	82.02	1.3686	2.756
Cl	115	96.00	57.60	0.900	506.2	11474	107.12	111.58	2.1747	4.448
NO3	113	8.21	5.22	0.310	67.5	80	8.96	109.16	3.2593	16.763
F	114	2.46	1.48	0.000	18.0	10	3.11	126.43	2.7466	8.600
HCO3	115	413.40	375.40	48.700	1685.8	51211	226.30	54.74	2.0677	8.449
SO4	113	81.66	57.75	0.900	485.2	7234	85.05	104.15	2.3584	6.740

The discussion of major and important hydrochemical parameters of the groundwater and surface waters of the area are as follows:

PH: The hydrogen-ion activity in an aqueous solution is controlled by interrelated chemical reactions that produce or consume hydrogen ions. It is controlled by the presence of gaseous and dissolved carbondioxide from sources (Bicarbonate and carbonate ions) and its value in between 6.5 and 8.5 is potable based on WHO standards. The study area has a minimum of 6.8 at plateau area and 8.84 at a locality Sabure. Generally it is progressively increases towards northern and north east direction of the study area.

Electrical conductivity: is the degree of salinization of groundwater which is a widely used method for categorizing groundwater. Equally, a measurement of the EC of a solution will also give a relative indication of the amount of dissolved salts. The more salts that are dissolved in the water thus the higher electric conductivity. The relationship of conductivity versus total dissolved solids for all primary and secondary hydrochemical data gave the equation expressed by TDS = 0.647EC (Figure 4.4).

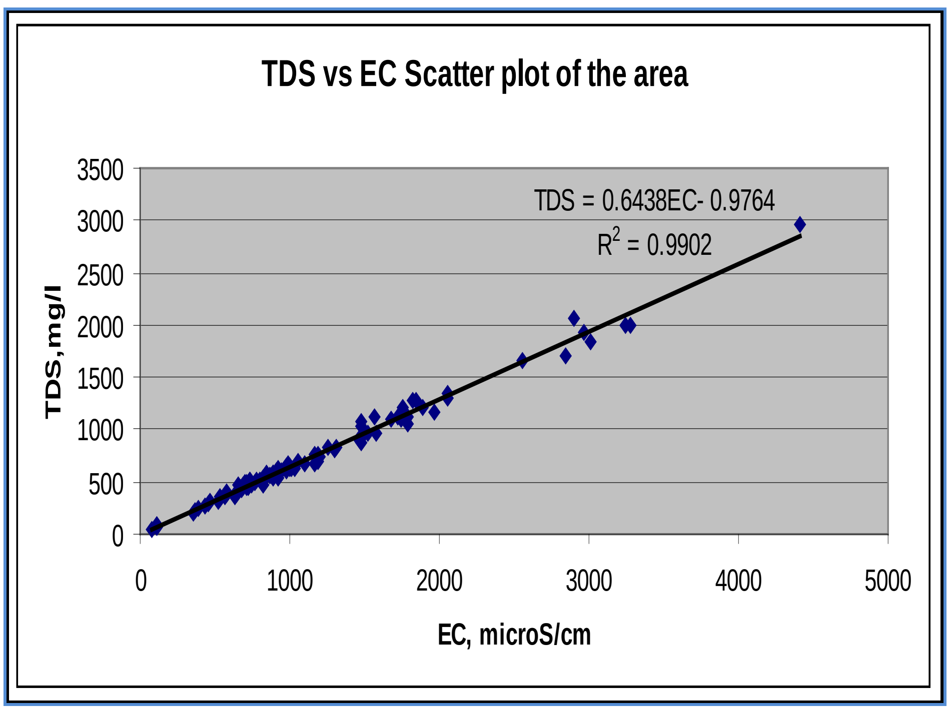

Figure 4.4: TDS as a function of EC plot for the study area hydrochemical data

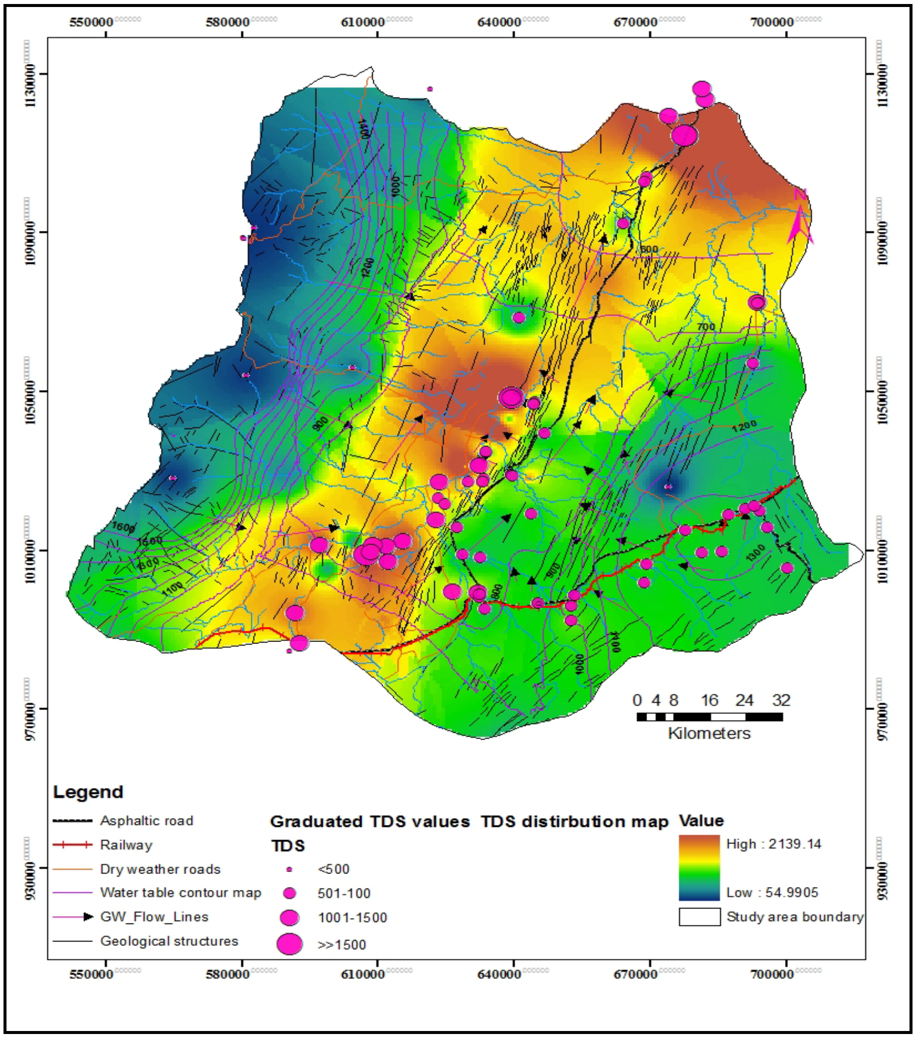

Figure 4. 5: TDS spatial distribution map

The result illustrated from the spatial TDS distribution map and TDS against EC relation created for hydrochemical data plot, TDS increases towards rift floor from the elevated highlands that surround it.

The minimum recorded TDS in the area is 54 (mg/l) and 109 mg/l, which correspond to the spring located around Asebot and Tarmaber of eastern Escarpment and north western plateau respectively. Whereas the maximum record is 2956 (mg/L) measured from a hand dug well drilled in the Awash valley alluvium around melka werer (HDW13) which is located in wonji fault belt (WFB). In general, Ground waters located within the active Wonji fault belt have higher EC (>1500 µS/cm) compared to ground waters circulating outside of this fault belt (EC < 1000µS/cm).

Based on the total dissolved solids classification Freeze and Cherry(1979), Fresh water is the water that contains less than 1000 mg/l of dissolved solids. Generally, out of 123 hydrochemical data, about 94.12 % fall within this range.

Temperature: The Study area is well known by its thermal effect, which is related to the active volcano-tectonic processes. The statistical hydrochemical data(Table 4.4) created for this study shows that the temperature of the groundwater from boreholes and surface waters vary from 23.3^{0}C to 50^{0}C and 15^{0}C to 42.7^{0}C respectively. Ground waters located within Wonji fault belt have relatively higher temperature than at the plateau and escarpments (Figure 4.6). Average groundwater temperature in the study area reaches about 33.1^{0}C. Temperature of the hot spring, Blen spring (SP-4) is the maximum of surface waters (42.7 ^{0}C) and that of well SW12 at Kesem reaches 50^{0}C.

Generally, temperature of groundwater increases down the gradient starting from the north western plateau, south eastern and eastern escarpment towards the lowlands.

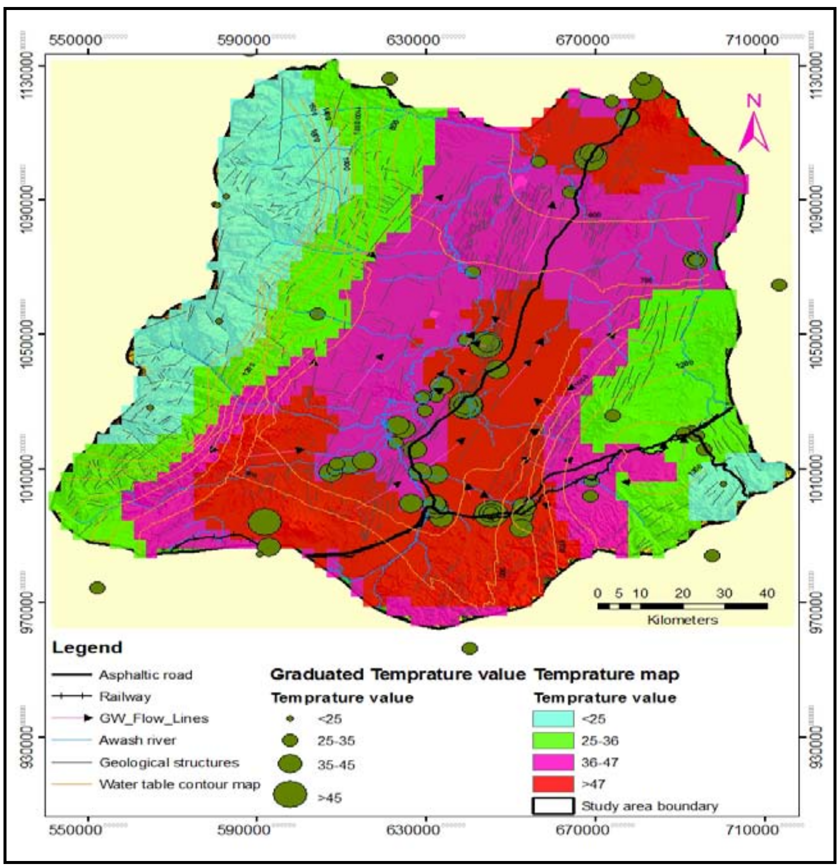

Figure 4.6: In-situ measured temperature spatial distribution map

Fluoride: is the most electronegative of all the elements i.e. it has high tendency to acquire negative charges. Fluoride ions have the same charge and nearly the same radius as hydroxide ions, thus the ions may replace each other in mineral structures (Hem, 1989). It can be found at significant level in a wide variety of volcanic and sedimentary rocks composed of fluoride-bearing minerals such as Fluorite (CaF2), rock phosphate ($Ca_5(PO4)_3(OH,F,Cl)$), cryolite (Na_3AlF_6), apatite (CaF_2), mica (XY_2-$3Z_4O_4(OH,F)_2$ and hornblende ($4Al(Si_7Al)O_{22}(OH,F)_2$ (Handa, 1975; Babulal et al., 2003; Abdelrahman et al.,2009 cited in Wagari, 2010). It is commonly associated with volcanic and geothermal activities, especially those of high pH (Edmunds and Smedley, 1996).

Fluoride concentration in potable water is permissible below 1.5mg/l and 3mg/l according to WHO and MOWE standards however, excessive amount results a number of adverse effect like dental fluorosis and neron impact (WHO, 2004).

The result of multivariate statistical hydrochemical data (Table 4.4) shows that its lower and higher values 0.1mg/l and 18mg/l is found in plateau and in rift floor (lowlands) respectively depending on the presence of fluoride bearing minerals and/or thermal effect.

There are several potential solubility controls that can limit the dissolved-fluoride concentration in water. In solutions that contain sufficient amounts of calcium there may be equilibrium with respect to fluorite (Tenalem, 2007). The total concentration of fluoride in such a solution generally will be somewhat greater owing to ionic strength and complexing effects, but it appears evident that high fluoride concentrations are more likely to occur in water that has a low calcium concentration (Hoefs, 2009).

Generally, the result (Figure 4.7) indicates that the concentration of fluoride ion increases significantly from highlands towards rift floor. Besides that the higher fluoride concentration is associated with thermal groundwaters and non-Ca-water types (Na-HCO_3, Na-HCO_3-Cl and Na-HCO_3-SO_4) of higher P^H.

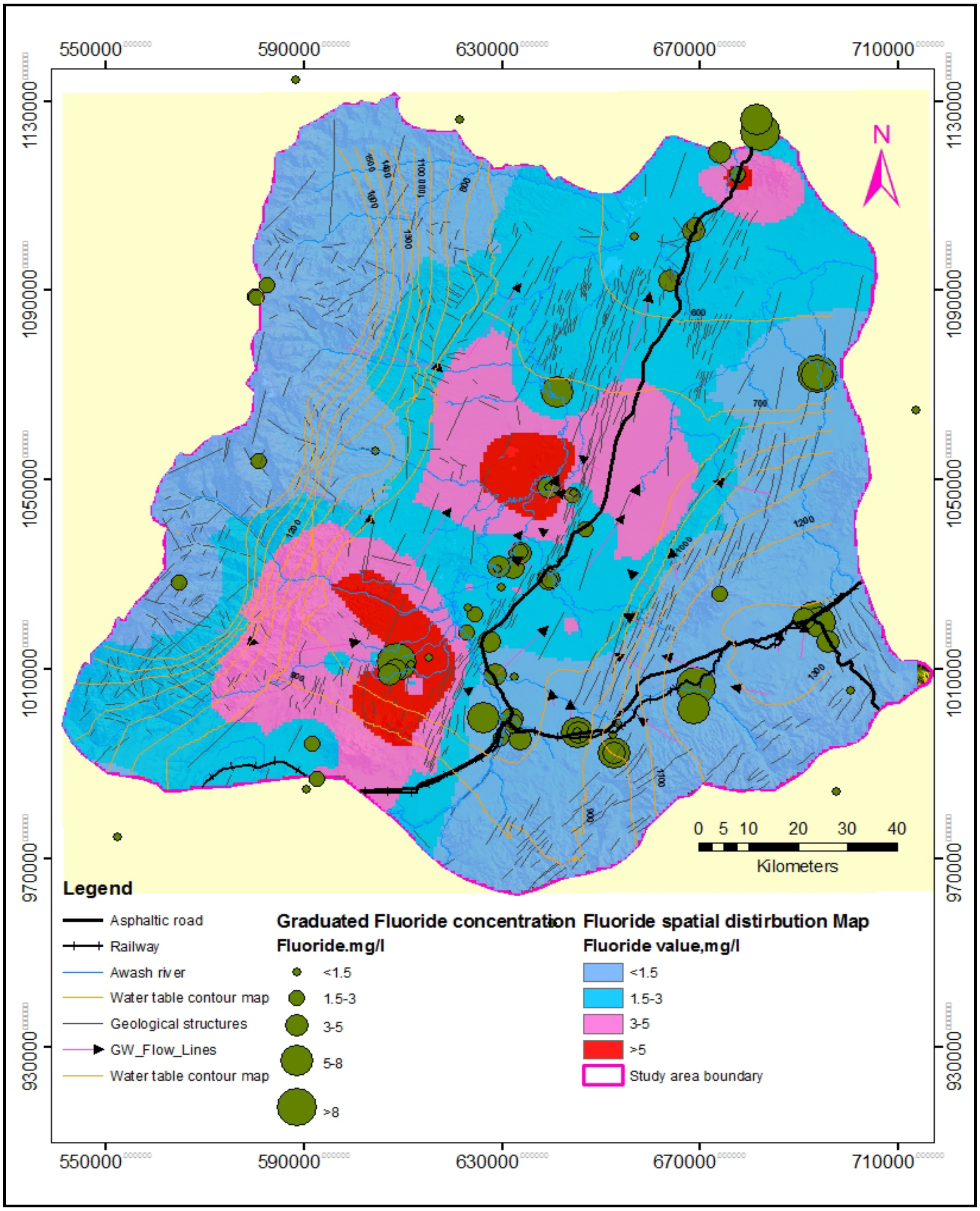

Figure 4.7: Fluoride spatial distribution map

Calcium and Sodium: The spatial distribution of major cations (Ca^{2+} and Na^{+}) concentration in the study area is inversely related (Figure 4.8 (a) and (b)). The maximum amount of Calcium and sodium is 209mg/l in highly elevated area and 1020 mg/l in lowlands respectively (Table 4.2). As one goes from the elevated high areas which bound the lowlands (rift floor), concentration of Ca^{2+} decreases, whereas concentration of Na+ progressively increases. Decreasing trend in Ca^{2+} concentration is associated with the contact between Acidic volcanic rocks with water. It is evidenced by hydrochemical data collected from boreholes and springs from topographically elevated areas of basic volcanic rocks (BH35,BH36,BH37,SP7,SP9,SP11 and SP12)which have high concentration rather than wells drilled in Awash valley alluvial aquifer and acidic volcanic rocks located in Allydegi plain (BH15,BH18,BH19).

In general, the concentration of alkaline metals, Na^{+} and K^{+} increases along Awash River course and the main geologic structure called WFB in the area, which is the result of cation exchange reaction or formation of aluminium silicate minerals along the groundwater flow path.

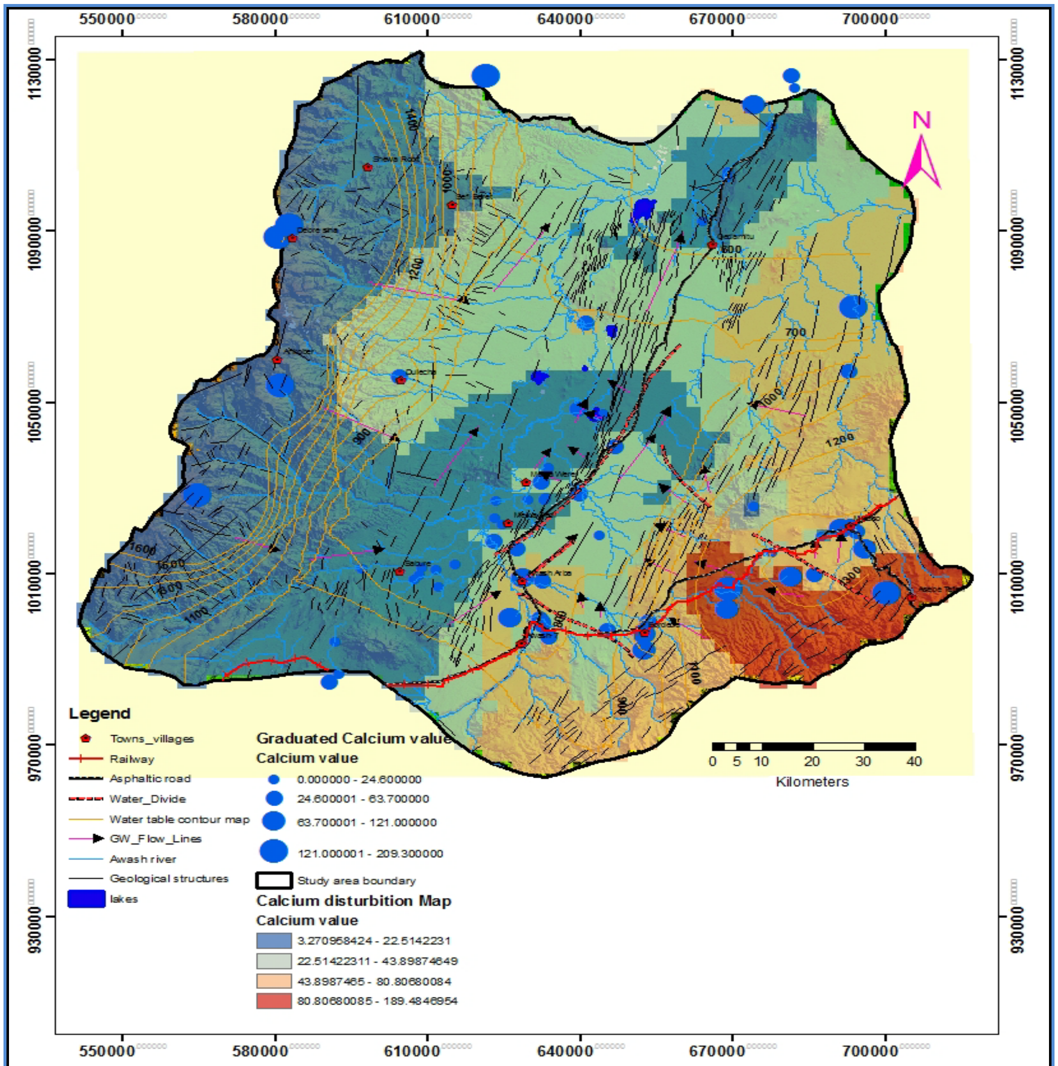

(a)

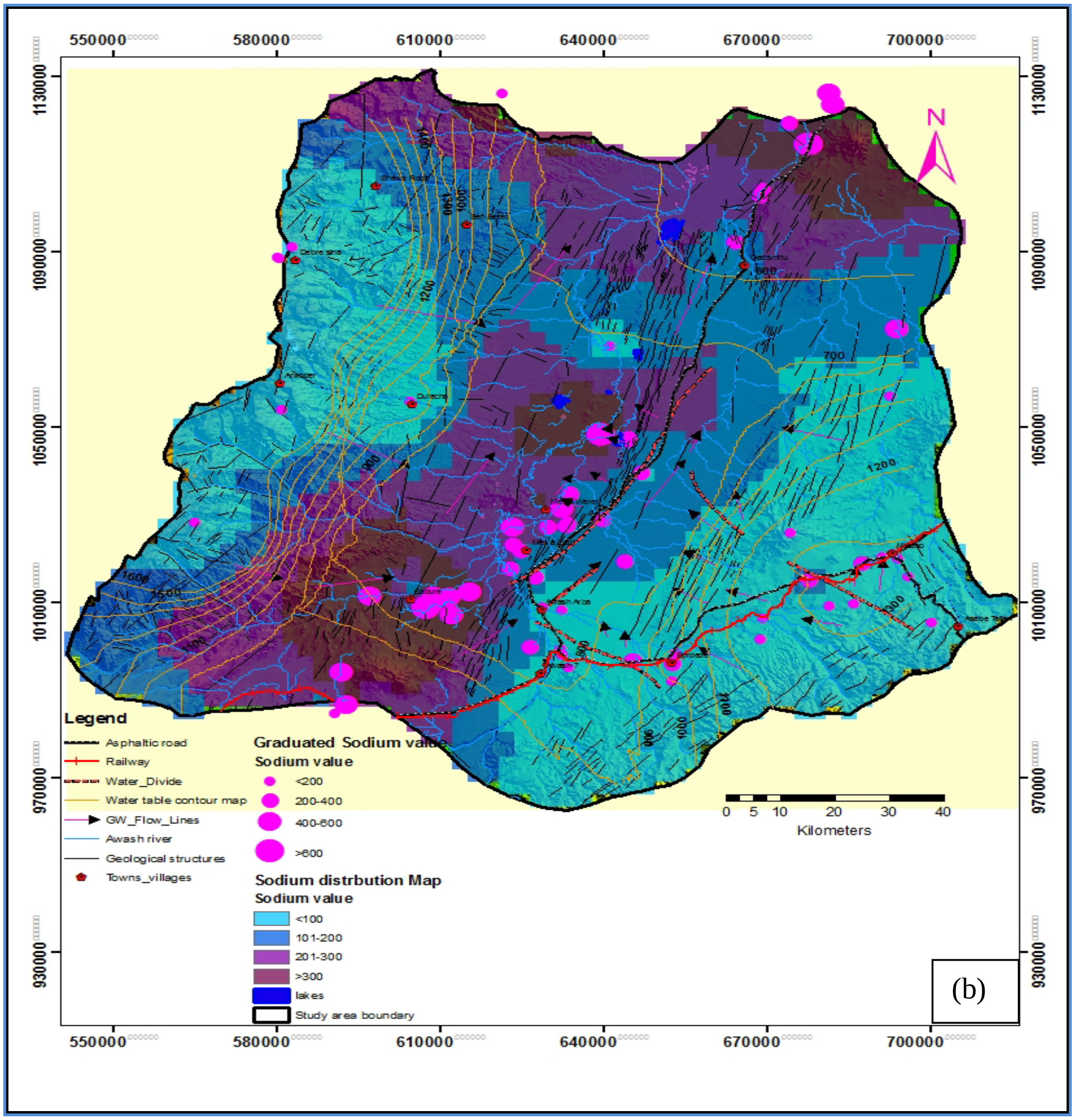

Figure 4.8: Major Cations (a) -Ca^{2+} and (b)-Na^{+} spatial distribution map

Bicarbonate, Chloride and Sulphate: The result of hydrochemical data shows that in highlands and escarpments of the study area HCO_3^- is dominant over chloride and sulphate ions. However, as one goes towards the northern and north eastern parts of the study area its dominance decreasd and increase in Cl^- and SO_4^{2-} ions exists with local anomalies exists. The result of hydrochemical data depicts that hot water schemes have relatively higher bicarbonate ion than cold water schemes which could be due to hydrolysis reaction facilitated by CO_2 consumption from deeper source.

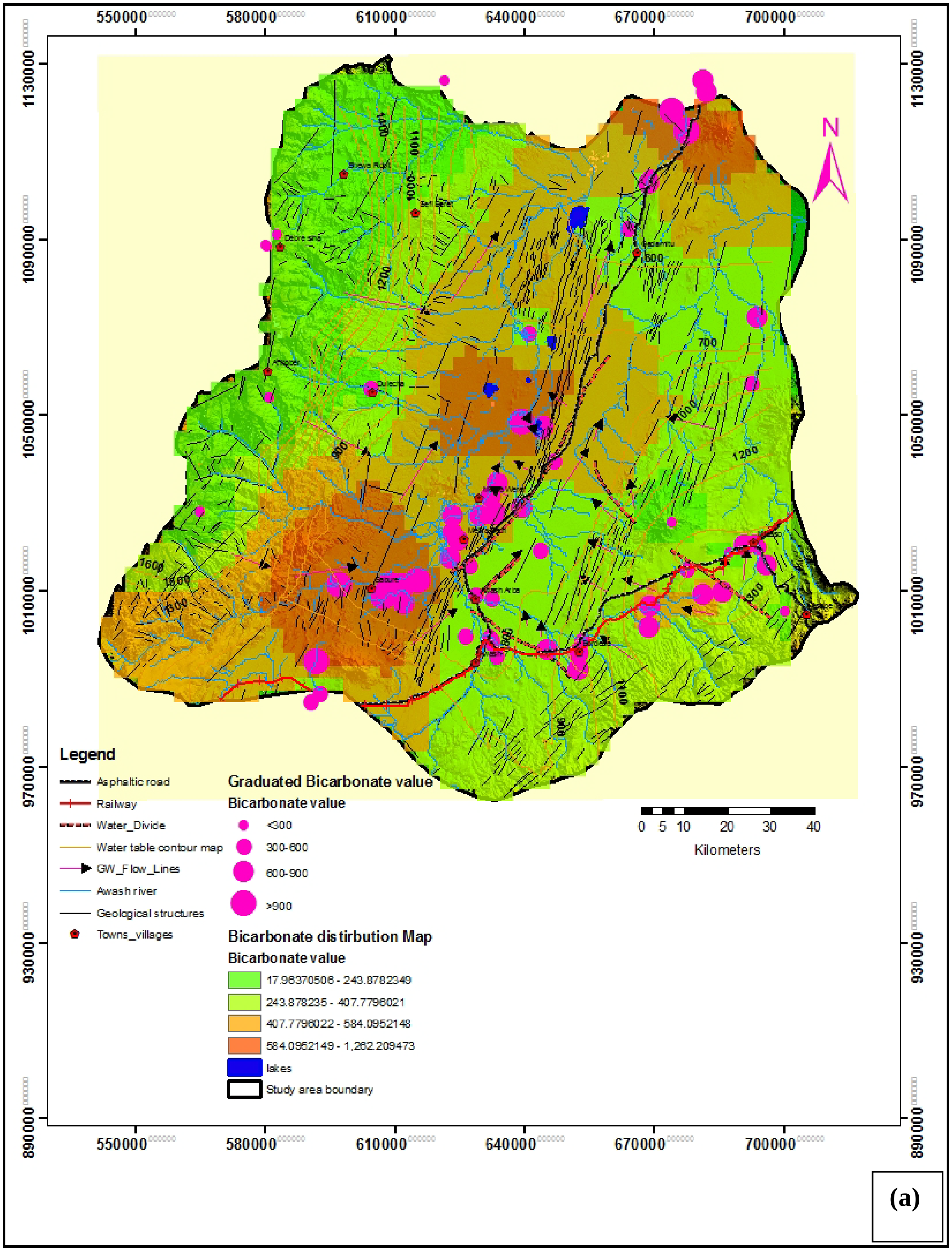
550000
580000
610000
640000
670000
700000
1130000
1090000
1050000
1010000
970000
930000
890000
N
Legend
Asphaltic road
Railway
Water_Divide
Water table contour map
GW_Flow_Lines
Awash river
Geological structures
Towns_villages
Graduated Bicarbonate value
Bicarbonate value
<300
300-600
600-900
>900
Bicarbonate distribution Map
Bicarbonate value
17.96370506 - 243.8782349
243.878235 - 407.7796021
407.7796022 - 584.0952148
584.0952149 - 1,262.209473
lakes
Study area boundary
0 5 10 20 30 40
Kilometers

(a)

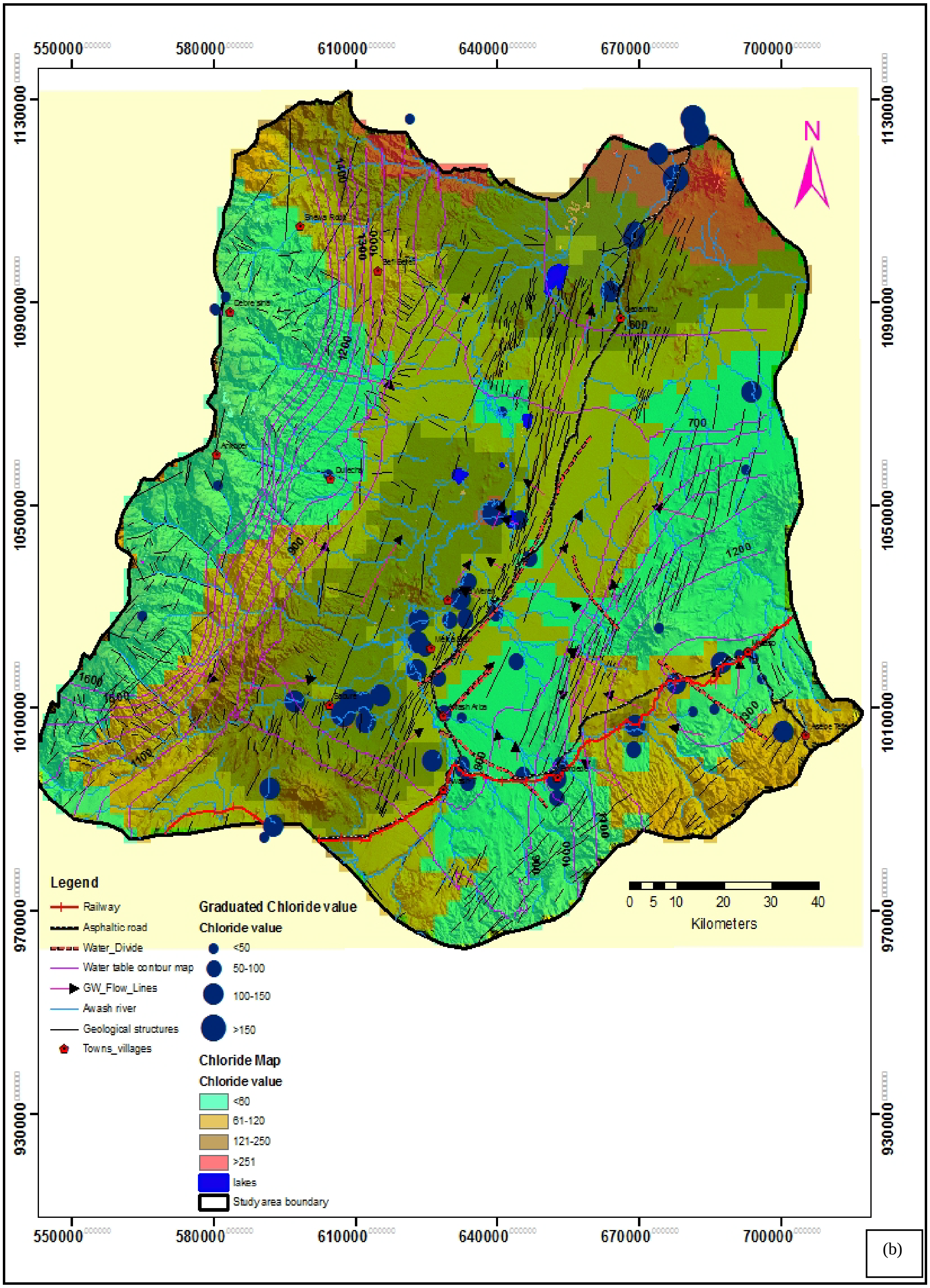
550000
580000
610000
640000
670000
700000
1130000
1090000
1050000
1010000
970000
930000
N
0 5 10 20 30 40
Kilometers
Legend
Railway
Asphaltic road
Water_Divide
Water table contour map
GW_Flow_Lines
Awash river
Geological structures
Towns_villages
Graduated Chloride value
Chloride value
<50
50-100
100-150
>150
Chloride Map
Chloride value
<60
61-120
121-250
>251
lakes
Study area boundary

(b)

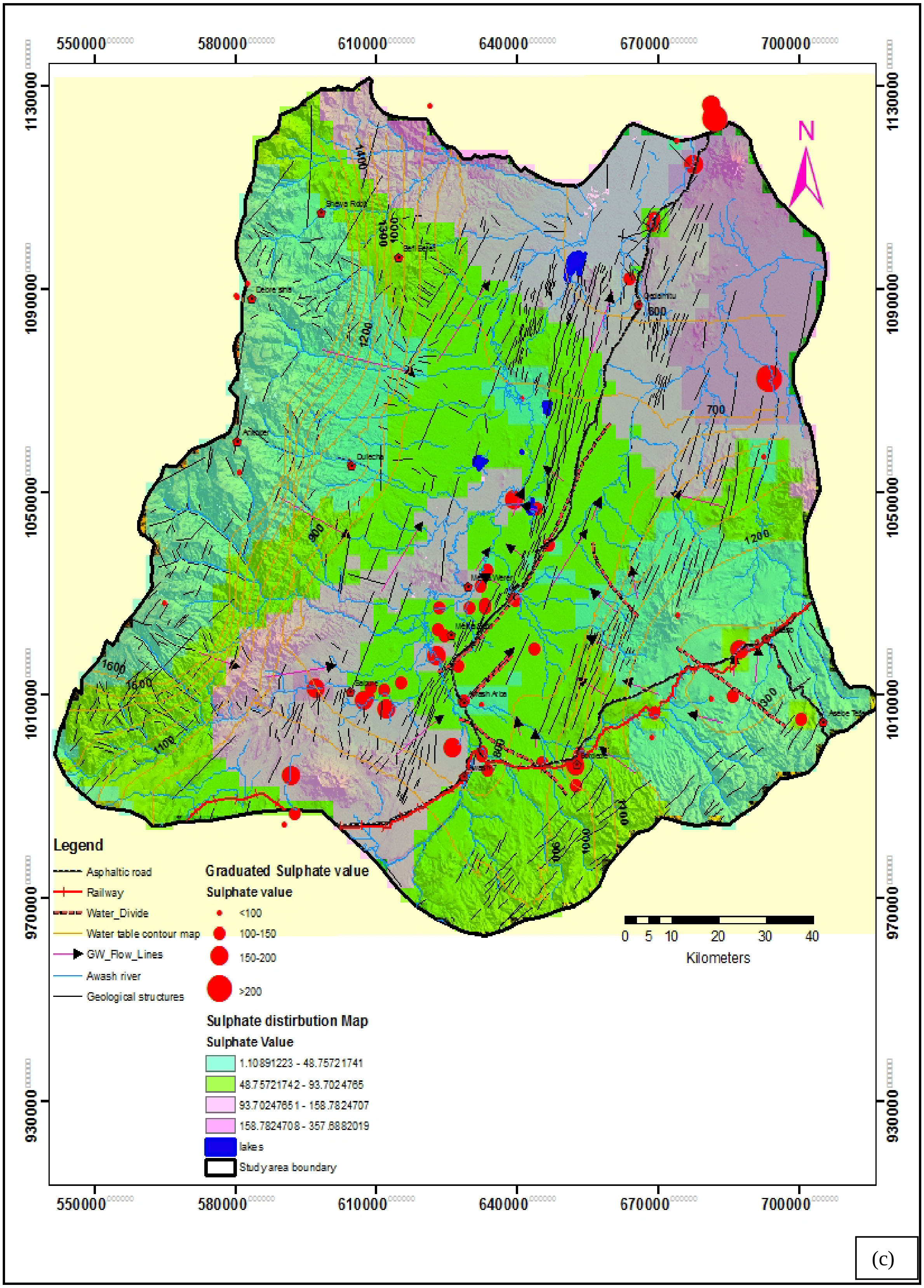

Figure 4. 9: Major Anions (a) –Bicarbonate, (b)-Chloride and (c)-Sulphate Spatial distribution map of the study area

Figure 4.9 (a), (b) and (c) illustrate that SO_4^{2-} and Cl^- concentration increases from surrounding highlands through Allydegi plain towards northern direction with local anomalies associated with active thermal fields along WFB. Higher $SO4^{2-}$ is mainly concentrated on alluvial aquifer of awash valley resulted from dissolution of salts from sediment deposits and increase in Cl^- amount linked with dissolution of basic volcanic rock like Sylvite (KCl) and Halite(NaCl) found in alluvial aquifers with in the soil matrix due to the evaporative enrichment prior to recharge.

In general, the variation in ionic concentration and kind in the study area could be the result of existing type of lithology, the time span for rock-water interaction, high evaporation rate and thermal effect.

4.5 Residual Alkalinity and Major cations ratio

Residual Alkalinity (RA=$[HCO_3^-]-[Ca^{2+}+Mg^{2+}]$ in meq/l) which increases gradually with increasing TDS (Figure 4.10) along the groundwater flow path in the area helps to identify recharge and discharge areas and inflow of meteoric waters in to the aquifer system (Fetter,1994). The increase in residual alkalinity and decrease in the ratio of divalent cations to univalent cations((Ca+Mg)/(Na+K)) is possibly due to the long residence time of rock-water interaction for removal of divalent cations (Ca^{2+}andMg^{2+}) through precipitation reaction and cation exchange along the groundwater flow direction.

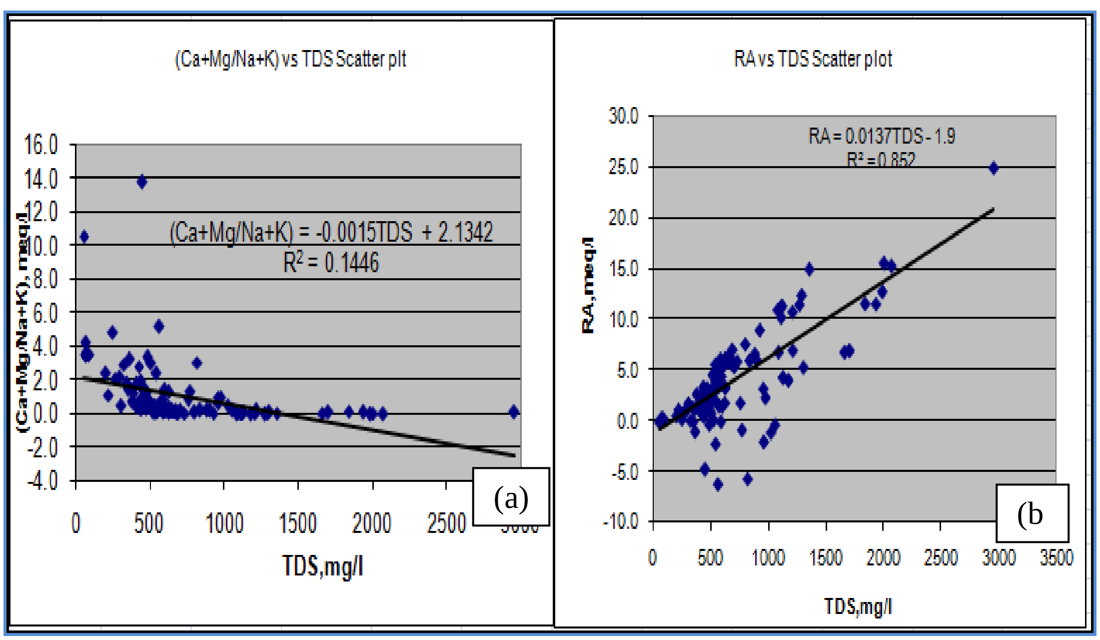

Figure 4.10: (a)-TDS against the ratio of divalent cation to univalent cation and (b) -TDS Against Residual Alkalinity (RA)

Except the local variation of divalent to univalent (Ca^{2+}+$Mg^{2+/}$$Na^{+}$+$K^{+}$) cations ratio with respect to the local variation in geology(lithology), the general trend of divalent to univalent cations ratio shows a decreasing tendency towards the rift floor from the surrounding elevated areas.

In general, the ratio of (Ca^{2+}+Mg^{2+}) to (Na^{+}+K^{+}) and RA are in good agreement with the conventional hydrogeology, groundwater head distribution and groundwater evolution trend to show the study area ground water is recharged from the north western, southern and south eastern plateau through Allydegi plain towards the northern direction.

4.6 Hydrochemical Facies

The diagnostic chemical character of water solutions in hydrogeologic system has been determined with the application of the concept of hydrochemical facies, which enables a convenient subdivision of water compositions by identifiable categories and reflects the effect of chemical processes occurring between the minerals within the subsurface rock units and the groundwater (Hiscock,2005).Statistical distribution diagrams such as Piper (trilinear) diagram is used to gain better insight into the hydrochemical processes operating in the groundwater system.

In the study area, the hydrochemical character of the groundwater is the integrated result of mineralogy, thermal condition, evaporation rate and the residence time. Thus, most of the groundwater in the area is characterized by different water facies. An important task in groundwater investigation is the compilation and presentation of chemical data in a convenient approach for visualization. For this purpose Piper (Trilinear) plot was used to study clustering of chemical data. Based on this four major water types were identified. These are:

- Ca-Mg-HCO_3 or Ca-Na-HCO_3
- Na-Ca-HCO_3
- Na-HCO_3 and
- Na-HCO_3-Cl or Na-HCO_3-SO_4 water types.

According to chebotarev (1955), as groundwater moves along its flow path, increase of dissolved solids and most of major ions normally occur. Ground water tends to evolve chemically towards the composition of sea water; this evolution is normally accompanied by the following regional change in dominant anion species.

$\longrightarrow$ Travel along flow path

$HCO_3^- \longrightarrow HCO_3^- + SO_4^{2-} \longrightarrow SO_4^{2-} + HCO_3^- \longrightarrow SO_4^{2-} + Cl^- \longrightarrow Cl^- + SO4_2^- \longrightarrow Cl^-$

$\longrightarrow$ Increasing age

These changes occur as the water moves from shallow zone of active flushing through intermediate zones in to zones where the flow is very slow and the water is old (Freez and cherry,1979).

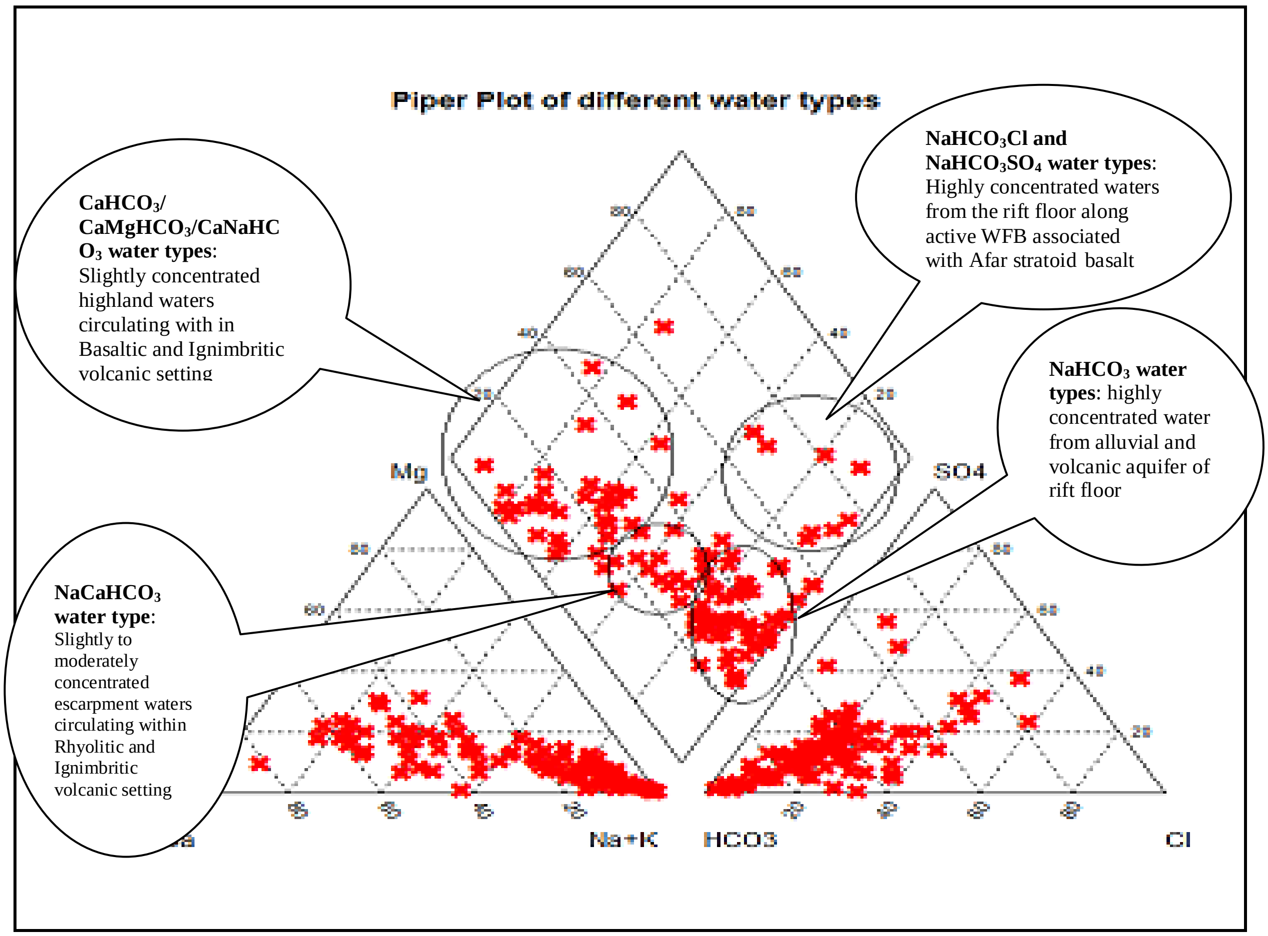

Figure 4.11: Piper plot for hydrochemical data

Water groups of Ca-Mg-HCO_3 or Ca-Na-HCO_3 with dominant in Calcium and bicarbonate ions located in the highland areas surrounding the rift floor of the study area. Most of them circulated through fractured basalt, ignimbrite, Rhyolite and trachyte and are characterized by low TDS value below 600 mg/l. As mentioned above in the general ground water chemical evolution model, these types of waters are considered as recharge area waters at their early stage of geochemical evolution.

Na-Ca-HCO_3 water type is obtained in between Bordede and Allydegi plain of volcanic aquifer. It drains in acidic rocks in the escarpment such as Ignimbrite, Tuff, rhyolite and trachyte characterized by a TDS in the range of 600-to-800mg/l. Water sample analysis result from test wells (BH14 and BH16) drilled in Allydegi plain with a depth of 300m with a succession of Ignimbrite and thick Scoracious basalt gives water of this type.

Hydrochemical facies of Na-HCO_3 types of waters in the study area are located in the vicinity of active thermal fields of central rift floor, which are evolved from highlands and escarpments Ca-Na (Mg)-HCO_3 and Na-Ca (Mg)-HCO_3 water types. As it is from active thermal field area where the water samples obtained, most of them have high fluoride concentration above the permissible WHO standard. Blen spring, the hottest spring (42.9 ^{o}c) but relatively less concentration emanating from the afar stratoid basalt is under this category. The water types rich in bicarbonate with increasing sodium and potassium concentrations is in the process of moving rather than Ca^{2+}, Mg^{2+}, Na^{+}, Cl^{-} and $SO4^{2-}$ as stagnant and is actively being mixed (Adam, 2001). Generally, it is associated with alluvial aquifer of Awash valley and deep volcanic rocks.

The fourth types of water named Na-HCO3-Cl or Na-HCO3-SO4 type is located along the Wonji Fault belt (WFB) and at the northern sector of the study area. It is spatially distributed in alluvial aquifer of Awash valley along its flow direction towards Gewane in the study area. These are highly concentrated with a TDS and temperature of more than 1000mg/l and 35^{o}c respectively. As the concentration of sodium, chloride and/or Sulphate values of the water increase, it is stagnant and relatively old (Adam, 2001).

In general, groundwater system in the area evolves from Ca-Mg-HCO_3 type to Na-HCO_3-Cl or Na-HCO_3-SO_4 water types, with progressive increasing of Residual Alkalinity and TDS but (Ca^{2+} +Mg^{2+}) to (Na^{+}+K^{+}) ratio decreases .

4.7 Hierarchal Cluster Analysis (HCA)

Hierarchal Cluster Analysis is a statistical algorithm that put observed data into meaningful structures in their hierarchical order (Davis, 1986). The idea is to join together hydrochemical data of different water points in the study area together using some measure of similarity or distance. The classification of samples according to their parameters is termed Q-mode classification. The linkage rule used here is Ward's method (Ward, 1963). Linkage rules iteratively link nearby points (samples) by using the similarity matrix. It is generally known that a large amount of groundwater chemistry data can be understand by simplifying the complex and diverse relationships that exist among a set of observed parameters using some multivariate analyses (Sukand Lee, 1999). The result is explained by hierarchal tree to represent hydrochemical facies and used to assess the geochemical factors associated with each cluster.

Twelve variables (TDS,PH,Na^+, K^+, Ca^{2+}, Mg^{2+},Cl^-,$HCO3^-$, $SO4^{2-}$, $NO3^-$ and F^-) of 86 (Eighty six) water samples were used in HCA presented as a dendrogram in (Figure 4.13). Based on the result of the dendrogram, six major groups (Clusters) were selected.

Table 4.3: Mean value of Hydrochemical variables for Clusters
(RA in meq/l, PH dimensionless and the rest in mg/l)

Hydrochemical variables	Cluster-I	Cluster-II	Cluster-III	Cluster-IV	Cluster-V	Cluster-VI
TDS	414.9	621.0	1171.4	962.5	2000.0	2956.0
PH	7.5	8.0	8.3	7.8	8.3	7.8
Na^+	72.5	177.0	405.1	257.2	765.0	1020.0
K^+	9.1	11.0	14.5	12.0	15.0	6.1
Ca^{2+}	58.0	24.5	19.4	44.8	14.2	30.0
Mg^{2+}	13.1	8.9	6.5	10.1	6.0	14.8
Cl^-	36.3	73.8	154.6	144.8	402.1	425.3
$NO3^-$	8.1	8.7	7.6	12.3	7.1	8.5
F^-	0.9	2.6	6.7	2.1	7.9	18.0
HCO_3^-	324.5	405.3	725.0	405.5	915.1	1685.8
SO_4^{2-}	37.7	62.8	85.7	173.0	242.2	143.0
RA	1.3	4.7	10.4	3.6	13.8	24.9
(Ca+Mg)/(Na+K)	0.87	0.18	0.06	0.20	0.03	0.04

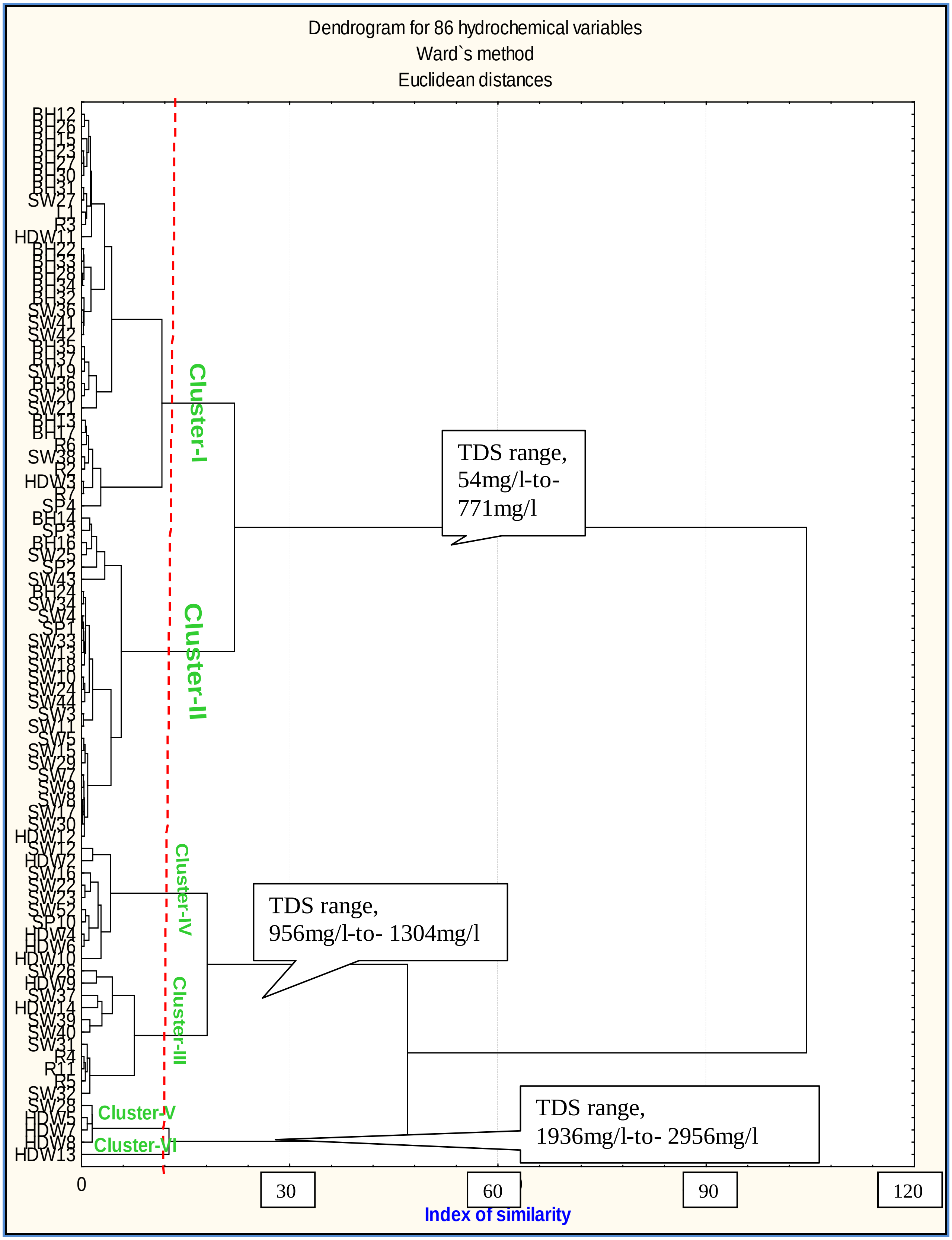

Figure 4.12: Dendrogram of the hydrochemical data

The clusters in the dendogram are ordered from top to bottom in increasing order of TDS, ionic concentration and Residual alkalinity from Cluster I to Cluster VI.

Cluster-I

This cluster include thirty water points hydrochemical data which have low TDS value on average less than 415mg/l located at topographically higher areas (Debresina, Ankober and Asebot) which bound the lowlands (rift floor). These areas have higher rainfall amount (Annex-I) implies high hydraulic gradient and fast flow system. The water in this group drains Basic and acidic volcanic rocks like Tarmaber-megezez and kesem sub-alkaline basalt, Seladingay-Debrebrhan-Gorgo Ignimbrite, rhyolitic domes and trachyte. It is characterized by very weak alkalinity with average P^H of 7.5 and relatively low TDS associated with fast circulation. Ca^{2+} and HCO_3^- are the dominant ions which correspond with $CaHCO_3$, $CaNaHCO_3$ and $CaMgHCO_3$ water types. Thus, this group shows the initial stage of chemical evolution (recent recharge) and they represent the recharge area for the groundwater system in the area.

Cluster-II

Twenty six water samples in this group are concentrated in transition zone along local fault zones. Few relatively deeper wells drilled in south eastern Allydegi plain with aquifer of fractured basalt and scoracious basalt belong to this group. The salinity character is marked by moderately diluted water with an average TDS of 621mg/l. In comparison with group-I water samples; each hydrochemical variables concentration increased which shows the rock-water interaction is on the way for chemical hydrolysis that adds chemical concentration to water. Ca^{2+} and HCO_3^- are slightly decreased while Na^+, K^+, Cl^- and SO_4^{2-} concentration are increased corresponds to a water type $NaCaHCO_3$. In general, the water samples belong to this cluster joined with low linkage distance to cluster-I describe both groups drain the same geological formation, source and hydrochemical character. Therefore, it represents early stage chemical evolution next to cluster-I and it may be due to the active flashing of meteoric water to the aquifer system from the highland area through local faults.

Cluster –III and Cluster IV

Cluster three and four include twenty one water points of nearly similar hydrochemical character but are moderately to highly concentrate with an average TDS of 1171mg/l and 962.5 mg/l respectively. It includes chemical data located in Afar stratoid lower basaltic rock and Awash Alluvial plain along local faults and highly permeable formation. Blen hot spring belongs to this group characterized by thermal nature due to its location at the foot of wonji fault belt (WFB). The occurrence of Ca^{2+}, Cl^- and SO_4^{2-} ions in this cluster reveals the higher rock-water interaction and hydrolysis reaction. This group is dominated by a $NaHCO_3$ hydrochemical facies with few $NaHCO_3SO_4$ types.

Cluster -V and Cluster-VI

Cluster five and six are generally similar with a very high TDS of an average being 2000mg/l and 2956mg/l respectively. These groups are characterized by high thermal property and high concentration of $HCO3^-$, Cl^-, SO_4^{-2}, Na^+ and F^- ions. Most of them are located around wonji fault belt, local faults and northern part of the study area. High Fluoride concentration up to 18mg/l in rift floor found associated with thermal waters and some of them found near acidic volcanic centers to the CO_2 input from the deeper source affect the water chemistry (Seifu et al., 2007). All of the group members situated within the valley following the Awash river cource leading to slow groundwater velocity and long residence time. As a result, they have salinity (TDS> 2000mg/l) and alkaline waters with pH more than 7.8. The water points location from which water sample collected is alluvial deposits of shallow depth gives Na^+ and HCO_3^- are the major ions with subordinate Cl^- and SO_4^{2-} concentration leads to a $Na\text{-}HCO_3\text{-}Cl$ or $Na\text{-}HCO_3\text{-}SO_4$ water type. However, Ca^{2+}, and Mg^{2+} are detected only in two water samples gives clue towards the precipitation of the divalent cations along the groundwater flow direction.

Thus, cluster five and six are represented by $Na\text{-}Cl\text{-}SO_4$ and/or $Na\text{-}HCO_3\text{-}Cl$ water types respectively and these groups show the final stage of chemical evolution in the study area which represents the discharge area of the groundwater system.

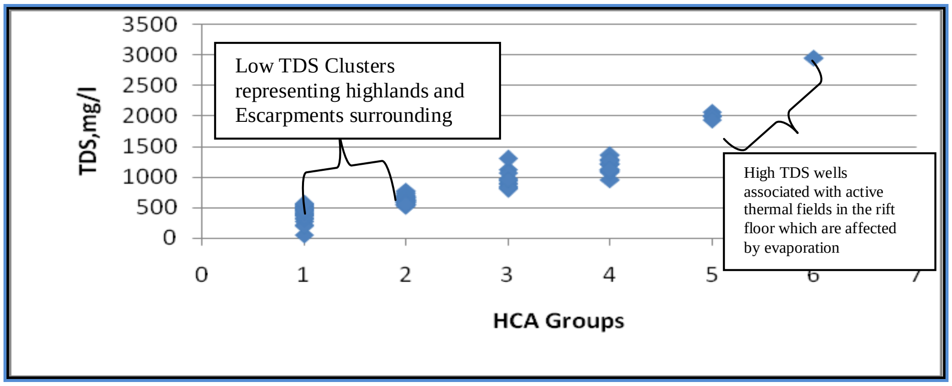

Figure 4.13: TDS against HCA clusters of hydrochemical data.

4.8 Correlation matrices

The relationship between hydrochemical variables has been analyzed using a statistical correlation matrix. Table 4.4 describes that TDS, Na^+ and HCO_3^- are positively and highly correlated with each other whereas weekly correlated with $Cl^-$and SO_4^{2-}. This shows that they are gradually increasing along the groundwater flow direction. It is evidence that an increase in such variables leads enrichment of salinity of water. Aside this Ca^{2+} and Mg^{2+} are negatively correlated with Na^+, K^+, Cl^-, PH and SO_4^{2-} which indicates along the groundwater flow direction removal of such variables facilitated through precipitation. The weak correlation of HCO_3^- with Cl^- and SO_4^{2-} implies Cl^- and SO_4^{2-} evolution in the northern direction along the active thermal fields.

Table 4.4: Correlation matrices of Hydrochemical parameters
(In mg/l, except PH) in the study area, at significant level of $p < .05$)
Number of water points=111

Parametrs	TDS	PH	Na^+	K^+	Ca^{2+}	Mg^{2+}	Cl^-	NO_3^-	F^-	HCO_3^-	SO_4^{2-}
TDS	1.00										
PH	0.51	1.00									
Na^+	0.96	0.60	1.00								
K^+	0.21	0.13	0.20	1.00							
Ca^{2+}	-0.18	-0.47	-0.38	-0.13	1.00						
Mg^{2+}	-0.05	-0.38	-0.24	-0.05	0.78	1.00					
Cl^-	0.90	0.41	0.87	0.22	-0.13	-0.01	1.00				
NO_3^-	0.12	0.10	0.03	-0.21	0.33	0.28	0.21	1.00			
F^-	0.70	0.54	0.74	0.09	-0.38	-0.26	0.50	-0.16	1.00		
HCO_3^-	0.85	0.43	0.83	0.11	-0.11	0.04	0.64	-0.07	0.75	1.00	
SO_4^{2-}	0.65	0.30	0.60	0.20	-0.05	-0.05	0.70	0.28	0.19	0.31	1.00

It is also supported by the correlation of major ions with Total dissolved ions (TDI).This relation is used to identify the contribution of major ions to the ground water salinity. Figure 4.15 shows that Na^{+} and Cl^{-} are strongly correlated and $SO4^{2-}$ is weekly correlated with TDI. Relatively weak HCO_3^- correlation with TDI is due to the conversion of HCO_3^- to CO_3^{2-} takes place as PH increases along the groundwater flow path. The result of such correlations shows that these ions are the major contributors for the groundwater salinity of downstream water schemes.

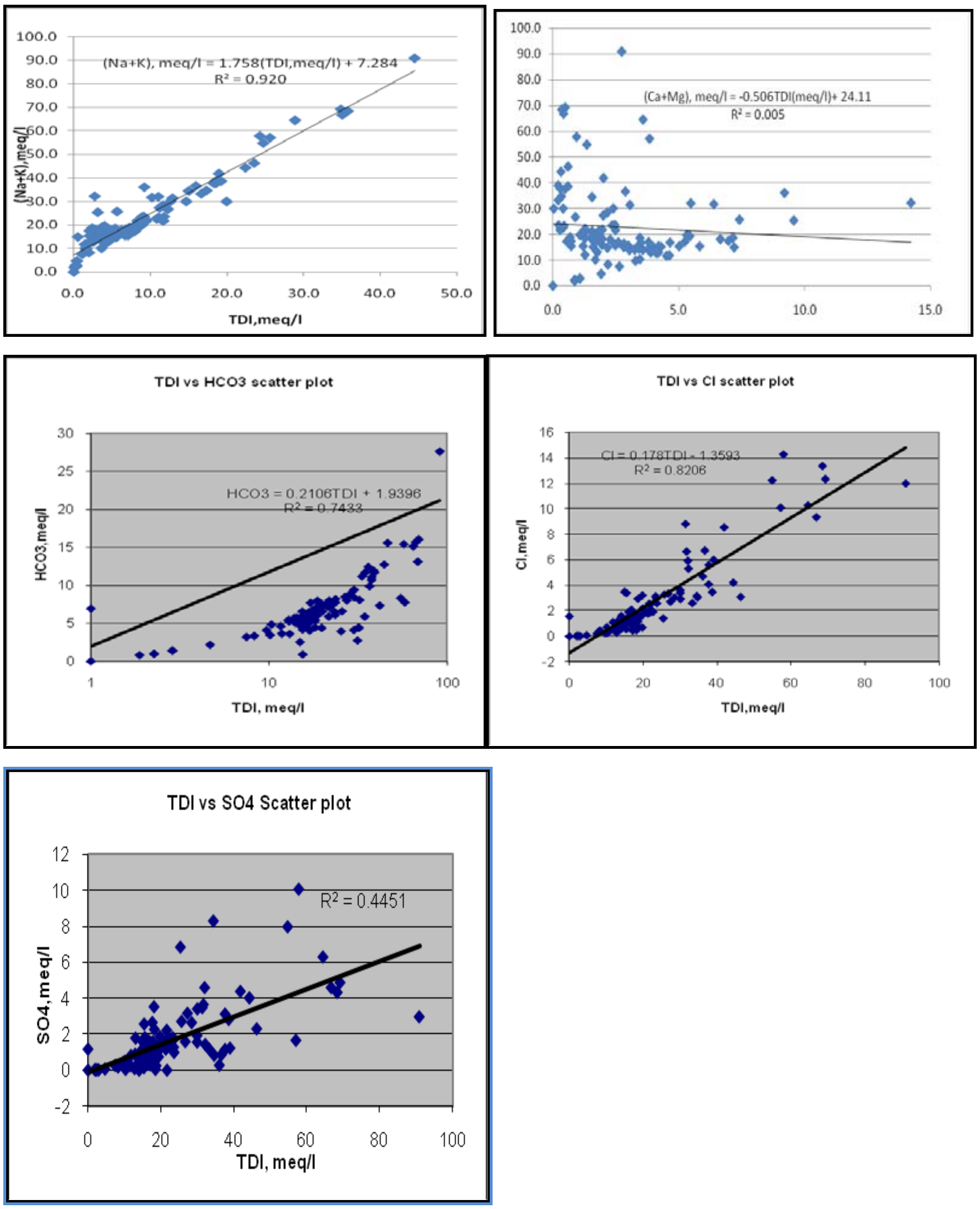

Figure 4.12: Major ions against Total Dissolved Ions (TDI) Scatter plot

4.9 Inverse Geochemical Modeling (IGM)

Inverse geochemical modeling approach applies geochemical mass balances to the observed chemical composition of evolutionary ground waters to estimate masses of mineral and gas transfer either through dissolution or precipitation of phases that account for changes in water chemistry between initial and final water composition along the groundwater flow direction. The initial and final water points hydrochemical data were selected based on the knowledge of geological, morphological setup, geochemical changes observed, groundwater flow direction created for this research and previous works.

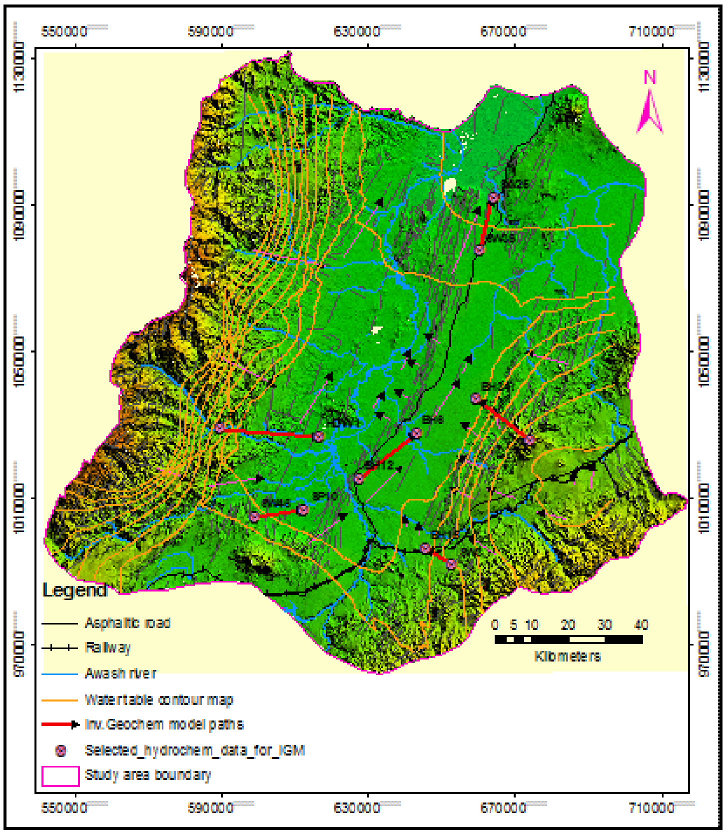

Figure 4.13: Selected inverse geochemical model paths

Inverse geochemical modeling can require appreciable knowledge of the reactions that may be responsible for the observed evolution is needed. Therefore, mineralogical knowledge is needed to make reasonable guesses as to which minerals and gases might be dissolving and/or precipitating. In order to do the modeling work, selection of the mineral phase was done based on the mineralogical composition knowledge gathered from (WWDSE, 2011) and (GSOE, 2010).

The study area is characterized by volcanic terrains, alluvial and/or eluvia deposits. Due to these primary and secondary silicate minerals like Plagioclase, k-feldspar, olivine, pyroxene, amphiboles, crysotile, kaolinite, montimorilonite, illite (k-mica) are among the mineral phases selected to run the model. Beside this Calcite occurs in volcanic rocks as late crystallization in cavities of lava and Anhydrite and gypsum can occur in amygdaloidal cavities of basalt or clay material. Halite and sylvite occur in clay, sand or paleosols due to the pre-burial evaporative process (Tilahun Azagege, 2008). Fluorite is commonly found associated with acidic volcanic minerals as rare mineral (Dana, 1995).

For inverse geochemical modeling, the PHREEQC interactive version 2.8 code within Aquachem 4.0 version software was used (Pankhurst 1995; 1999) takes in to account with uncertainty limit of 5% to satisfy the mole balance for each element within the solution. Five major flow paths with Hydrochemical data for initial and final solutions were selected to proceed the modeling (Table 4.4) and the result of each flow path is discussed in detail below.

Table 4.5: Selected water points hydrochemical date for inverse geochemical modeling Units (all in mg/l). Except EC, µs/cm, T-Temprature,°C

No.	Solution	ID	UTME	UTMN	TDS	PH	Na+	K+	Ca^{2+}	Mg^{2+}	Cl-	$NO3^-$	F-	$HCO3^-$	$SO4^{2-}$	WATER_TYPE
1	Initial	R10	589368	1029172	250	8.5	8	2	30	5	3	0	0.7	132	3	$CaHCO_3$
	Final	HDW1	616633	1027149	658	7.3	210	12.1	20	3.36	73.7	1.03	3.23	451.4	83.54	$NaHCO_3$
2	Initial	SW46	598836	1005342	345	7.31	47	3.9	53.1	14.8	22.6	8	0.8	320	42.7	$CaNaHCO_3$
	Final	SP10	612163	1007102	1110	8.5	415	20	6.4	1.92	144.8	5.08	3.41	653.68	150.4	$NaHCO_3Cl$
3	Initial	SW3	652583	992169	622	7.6	85	13	60.8	27.3	58.25	15.4	0.81	435.5	59.02	NaCaMgHCO3
	Final	BH16	645334	996709	623	7.4	188	7.8	36.1	8..2	91	1.2	1.2	359	107	$NaHCO_3ClSO_4$
4	Initial	SP4	674163	1025893	54	6.99	1.3	1	15.5	2.1	15	4.8	0	48.7	1.1	CaHCO3
	Final	BH34	659425	1037284	514	7.6	120	12	26.6	10	41.86	5.22	0.92	294	44.65	NaCaHCO3
5	Initial	SW39	660074	1077852	1058	7.26	290	11.2	45.5	9.4	312.9	22.5	0.9	166.5	167.7	$NaClSO_4$
	Final	SW25	663997	1092189	626	8.3	196	12	15.1	3.8	114.2	10	1.84	267.2	89.8	$NaHCO_3Cl$
6	Initial	BH12	627464	1015684	534	7.5	123	19	34.9	8.96	68.2	7.4	1.52	281.3	47	$NaCaHCO_3Cl$
	Final	BH6	643091	1027968	1022	8	178	8.5	8	3.84	60.1	2.5	0.66	329	72.6	$NaHCO_3$

Path-1: In this, modeling path was selected in between Kebena river drains from north western plateau(R10) from cluster-I as an initial solution and Marinto hot hand dug well(HDW1) from cluster-III as a final solution with a TDS of 87mg/l and 658mg/l respectively. The initial solution (R10) is emanating from the plateau of basaltic geology with $CaHCO_3$ water type and the final solution (HDW1) sunk in alluvial deposit with $NaHCO_3$ water type from rift floor. The distance between the initial and final water points for the modeling is about 27km and the major geological structures in between them is NNE-SSW marginal faults that control the geochemical processes locally in the area.

Phase	mole transfers:	Chemical composition
Halite	1.543e-003	NaCl
Ca-Montimorill	9.6e+001	$CaO.165Al_2.33Si_3.67010(OH)_2$
Kaolinite	-1.603e+002	$Al_2Si_2O_5(OH)_4$
Chrisotile	-2.472e-004	$Mg_3Si_2O_5 (OH)_4$
K-mica	6.433e+001	$KAl_3Si_3O_{10}(OH)_2$
Anorthite	-1.584e+001	$CaAl_2Si_2O_8$
Alibite	7.069e-003	$NaAlSi_3O_8$
K-feldspar	-6.433e+001	$KAlSi_3O_8$
Anhydrite	7.044e-004	$CaSO_4$

The model result shows that the main hydrochemical process taking place along the ground water flow path are dissolution of silicate mineral (Albite), clay minerals(Ca-montimorilonite, K-mica) and preceptation of minerals (K-feldspar, Kaolinite, Chrisotile and Anorthite).Halite and Anhydrite dissolve along the path.

Path-2: Inverse geochemical modeling was conducted in between Sabure shallow well around Kesem dam (SW46) from cluster-I as the initial solution($CaNaHCO_3$ water type) and hot stream emanating from Fentale mountain (SP10) from cluster-V as a final solution($NaHCO_3Cl$ water type). TDS of the initial and final hydrochemical data is 345 and 436mg/l respectively. The distance between the selected water points is about 14km and characterized by a series of normal faults known as WFB.

Phase	mole transfers:	Chemical composition
Anorthite	5.305e+003	$CaAl_2Si_2O_8$
CO2(g)	6.678e+003	CO_2
K-felds	9.921e+002	$KAlSi_3O_8$
Calcite	-6.678e+003	$CaHCO_3$
NaX	4.162e-001	NaX
CaX2	-2.081e-001	CaX_2
Halite	5.179e-004	NaCl
Anhydrite	1.984e+003	$CaSO_4$
Chrysotile	-2.394e+003	$Mg_3Si_2O_5(OH)_4$

According to the model result obtained, the main hydrochemical reactions taking place along the flow path are dissolution of Anorthite (Calc-plagioclase), K-feldspar, Halite and anhydrite followed by calcite precipitation by consuming carbon dioxide. The other process is cation exchange in between Ca^{2+} and Na^{+} in clay surfaces as sodium discharged to the solution and clay mineral chrysotile formed from weathering of basic volcanic rocks.

Path-3: Inverse geochemical modeling was conducted along the bordede-Allydegi plain flow path. The initial and final solutions selected are shallow well (SW3) in bordede and (BH16) in Allydegi plain with a distance in between is about 9km. The initial solution used for this path is NaCaMgHCO3 water type and $NaHCO_3ClSO4$ water type for the final solution. The basic fault system controlling the geochemical reaction is NE – SW trending Nazareth series Fault system.

Phase	mole transfers:	Chemical composition
Albite	2.934e+002	$NaAlSi_3o_8$
K-feldspar	-4.904e+001	$KAlSi_3O_8$
Pyroxene	5.58e+002	$MgO.5CaO.5SiO_3$
Ca-Montimorill	0.281e+002	$CaO.165Al_2.33Si_3.67010(OH)_2$
CO2(g)	6.221e-003	CO_2
CaX2	-3.671e+001	CaX_2
NaX	2.834e+002	NaX
Calcite	-4.322e-004	$CaHCO_3$
Anhydrite	3.76e-004	$CaSO_4$
Anorthite	-5.361e+001	$CaAl_2Si_2O_8$
Halite	1.609e-003	NaCl

The modeling result reveals that a silicate mineral (Pyroxene), Anhydrite, halite and illite (clay mineral) dissolve along the flow path by using up CO_2 gas as a steam through fractures from the magma chamber whereas Calcite, Anorthite and silicate mineral (K-feldspar) precipitate along the flow path. Clay mineral (chrysotile) is the weathering product and there is also a cation exchange reaction in the flow path between Na^{+} and Ca^{2+}.

Path-4: The model was conducted in between spring (SP4) as initial solution emanating from Asebot rhyolitic volcanic mountain with a lower TDS of 54 mg/l and is $CaHCO_3$ water type. The final solution selected was a deep borehole (BH34) from the rift floor with higher TDS value (514 mg/l) of NaCaHCO3 water type. The distance between the selected hydrochemical data is about 18km and has numerous NNE-SSW trending faults exist in between them.

Phase	mole transfers:	Chemical composition
Halite	1.655e-001	NaCl
K-mica	5.072e+001	$Kal_3Si_3O_{10}(OH)_2$
Ca-Montimorilon	-7.132e+001	$CaO.165Al_2.33Si_3.67010(OH)_2$
CO2(g)	5.570e+001	CO_2
CaX_2	-3.461e-001	CaX2
NaX	1.85e-001	NaX
Calcite	-6.59e+001	$CaHCO_3$
Gypsum	8.261e+001	$CaSO4:2H_2O$
Allunite	-1.298e+001	$KAl3(SO_4)(OH)_6$

The chemistry of the groundwater in this flow path is controlled by the dissolution of clay minerals (K-mica), Gypsum and halite with the consumption of CO_2. Beside this, precipitation of calcite, Alunite and Ca-montimorilonite with a cation exchange in between Ca^{2+} and Na^{+} in the clay surfaces of silicate minerals.

Path-5: In this final flow path, modeling was carried out in between Gelalay shallow well(SW39) with $NaClSO_4$ water type and a shallow well (SW25) with $NaHCO_3Cl$ both from the active NNE- trending wonji fault belt with a TDS of 1058mg/l and 626mg/l respectively. The distance in between them is about 15km.

Phase	mole transfers	Chemical composition
Albite	3.012e-003	$NaAlSi_3o_8$
Anorthite	-6.065e-003	$CaAl_2Si_2O_8$
Chrisotile	-5.167e-002	$Mg_3Si_2O_5(OH)_4$
CO2(g)	6.029e-003	CO_2
Halite	1.243e-002	NaCl
K-feldspar	6.248e-004	$KAlSi_3O_8$
Olivine	3.298e-005	$Mg2SiO_4$
Anhydrite	-2.775e+001	$CaSO_4$
Calcite	8.136e-003	$CaHCO_3$

The model result shows that the main processes along the path are dissolution of silicate minerals like (olivine, K-feldspar and Albite) and calcite with consumption of CO_2, which is balanced by a precipitation of clay mineral(Chalcedony) and Anhydrite.

Path-6: modeling was carried out in between two deep wells (BH12) with $NaCaHCO_3Cl$ water type as initial and (BH6) with $NaHCO_3$ water type as a final hydrochemical data. Both water points selected from Allydegi plain in the groundwater flow path with a TDS of 534mg/l and 1022mg/l respectively. The distance in between the water points is about 19km.

Phase	mole transfers	Chemical composition
Chalcedony	6.120e-003	SiO_2
Halite	-2.285e-004	NaCl
K-feldspar	-1.553e-004	$KAlSi_3O_8$
Calcite	3.379e-003	$CaHCO_3$
Ca-Montimorilon	-4.039e-003	$CaO.165Al_2.33Si_3.67010(OH)_2$
Chrisotile	-7.024e-005	$Mg_3Si_2O_5(OH)_4$
Anhydrite	-2.301e-003	$CaSO_4$
Plagioclase	5.153e-003	$NaO.62CaO.38Al.38Si_2.62O_8$
Alunite	1.284e-003	$KAl_3 (SO4)_2(OH)_6$

Based on the result obtained from this path, the major geochemical processes takes place are dissolution of minerals like plagioclase, Calcite, chalcedony and Alunite balanced with precipitation of K-feldspar and Anhydrite. Weathering products of mafic as well as felcic rocks like Ca-montimorilonite and Chrisotile appeared in this flow path.

Ingeneral, due to the complex volcano-tectonic processes in the area; the modeling paths were selected carefully not for more than 20km except for path 1 which is 27km. The major geochemical processes which control the hydrochemistry of the area are chemical reactions such as dissolution and/or precipitation of silicate minerals, calcite, halite and Anhydrite followed by cation exchange in between Ca^{2+} and Na^+ in clay surfaces and formation of different clay minerals by weathering process by consuming CO_2(g) from deeper source through fractures.

4.10 Salinity source of the area

Understanding of the cause of salinization is a crucial activity to its management and remedial measures for the groundwater resource exploitation (Freez and Cherry, 1979). In Arid and Semi-Arid areas like the present study area, the effect of evaporation subsequently concentrates salts. The salinity source of ground waters can be of three major categories. The first is originate from atmospheric deposition (both in precipitation and as dry fallout) and from weathering reactions of precipitation with surficial rocks and soil in the watershed. The second category is the inflow of subsurface-origin saline waters. Such waters may be derived from solution of evaporite deposits. The third category is anthropogenic salt inputs (Fetter, 1994). In arid and semiarid river basins the effects of evaporation and transpiration subsequently concentrate salts.

Measurement of the stable isotope composition of salinized water is a useful method to testify the cause of the salinity because water that is saline due to evaporation will be isotopically more enriched than the source water, whereas water that is saline due to salt addition or transpiration will not change isotopic composition (Hem,1989).

The spatial TDS distribution map (Figure 4.5) illustrates that the salinity increases towards rift floor along the WFB including Awash river valley alluvial aquifer from north western plateau and south eastern escarpment. The increase in salinity marked in water points from alluvial valley and rift floor shows isotopically ($\delta^{18}O$) enriched which fall on evaporation line rather than water points sitting in volcanic rocks of Allydegi plain which show dissolution (Hydrolysis).

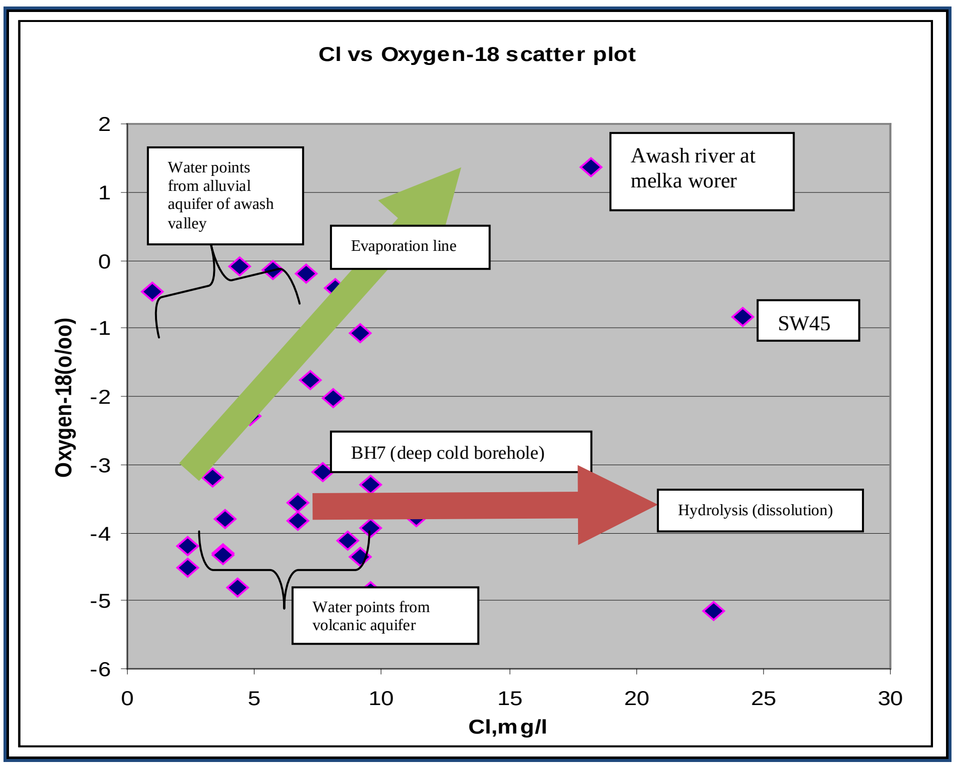

Figure 4.14: Scatter plot of Chloride against $\delta^{18}O$

Thus, the correlation between chloride ion and stable isotope ($\delta^{18}O$) concentration describes the presence of two different processes for the evolution of salinity in the study area. These are salt deposition due to evaporation and different minerals dissolution (hydrolysis) along the WFB (Figure 4.16). Beside these, Awash river water samples were collected along its flow path before and after Beseka lake drains to it to see the impact of Beseka lake on a downstream ground water salinization.

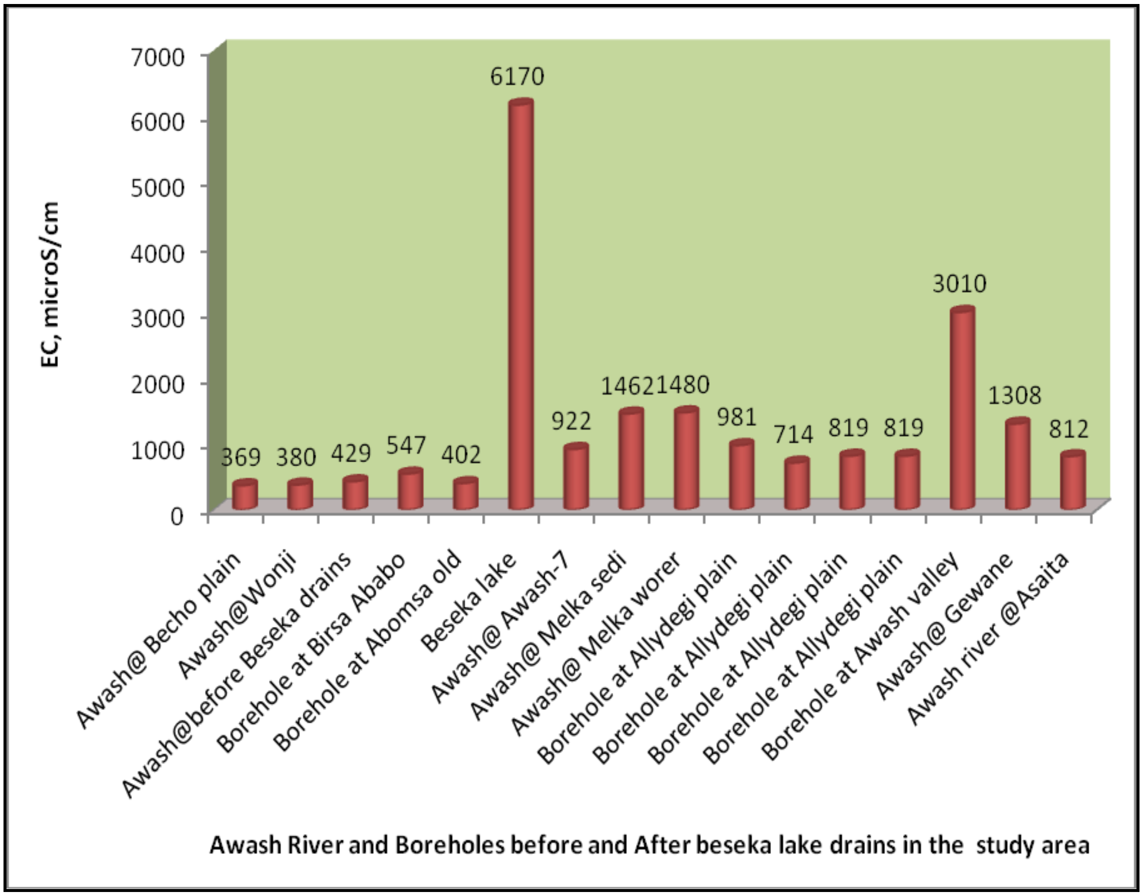

Figure 4.15: Graph showing electrical conductivity of Awash river at different locations and boreholes along the flow direction before and after Beseka Lake drain (Sampling date February 2013)

The graph of EC against water points location (Figure 4.18) shows that the salinity of downstream surface and subsurface waters after Beseka lake drain enhanced. It could be one factor for the cause of salinity for the water schemes located downstream of Lake Beseka which needs further study to assess its impact on downstream aquifers.

4.11 Groundwater Recharge Estimation

Groundwater recharge can be defined as the water that replenishes the underground water stock. Natural recharge mechanisms can either be direct, localized or indirect (Simmers, 1997). Quantification of the rate of natural ground water recharge is a pre-requisite for efficient ground water resource management. It is particularly important in regions with large demands for ground water supplies where such resources are the key to economic development (Freez and Cherry, 1979). However, the rate of aquifer recharge is one of the most difficult factors to measure in the evaluation of ground water resources. Estimation of recharge, by whatever method, is normally subject to large uncertainties and errors due to the interaction of climate, geology, morphology, soil condition and vegetation determine to varying degrees the recharge process (Simmers, 1997, De Vries & Simmers; 2002).Groundwater recharge in semi-arid and arid areas is more susceptible to near surface conditions as compared to humid areas. Further, the potential evaporation is higher than the rainfall making recharge dependent on rainfall intensity and the existence of fissures and cracks that favors preferential flow in the receiving soil mass. Selection of cost-effective and simple rapid assessment methods for estimating recharge that allows real-time water resource management decisions to be made for the future use.

Tracer method of estimating recharge is more successful than the indirect physical methods because they are simple to use, relatively cheap and universally applicable (Lerner and Simmers, 1997). Among the tracer techniques, Chloride mass balance technique shows the simplest, least expensive, and most widely used for recharge estimation (Sophocleous, 2004). Despite the shortcomings like temporal and spatial chloride deposition, tracer methods remain the most widely used for groundwater recharge estimates in semi-arid areas. To reduce the uncertainties and errors in estimation the development has been made to use methods in combination either as multiple tracer methods or as tracer and some physical method.

Previously, WWDSE had estimated the groundwater recharge rate of Allydegi plain using Darcinal approach. The result obtained from such approach shows that more than 112.42MCM/yr (66.92mm/yr) water recharges the groundwater system of the Allydegi plain.

4.12 Chloride Mass Balance Recharge Estimation Method (CMB)

Chloride is the most commonly used hydrochemical parameter in groundwater used for indirect recharge estimation using mass conservation principle in between atmosphere and subsurface. The chloride balance method assumes that sources of chloride ion in the ground water come entirely from rainfalls. According to Edmunds (1988), the assumption is that the only source of chloride is from the soil surface through rainfall or as a dry deposition and no contribution of chloride from weathering of geological materials. Therefore, the equation for the recharge estimation is reduced to the following form:

$$\boxed{(P * Clp) + D = (R * Clgw) + (Ro * Cl_{ro})}$$

Where, P is mean annual rainfall in mm/yr, Clp, Clgw and Clro is the mean chloride concentration of rainfall, groundwater and runoff in mg/l respectively, D is dry deposition; R is the mean annual recharge rate.

Due to the absence of the water as a runoff in the area, the runoff part is neglected. In middle Awash river basin including the study area no any Chloride amount data documented as a dry deposition. Thus, it is assumed as negligible. Beside this the thickness of unsaturated soil is generally high (Annex-VII) and the depth to water level is so deep that the chloride concentration saturation reaches at equilibrium until reaches to the depth of groundwater. In such circumstances the concentration of chloride from dry deposition fallout is not significant with respect to the ground water depth. Due to this reason the above equation finally become;

$$\boxed{R = \frac{(P * Clp)}{Clgw}}$$

Arid and semi-arid areas like Allydegi plain and surroundings are characterized by higher evapotranspiration rather than precipitation and spatially variable alluvial deposits in the rift floor favors chloride content of ground waters higher than that of rainfall waters which underestimate the annual groundwater recharge. Therefore, CMB approach is in question unless water points from thin sediment deposits should be used. Therefore, open and hand dug wells in the thick sediment with high concentration of chloride were unused and chloride content from shallow wells, hand dug wells in the thin alluvial setting, springs and boreholes especially hydrochemical data in cluster-I and II of less mineralized once selected.

The major assumptions for the selection of water points are,

- The bulk precipitation (dry fall and precipitation) is the only source of Cl^- in the system,
- Cl^- deposition rate and mean annual precipitation are accurately estimated and have been constant over the period of groundwater residence time
- The measured Cl^- content of groundwater more or less represent the mean value of the total groundwater

The data required for the estimation of groundwater recharge of the study area using CMB method is long term average precipitation, Cl^- content of precipitation, Cl^- content of groundwater.

The areal depth of precipitation averaged for the research area using Isohytal method is 649.4mm/year. The mean wet chloride concentration in precipitation for the research area is 0.91mg/l which is adopted from previous thesis one month monitoring rainfall hydrochemical data (Addisu, 2012). Dry deposition rates are quite variable, depending on distance from the ocean, wind patterns, and local sources of Cl (Plummer, 1996; Davis et al., 1998). However, the chloride concentrations from dry deposition are not considered for this investigation area due to lack of data, the logical assumptions of the existence of deep groundwater table and in semi-arid areas like the research area, the chance of rising of groundwater table to the evaporation zone (root zone) is rare. Because of this fact, the leaching of residual chloride during recharge in the unsaturated zone to the water table is negligible. The average groundwater chloride concentration should be calculated as harmonic mean (Eriksson,1985). The harmonic mean of the chloride concentration in the ground water is calculated using the expression indicated below.

$$\boxed{\text{Harmonic mean} = \frac{N}{\sum_{i=1}^{n}(1/Cl_{gw})}}$$

Where N represents the number of data used for estimation and Clgw for chloride concentration of each selected water points.

Forty four (44) water points hydrochemical data were used to estimate the recharge rate of the area (Annex-VII). All of the selected water points have chloride concentration less than 50mg/l to reduce the error caused by the evaporation effect. Thus, the computed harmonic mean of chloride concentration from groundwater is 6.0232mg/l and the estimated groundwater recharge of the area using CMB method is 98.11mm/yr. i.e. 15.12% of the annual rainfall amount (649.4mm/yr).

Recharge rate determined using Chloride mass balance method supports recharge rates obtained using Darcinal approach by WWDSE, which is 66.92 mm/yr. Due to the overestimated recharge rate obtained by CMB, further recharge estimates through relatively precise methods are required. Based on the recharge rates calculated for the selected water points, the recharge rate is varied from place to place. This is due to the factors mentioned above like climate, geology, morphology, soil condition and vegetation cover.

The spatial disturbition map of recharge rates in the area (Figure 4.18) shows that Chloride mass balance method relatively overestimates recharge rate for the north western and south eastern plateaus bordering the lowlands(rift floor) and relatively underestimate recharge rate in the low lands of the study area. The over estimation could be related to the recharge takes place through fractures without undergoing significant evaporation which reduce the ground water chloride concentration and relative underestimation is associated with significant evaporation effect of the rainfall prior to recharge and dissolution of minerals like halite and fluorite.

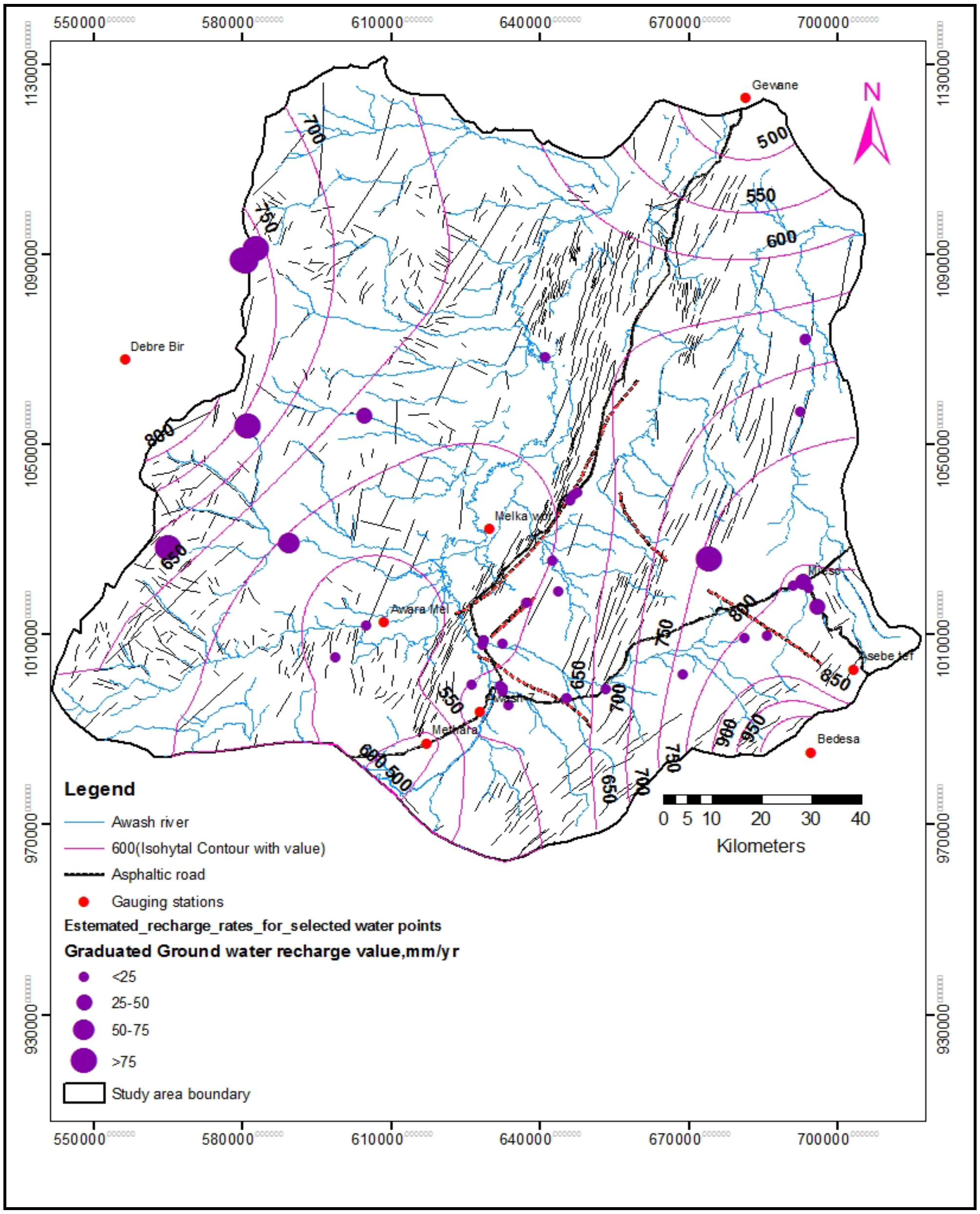

Figure 4.16: Spatial distribution map of graduated recharge rates for the area

4.13 Conceptual hydrogeochemical model

The study result reveals that as one goes towards the lowlands from the elevated highlands surrounding it, increase in major hydrochemical parameters concentration like TDS, Na^+, F^-, Cl^-, HCO_3^- and SO_4^{2-} with local anomalies occurred due to the complex volcano-tectonic processes in the study area.

One of the crucial aspects in hydrogeological system analysis of the area is evaluation of the hydrochemical evolution mechanism of the area which comprises understanding of sources and factors that control the rock-water reactions along the ground water flow path. In order to understand the various geochemical facies, two conceptual geochemical evolution sections created along the groundwater flow direction (Figure 4.19 and 4.20).

Hydrochemical facies with TDS<650 mg/l represented by $CaHCO_3$,$CaMgHCO_3$, $CaNaHCO_3$ and $NaCaHCO_3$ drains from the fractured Tarmaber-megezez basalt, Seladingay-Gorjo Ignimbrite, Rhyolite, trachyte and from acidic volcanic centers (Asebot, Afdem, Fentale) from elevated areas have diluted chemistry due to the high hydraulic gradient favors less rock-water interaction.

The $NaHCO_3$ facies is most likely evolved from the above water types by a heat emanating from deeper source through fractures giving up dissolution of plagioclase, olivine, pyroxene and halite deposition from soil surfaces with calcite precipitation and cation exchange between Ca^{2+} and Na^+ located in the central rift floor of the study area along the active fault line (WFB). It is moderately concentrated with TDS in between 650 and 1200 mg/l.

Hydrochemical facies of $NaHCO_3Cl$ and $NaHCO_3SO_4$ are highly concentrated which testifies the final stage of chemical evolution in the study area evolved by dissolution of anhydrite and precipitation of calcite and halite. They are characteristics of the discharge area of the present study area groundwater system. In general, the piper plot (Figure 4.11) describes that the trend of hydrochemical evolution is from $CaMgHCO_3$-to-$NaHCO_3Cl$ or $NaHCO_3$ SO_4 type towards the rift floor along the groundwater flow direction.

In the study area the water demand enhanced for the purpose of domestic as well as irrigation purpose. Due to the lack of surface waters in the study area, groundwater is the only solution for the enhanced need of water. Most of the boreholes rarely exceeds 200m depth except the boreholes undergoes drilling currently in Allydegi plain. The hydrochemical result of the boreholes (BH7, BH11-to-BH17, BH21-to-BH23 in Annex-V) located in Allaydegi plain and surroundings have a TDS <700 mg/l and F^- < 1 mg/l.

From these deep bore holes water quality result of moderate concentration. It is associated with deep boreholes penetrate various lithologies (Annex-IV) that may neutralize the concentrated waters types.

As a result good quality and sustainable groundwater could be found in deeper aquifers in volcanic aquifers of older, depleted both in δD and $\delta^{18}O$(Figure 5.2, isotopic part) and higher discharge (like BH7,84 l/s and BH11,50 l/S) from volcanic as well as alluvial aquifer of Awash valley.

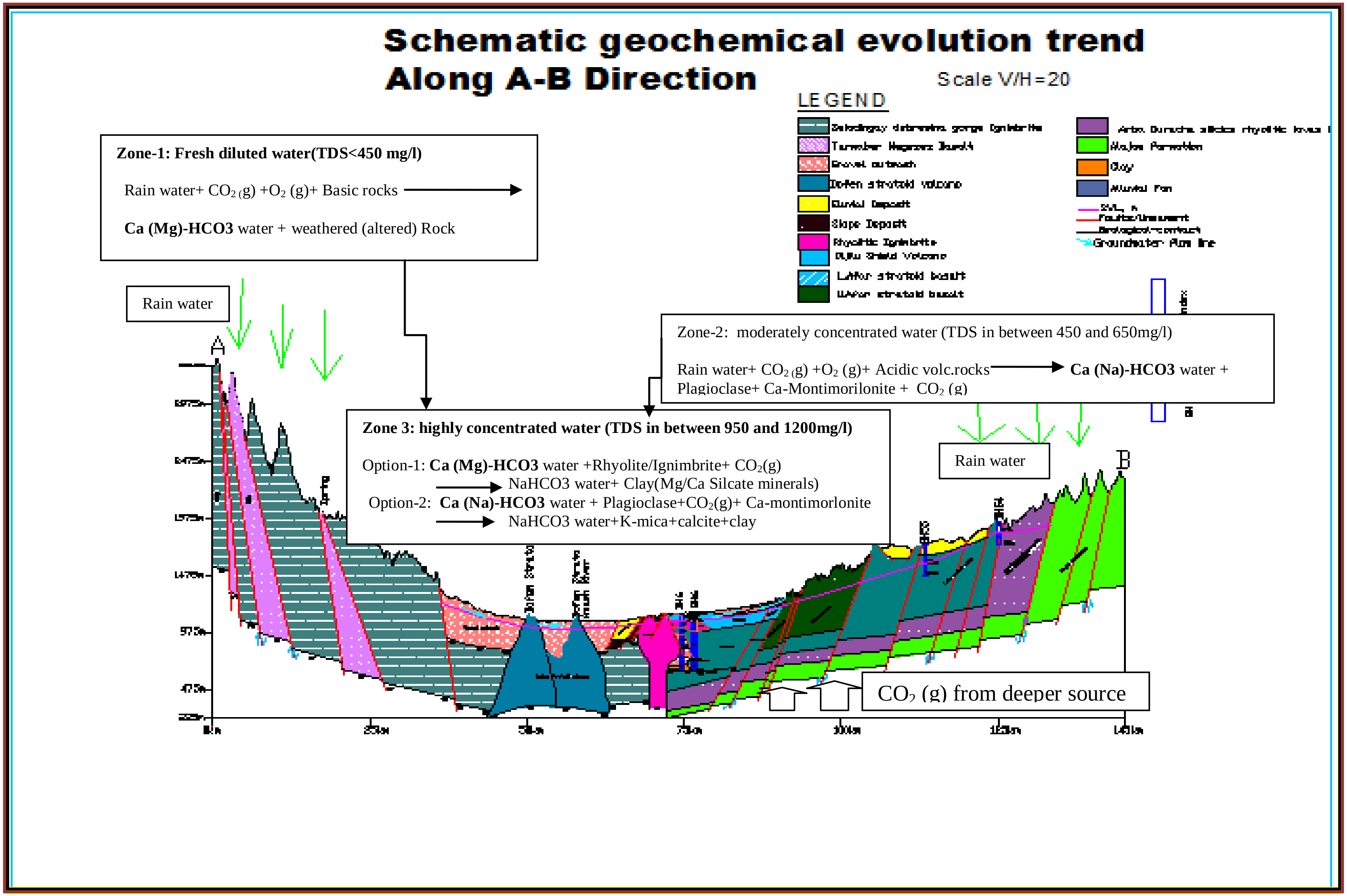

Figure 4.17: Schematic sectional conceptual geochemical evolution along the groundwater flow direction (A-B)

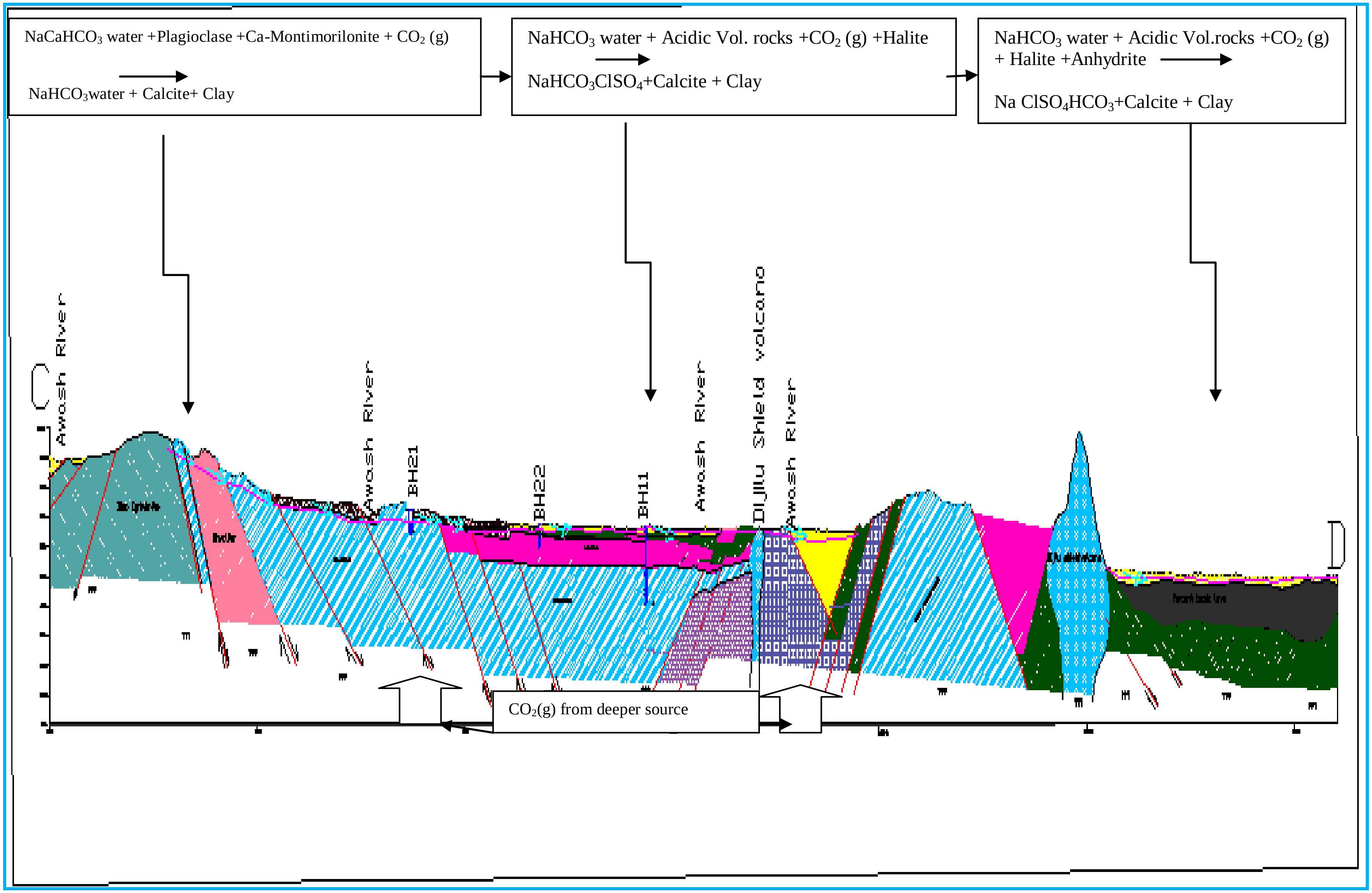

Figure 4.18: Schematic sectional conceptual geochemical evolution along the regional ground water flow direction(C-D)

5. Isotope Hydrology

5.1 Introduction

Water is a chemical compound of hydrogen and oxygen. In the gaseous state, at least, it has the molecular formula H_2O. Although the same formula also represents the compositions of liquid water and ice, the molecules in these two forms are associated structurally and it is a good idea to think of the condensed phases in terms of these associations rather than as simple aggregates of molecules. Because three isotopes of hydrogen and three of oxygen exist in nature, 18 varieties of water molecules are possible. Among these, ^{2}H, ^{3}H and ^{18}O are the most important applications for the study of hydrogeological system analysis (Hem, 1985). There are two types of isotopes of water under considerations, radioactive and stable isotopes. Radioactive isotopes are nuclides that spontaneously disintegrate through a time from other isotopes with emission of alpha or beta particles sometimes also gamma rays and stable isotopes are nuclides that do not appear to decay to other isotopes but may themselves be produced by the decay of radioactive isotopes (Fritz and Fontes, 1980).

Stable and radioactive environmental isotopes have now been used for more than four decades to study hydrological systems, and have proved particularly useful for understanding groundwater systems. Applications of stable isotope ratios of hydrogen and oxygen in the study of groundwater system are based up on isotopic variation in atmospheric precipitation and the general concept of tracing in which either intentionally introduced isotopes or naturally occurring environmental isotopes are employed. Environmental isotopes are advantageous over artificial tracers that they facilitate the study of various hydrogeological processes on a much larger temporal and spatial scale through their natural distribution in a hydrological system (Aggarwal, 2007). Among the most important applications where isotopes are useful in groundwater system of arid and semi-arid areas, study of recharge source and mechanism, flow path, interconnection between aquifers and relative dating of the water either pre-test or post test waters are common.

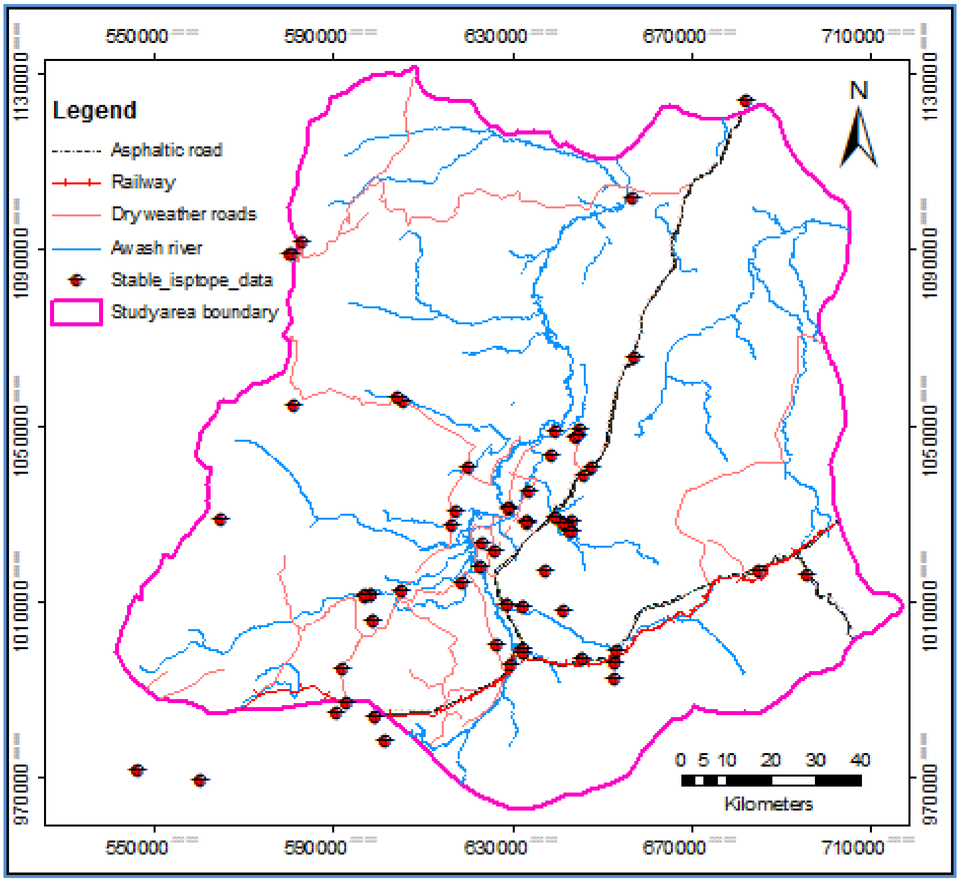

Figure 5.1: Environmental isotope data availability map

5.2 Stable Isotopes

Stable isotope ratios in hydrology and oxygen are conventionally reported as per mil(‰) deviation from those of a standard using the δ(delta) notation, i.e;

$$\boldsymbol{\delta(‰)=(R_{sample}-R_{standard})/R_{standard}*10^3}$$

Where R is isotopic concentration ratio ($^2H/^1H$ and $^{18}O/^{16}O$) of the sample or standard. The isotopic standard used for hydrogen and oxygen isotopes is the Vienna Standard Mean Oceanic Water (VSMOW).

The local meteoric water line was created using IAEA data of Addis Ababa station from 1961-to-2009 downloaded from GNIP isotopic data base web site (http://isohis.iaea.org/Database). Isotopic composition of these precipitations data ($\delta^{18}O$ (‰) against δ^2H(‰)) are plotted and resulted with a linear trend represented by the equation **δ^2H(‰)= 7.659$\delta^{18}O$(‰)+11.7** is known as the local meteoric water line(LMWL). The LMWL is the reference line to study the surface and subsurface water recharge sources, mechanism, interconnection between different aquifer units, to estimate mixing ratio of different sources for the seepage of kesem dam which is under construction, interaction between Awash river with aquifer of Allydegi plain and that of precipitations from all over the world plotted to give δ^2H (‰)= $8\delta^{18}O$ (‰)+10 which is given by Craig (1961)known as Global meteoric water line(GMWL)(Figure 5.2). The LMWL of Addis Ababa precipitation is plotted above the GMWL with d-excess of 11.7‰ which could be related with the source of rainfall, temperature and topographic effects and the average summer and winter rain s $\delta^{18}O$ compositions are -1.87‰ and 0.89‰ respectively for the year 1961-to-2009 precipitation. The average summer and winter rains δD compositions are -1‰ and 19.06‰ respectively for the same year.

In this study, 21 water samples for stable isotope and 19 water samples for tritium were collected to fill the data gap as a primary data. Both stable isotope and Tritium were analyzed in the hydrogeological laboratory of Earth Science Department of the Addis Ababa University by Liquid-Water Isotope Analyzer and Electrolytic Enrichment and Liquid Scintillation Spectrometry respectively. Due to the lack of chemical for the analysis of tritium, it was not possible to get the result but an attempt was made to use tritium data of Awash river at Melka- Sedi and five-wells from Allydegi plain aside to the secondary data collected from the previous works. Totally 89 water samples from different water schemes (Appendex-VI) were collected and organized from different locations of the area.

Rainfall pattern of the area varies seasonally which caused isotopic composition due to change in moisture sources, moisture transport mechanism and amount of moisture. Higher monthly precipitation corresponds to increasingly negative stable isotope results (Mazor,1997). Comparing to the summer rainfall isotope values, especially those of June, July and August (figure 5.2) with water points (groundwater, spring and river) shows summer rainfall being the source of recharge. Whereas, winter rainfall is lost through the higher evapotranspiration rate which characteristics of arid and semi-arid areas such as the present study area.

The isotopic composition of water samples vary from -5.87‰- to- 1.36‰ for $\delta^{18}O$ and -26.21‰-to -14.31‰ for δD respectively. The mean composition is -2.4‰ for Oxygen-18 and -6.52‰ for deuterium.

The water points like BH2 (Dulecha Bahiri),Awash valley water samples (SW14,SW6,SW7,SW18,SW26,BH26,BH51), Allaydegi plain water samples (BH29,SW30,SW45) along WFB and R3,R4,R5(Awash river @ Awash-7,Mlka-werer and Gewane respectively) nearly plot to groundwater evaporation line with a slope (5.4) corresponding to extensive evaporation prior to recharge and the relative enrichment might also be the result of openness of the water scheme exposed to the atmosphere.(Figure 5.2). In addition to that the isotopic enrichment of Awash river at Awash -7, Melka worer and Gewane with shallow and deep boreholes of Awash valley and Allydegi plain depicts that an evaporated awash river most likely flood water from highlands surrounding the study area (rift floor) recharged the Allydegi plain and Awash valley alluvial aquifer along its course through fractures, faults or cavities.

Groundwater and river samples from Allydegi plain like BH23, BH24, BH18,SW2, SW7,BH38,BH53 and BH44(water sample taken at a depth of 100m during air lift development) and R11(Awash river @ Melka-sedi) plot on a LMWL indicating groundwater of the area recharged by summer rainfall through the available fractures and faults. In addition to that their isotopic plot on or nearly LMWL depicts the usefulness of rock-water interaction and isotopic fractionation in these water points is generally insignificant.

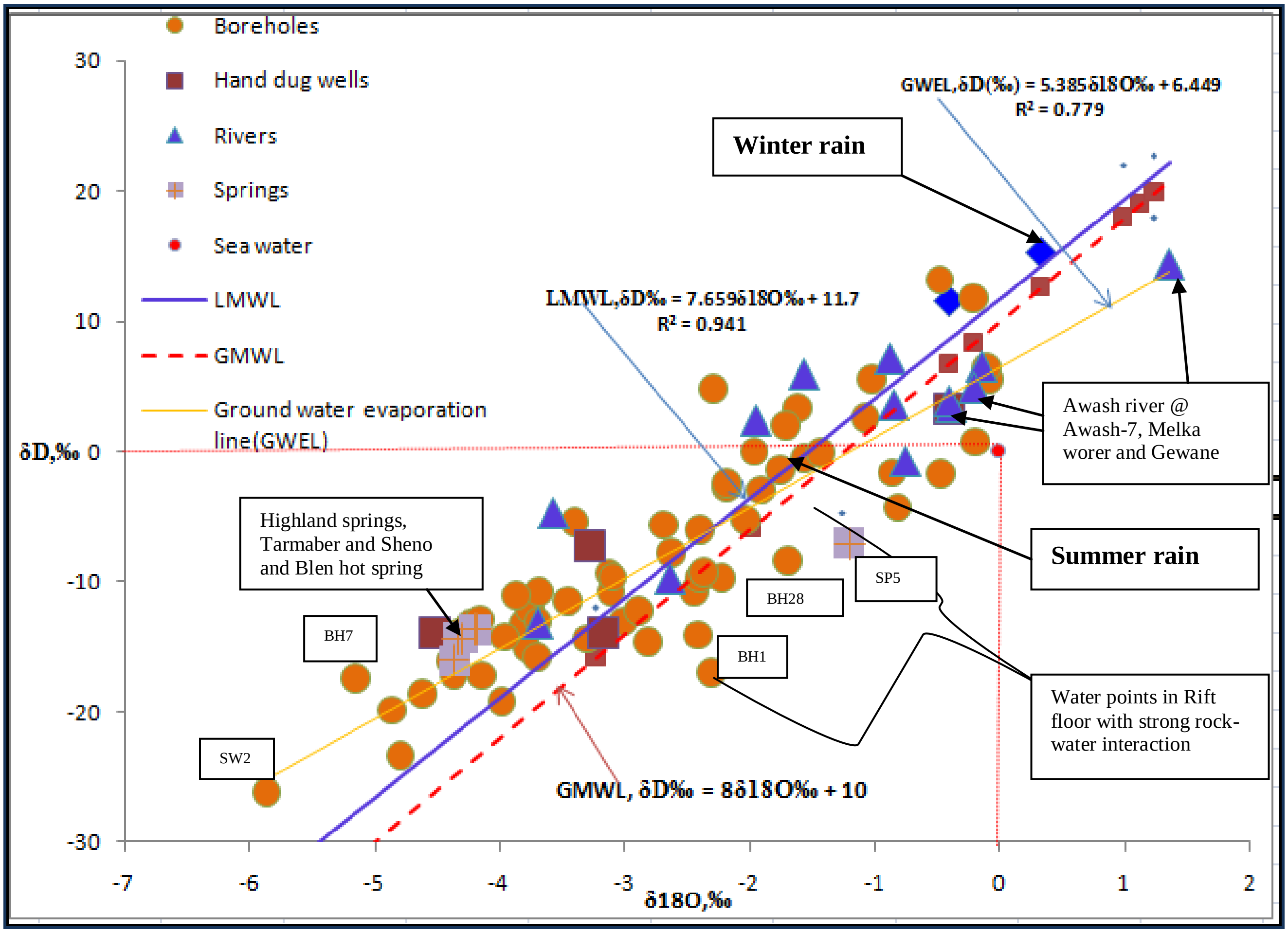

Figure 5.2: Scatter plot δD and $\delta^{18}O$ isotopes of study area water points

Water samples collected from deep sources like BH5,BH6(at a depth of 210m and 500m during air lift development), BH19,BH23(During pump test), BH25, BH32, BH44 (at a depth 200m, 300m, 400m and 500m during air lift development), SW2,SW35,HDW1,HDW2,HDW15,SP1, SP11(Plateau springs named Tarmaber and Sheno), SP8(Blen hot spring emanating from Thermal field, WFB), SP4(Cold spring emanating from Asebot mountain), R6(Kesem river), R9(stream from the foot of Fentale mountain) show significant depletion with respect to modern day summer rain fall. These water points represent very old waters which might be recharged in more humid conditions different from sampling time (it could be from southeastern and eastern highlands percolating through fractures/faults) or deep circulating meteoric water with isotopic exchange with CO_2(g) originating from deeper sources or both. Such a negative $\delta^{18}O$ shift has been attributed to interaction of meteoric water (H_2O) with deep CO_2- rich source (Clark and Fritz, 1997). Most of the water samples collected from the plain of geothermal area leads to the slow groundwater flow velocity which corresponds to the long residence time to enhance a strong rock-water interaction for the isotopic fractionation.

Among the water samples like BH1, BH28 and SP5 located in western and eastern part of Awash river shows enrichment with in $\delta^{18}O$ without significant change in δD. Enrichment related with $\delta^{18}O$ is due to rock –water interaction of isotopic exchange between ^{18}O from rock and ^{16}O from solution to reach the equilibrium condition. In rift floor of flat hydraulic gradient the groundwater flow velocity is slow which facilitate the rock-water interaction, some part of ^{18}O is move from the rock to water and some ^{16}O from the water go away to rock (Kebede et al., 2008).

In general, stable isotopes study of the present study area distinguishes the groundwater origin and recharge mechanism. The result illustrates that the ground water system is recharged from the combination of direct/diffuse recharge, from highlands that bounds the study area through fractures, faults or cavities and from Awash river.

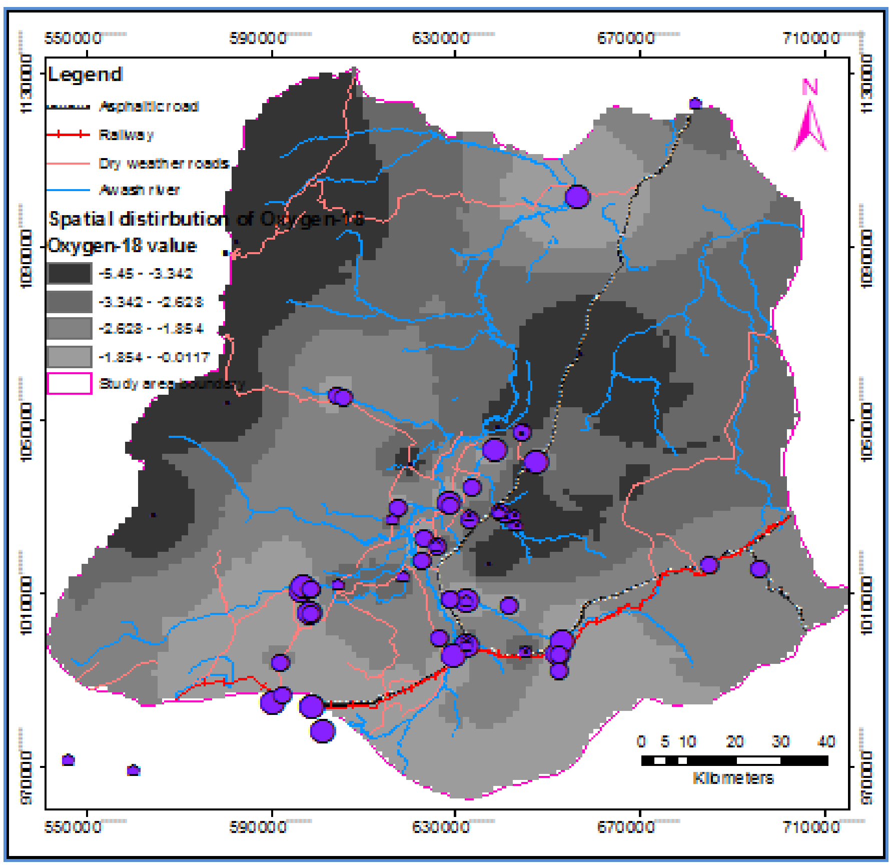

Figure 5.3: Spatial distribution map of stable isotope $\delta^{18}O$ (‰)

5.3. Environmental isotope monitoring of Awash river and wells in Allydegi plain

Groundwater often consists of a mixture of recharge from surface water and local precipitation. It is important to know the proportions of these recharge components in order to increase the sustainable supply of drinking water through bank infiltration, and to prevent drinking water pollution by infiltration of water from a contaminated surface water source and to manage the ground water resource. To assess the temporal variation of the stable isotope, Awash river with different five boreholes in Allydegi plain and Awash valley environmental isotope monitoring was conducted since Auguest,2012 on a monthly basis to understand the interaction of Awash river with groundwater system in Allydegi plain (Annex -VIII).

Table 5.1: Location of Environmental isotope monitoring water points

No.	Water source	ID	Local Name	UTME	UTMN	Elv, masl	Distance from R11,km	Borehole depth,m	Aquifer Geology	Yield ,l/s
1	Shallow well	SW2	Andido	646032	1038432	755	31.2	90	Volcanics	19
2	Borehole	BH20	Awash Arba	628683	1008918	827	10.7	150	Alluvial	6
3	Borehole	BH19	Allydegi plain	643290	1025519	831	21.8	126	Alluvial	2
4	Borehole	BH18	Gonita Birka	637189	1016763	774	14.4	220	Alluvial	20
5	Shallow well	SW1	Adebtole	633279	1027937	815	14.8	80	Volcanics	8
6	River	R11	Sidafage	622893	1017591	817	0	0	River	0

River water can show a seasonal variation in isotopic composition, usually observed with reduced amplitude and after a time lag in wells near the river. This time lag as well as the change in mean isotopic composition provides the minimum time (transit time) required for river water and possibly it’s dissolved pollutants to reach a groundwater supply well. Isotope composition also provides insight into the fraction of river water in recharge (possibly polluted) relative to other recharge sources.

The parameters monitored on a monthly basis are δD (‰), $\delta^{18}O$ (‰) and Tritium (TU). Due to the monitoring data plot of both $\delta^{18}O$ and δD as a function of time gives the same trend, consideration was given for $\delta^{18}O$ against time plot only. Monitoring data is plotted for $\delta^{18}O$ isotope parameter as a function of time and it was found that Awash River at Melka-sedi shows pick enrichment on months of October and January whereas on August, December and March it shows pick depletion (Figure 5.4). Enrichment is most probably related with dry season for evaporation of river water prior to recharge after the summer rainy season ceases and depletion is related with winter and summer rains that fall within or away from study area feed the Awash River.

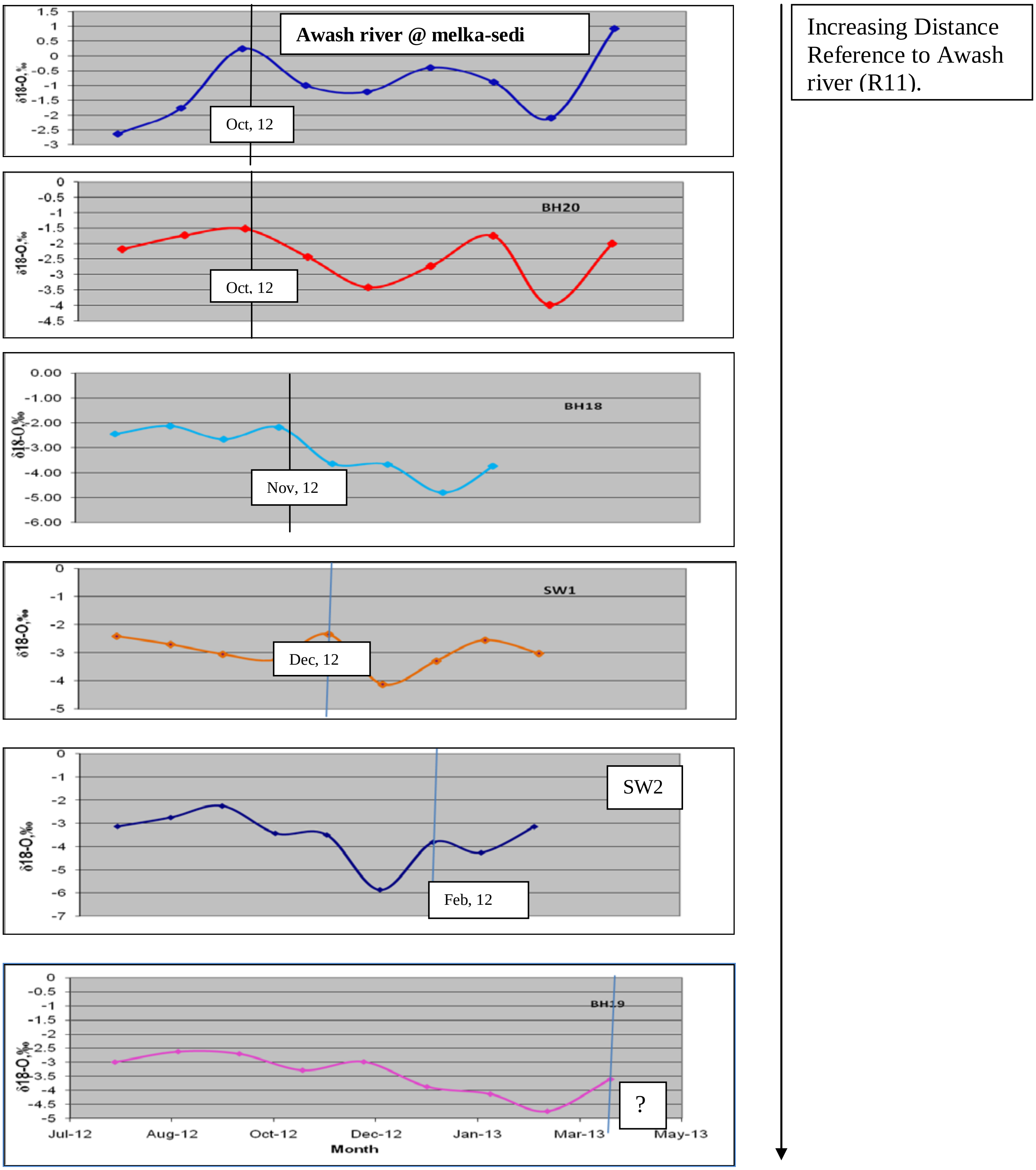

Figure 5.4: Heavy isotope δ18O vs Time monitoring graph for each water Points (August, 2012 –April, 2013)

Monitoring data plot of each water points as a function of time found that pick isotopic signature ($\delta^{18}O$) of Awash river is shown in bore holes BH18(14.4km far from R11), SW1(14.8km far from R11) and SW2(31.2km far from R11) in November, December and February respectively. However, BH20 (10.7km far from R11) shows the same trend (signature) of Awash river. This clearly indicates that these wells are recharged from Awash river with a residence time of approximately one, two and four months respectively. BH19 located at the center of Allydegi plain, 21.8km away from R11 do not show significant signature of Awash river for this short period of time (9-months data) may be defined after long time monitoring result.

Aside from these comparison of Awash river with boreholes (BH20, BH18 and BH19) along traverse-1 and boreholes (SW1 and SW2) along traverse-2 located at the same line was made (Figure 5.5 and 5.6). With these nine-month monitoring data, boreholes located further distant from Awash river, the signature (enrichment and depletion) of Awash river on boreholes decreases and the lag time for the boreholes increases. The result clearly depicts that the Allydegi plain was recharged from Awash river through fractures significantly. It also supports the result obtained from Awash River discharge analysis discussed earlier (Hydrology part), which is more than 314MCM/year of water as a deficit in between Awash @ Awash-7 and Awash @ Melka-sedi.

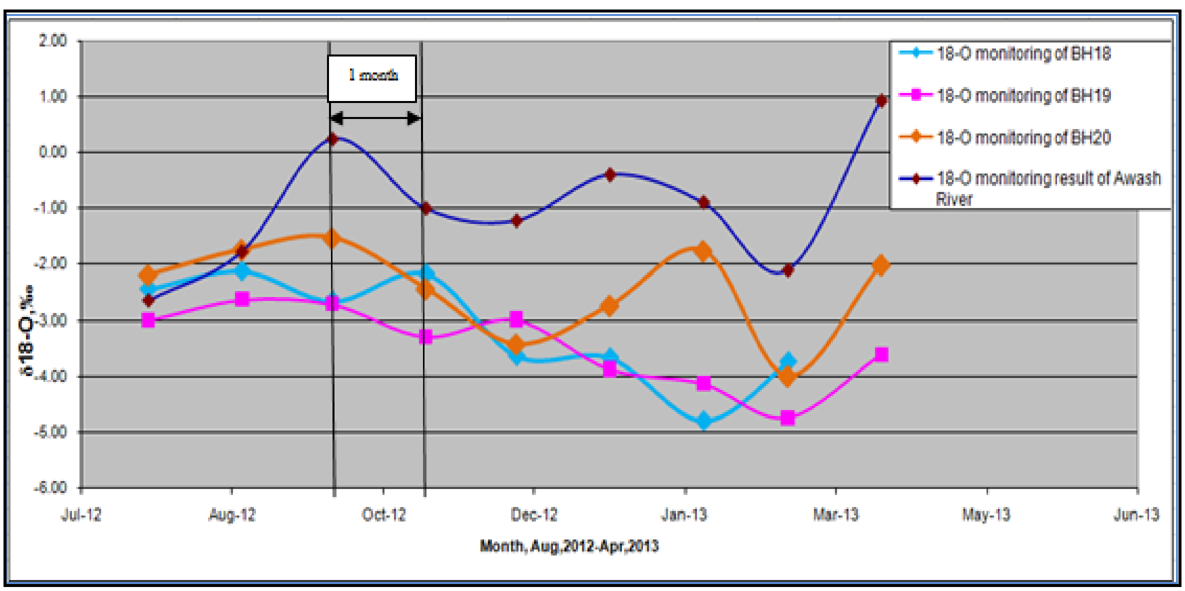

Figure 5.5: $\delta^{18}O$ monitoring plot for R11, BH20, BH18 and BH19 (Along traverse-1)

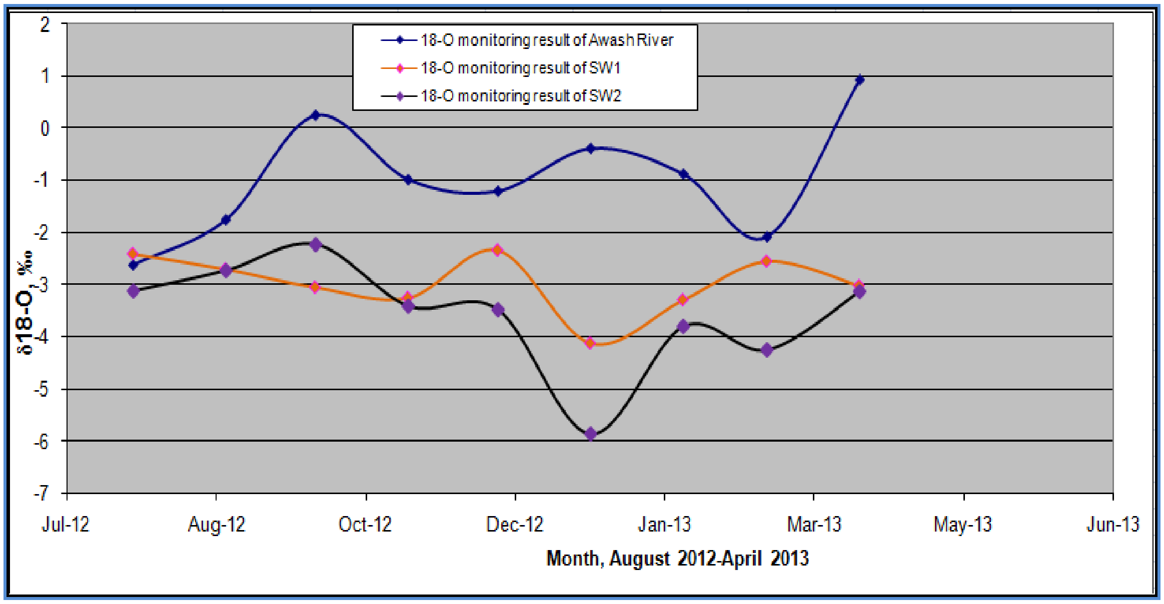

Figure 5.6: $\delta^{18}O$ monitoring plot for R11, SW1 and SW2 (Along traverse-2)

From figure 5.5, it is also possible to estimate roughly the groundwater flow velocity in Allydegi plain using the monitoring result of Awash river with traverse-1 boreholes distance between them. Distance between Awash river monitoring site @ melka-sedi(R11) and BH18 in Allydegi plain is about 14.4 km and the lag time for the $\delta^{18}O$ enrichment signature shows in a well is about 1 month. Therefore the roughly estimated ground water flow velocity is about $5.6x10^{-3}$ m/sec.

5.4. Source Identification of leakage at the left Abutment of Kesem Dam

Kesem Dam is located at about 245 km Asphaltic road northeast from Addis Ababa city to Beseka lake and turns to northwest off-road 45km distance all weather gravel road constructed for the supply of water for irrigation. Currently, Leakage problem encountered at the left abutment which may create serious problems related to the stability of dams. Many seepage problems and failure of dams have occurred because of inadequate seepage control measures (Freez and Cheery, 1997). Therefore, Determination of source, rate and path of leakage is very important as precisely as possible requires the combined use of different techniques. Some cases of abnormal dam seepage are related to reservoir leakage and or the leakage derives from the adjacent catchment. This kind of leakage is geological, reservoir or catchment infiltrating water flows into the dam's structure through weak strata in the dam region. Therefore, geology as well as dam integrity needs to be considered when abnormal dam seepage occurs.

Water samples from the reservoir, hot well at the dam axis, filter drainage (Toe drain) and leakage were collected for the stable isotope analysis. To support the monitoring result of hydrochemical parameters (EC and Temperature) as well as measurement of water level of reservoir and piziometric water level of the well at dam axis to assess the source of leakage. The water sample collection sites location illustrated in Table 5.2 and Figure.5.7.

Table 5.2: Location and stable isotope results of water points in kesem dam

No.	ID	Month	Data Source	LOCALITY	UTME	UTMN	SOURCE	$\delta^{18}O$	δD	Temp .ºC
1	KDLA 1	April,2014	Primery data	Kesem Dam @Left abutment	598557	1011161	Left Abutment	-2.02	-8.11	37.0
2	KDR	April,2013	Primery data	Kesem Dam @ Reserviour	596844	1010793	Reservoir	-0.44	-0.04	28.2
3	KDTd	April,2015	Primery data	Kesem Dam@Toe drain	598557	1011152	Toe drain	-1.67	-3.34	31.1
4	KDW	April,2016	Primery data	Artessian hot well@Kesem Dam axis	598579	1011118	Well	-2.31	-10.46	52.0
5	RGW	Previous data	Previous work	Regional ground water(well)			Well	-3.03	-14.01	

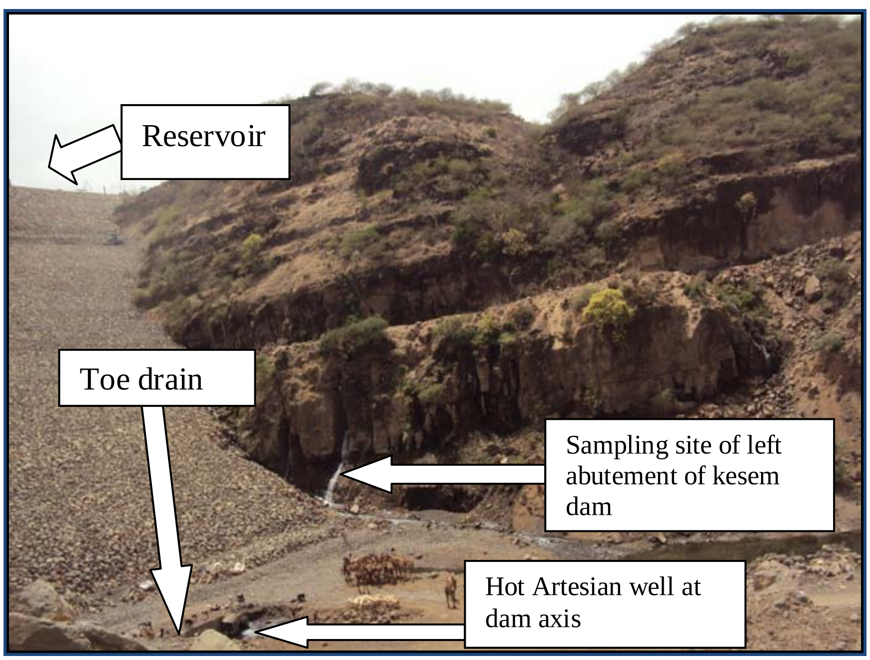

Figure 5.7: Plate showing location of water sampling sites

Stable isotopes, δD and $\delta^{18}O$ are ideal conservative tracers of water sources, they are mainly used in the identification of water from different origins. They are also applied in cases when there is isotopic stratification of deep reservoirs. In general, two waters with different hydrogeologic origin will have a different isotopic composition. This isotopic contrast is used as a natural water tracer, which allows identification of water of different origins and mixing process (Fritz and Fontes, 1980). The application of the technique in the study of dam leakages is Valuable when waters with different isotopic composition exist at the site. When there is an isotopic contrast between the waters in the study area this technique is very useful to distinguish source of leakage.

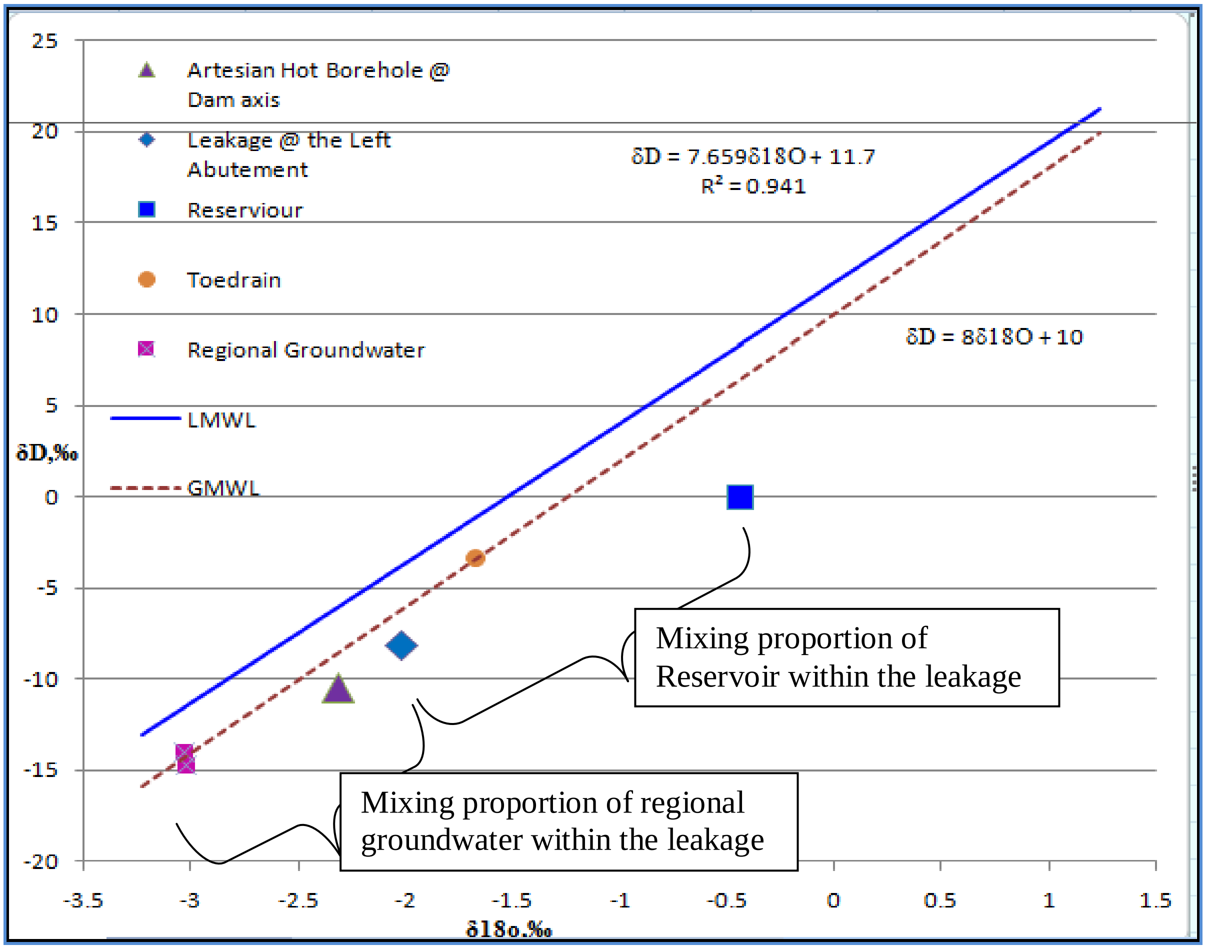

Figure 5.8: Scatter plot of water points stable isotope ratio related with LMWL/GMWL

The relationship between δD and $\delta^{18}O$ for the waters involved at kesem dam reservoir, artesian well at dam axis, Toe drain and leakage at left abutment. The relation shows that there is a strong rock-water interaction exists and the leakage water is the mixed water of groundwater (about 58%) and reservoir (about 42%) water. The mixing ratio is estimated using $\delta^{18}O$ values of water points. However, it is one time sampling result and generally the result doesn't support the hydrochemical and water level monitoring results, In addition to the stable isotopes result, monitoring of hydrochemical parameters (EC, Temperature), piziometric water level of the well at dam axis and water level of reservoir were carried out since November 2012.

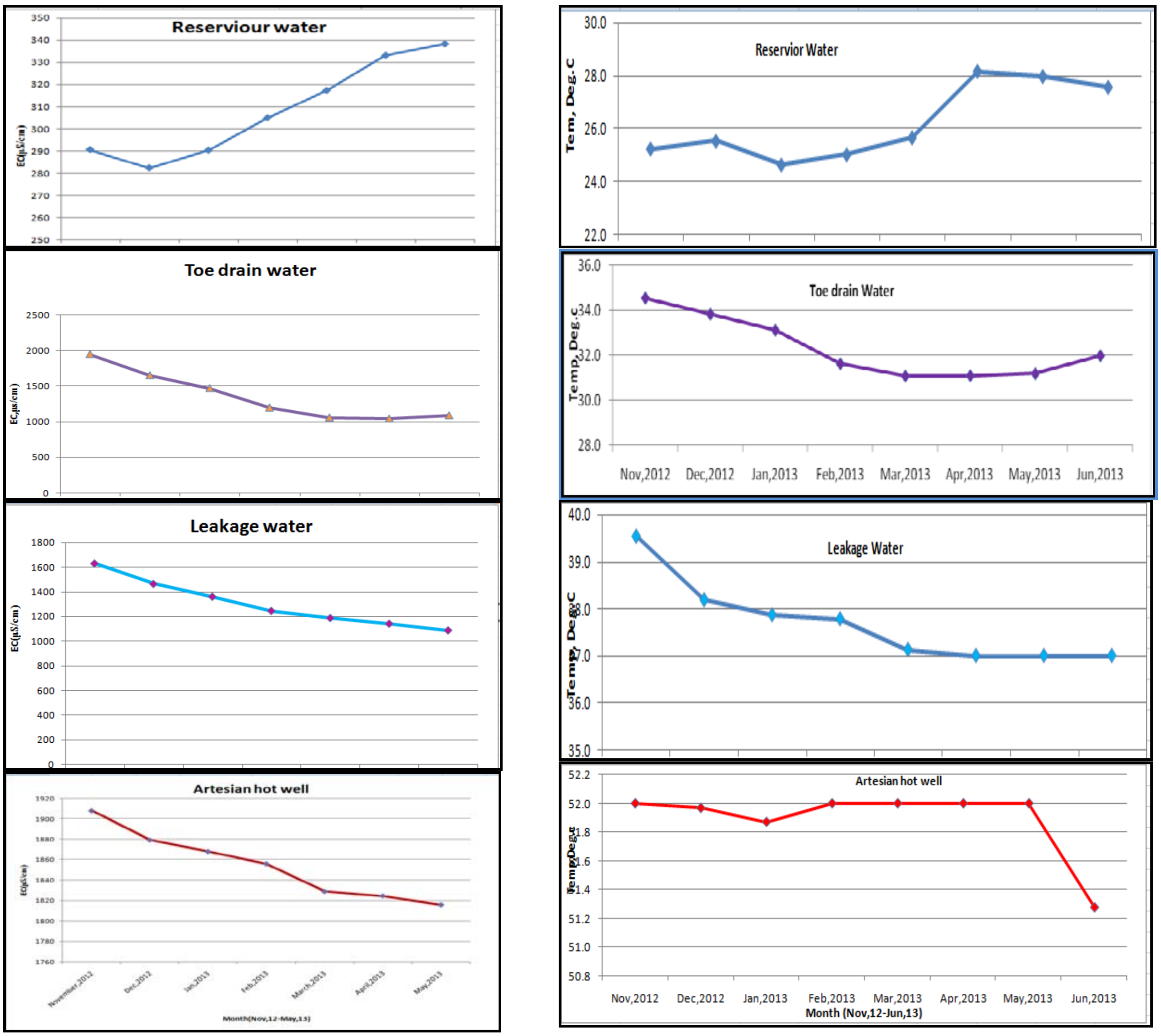

Figure 5.9: Electrical conductivity and Temprature monitoring graph for Kesem Dam water points
(Reserviour,Toe drain, Leakage and Artesian Hot well at Dam Axis)

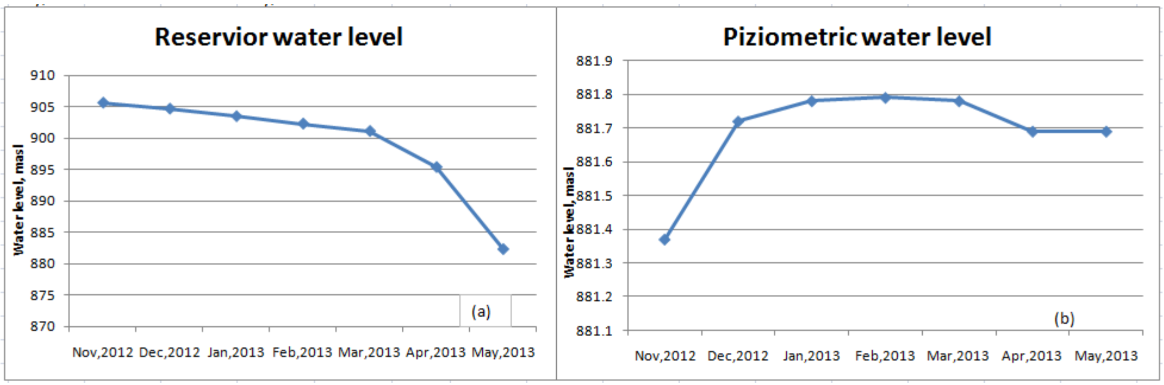

Figure 5.10: Water level monitoring graph for (a) Reserviour and (b) Artesian well at Kesem Dam axis (Nov,2012-to-May,2013)

Monitoring result of electrical conductivity and temperature as a function of time of water from Toe drain, leakage and artesian well shows gradual decrease and the trend of constant value for the last three-months, whereas the reservoir water conductivity and temperature increases (Figure 5.10). The higher value of conductivity and temperature especially for the leakage and borehole is associated with the NW-SE trending step faults(Marginal fault) intersected by W-E fault to give up heat from the deeper source through fractures to dissolve the minerals to enhance the electrical conductivity of leakage water as well as water from the well. Beside these result, the water level monitoring graph (Figure 5.10) also implies that the level of reservoir water dropped 5.65m and the piziometric water level increases only about 0.56m for the last seven-months. It is also well-known that the leakage water level is about 20m above the pizeometric water level and the regional groundwater level is far below the reservoir water level.

Thus, the monitoring results, the location of leakage above the piziometric water level and the regional groundwater level far below the reservoir water level illustrate that the source of leakage water is most likely from the reservoir water.

5.5. Tritium

In the earth, small amounts of natural tritium are produced by alpha decay of lithium-7. Naturally, it is also formed by bombardment of nitrogen by neutrons in cosmic radiation results with decay product of carbon-12 and tritium. Tritium atoms then combine with oxygen, forming water that fall as precipitation. Tritium has two neutrons in its nucleus which makes it unstable and it is therefore a radioactive isotope of hydrogen. This instability cause tritium to decay spontaneously to helium-3(^3He) through beta decay and during this decay process, a beta particle (high energy electron) is released. (Mazor, 1991).

Tritium has a half life of 12.32 years. The most common forms of tritium are tritium gas and tritium oxide also named tritiated water or HTO. Naturally occurring tritium exists in concentrations of about 1-to-5TU prior to atmospheric nuclear bomb testing in the 1950s, tritium's natural average concentrations ranged from approximately 2 to 8 TU. Approximately 1.13 x 109 TU were added in the northern hemisphere from atmospheric nuclear bomb testing with the largest tritium concentrations peaking in 1963. Since cessation of atmospheric nuclear tests, tritium concentrations have dropped to between 12 and 15 TU, although small contributions from nuclear power plants occur (Clark and Fritz, 1997). Tritium concentrations are measured by a scintillation counter which measures the ionizing radiation in a sample and as reported in tritium units (TU) where 1 TU is defined as the presence of one tritium in 10^{18} atoms of hydrogen. Because most tritium is disseminated in the environment as water, it enters the hydrologic cycle as precipitation and eventually becomes concentrated in levels detectable in groundwater. Tritium atoms then combine with oxygen, forming water that subsequently falls as precipitation.

Because groundwater tritium concentrations reflect atmospheric tritium levels when the water was last in contact with the atmosphere, it can be used to date groundwater recharge. Due to the tritium values vary both spatially and temporally which is not significantly affected by chemical reactions, therefore tritium values in water samples used to know the age of groundwater.

Nineteen Water samples were collected during field work and submitted to AAU school of earth science laboratory for ^3H analysis. However, it was not possible to conduct the analysis due to the chemical problem. Hence, only six primary and eleven secondary ^{3}H data were collected from different sources (AAU and WWDSE) used to characterize the groundwater system of the area (Annex-VI).

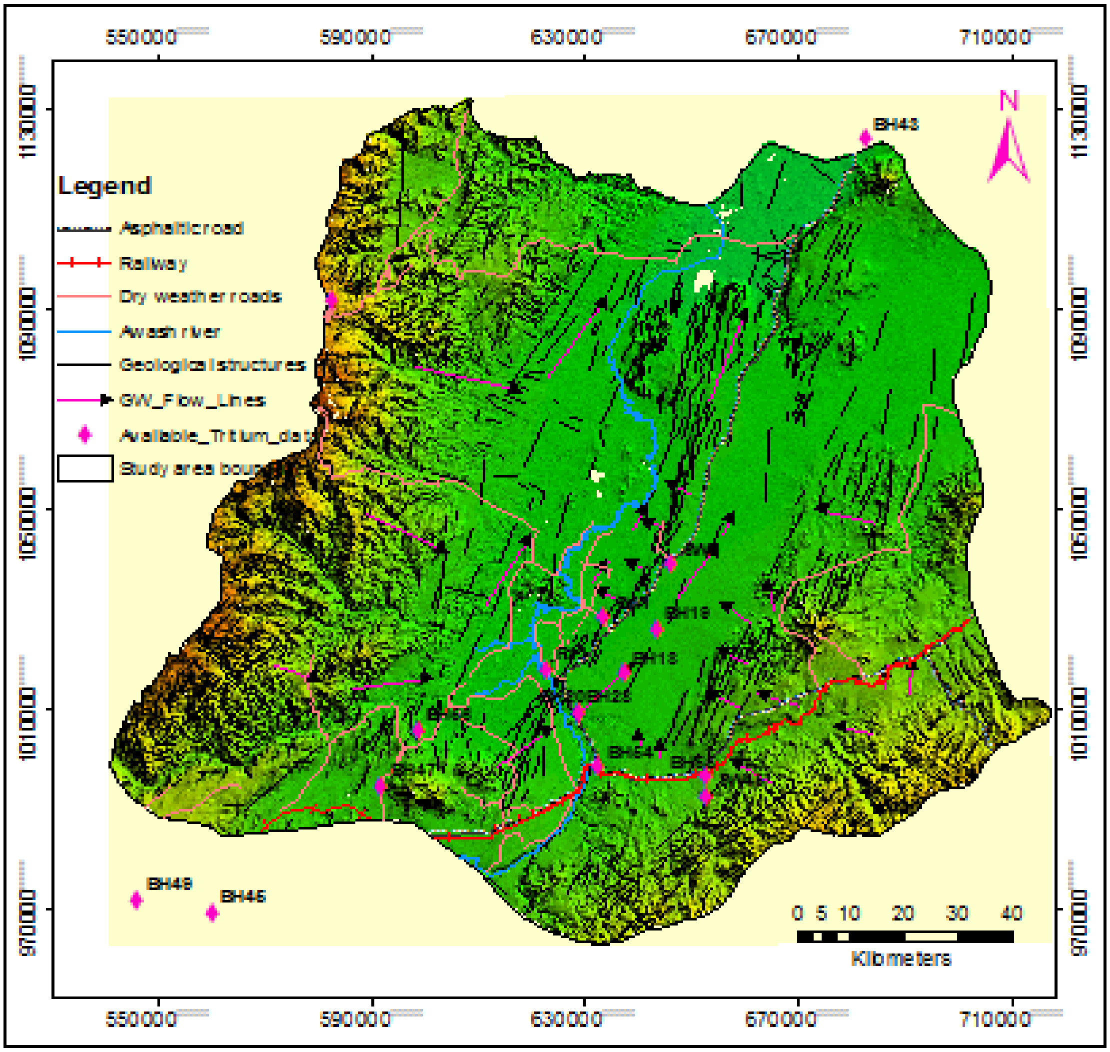

Figure 5.11: Available Tritium data distribution map

The limitation to use ^{3}H data is most of the available data were located along the regional ground water flow direction (Figure 5.11) through Allydegi plain rather than the highlands surrounding the lowlands(rift floor) of the area. Hence consideration was given only for Allydegi plain.

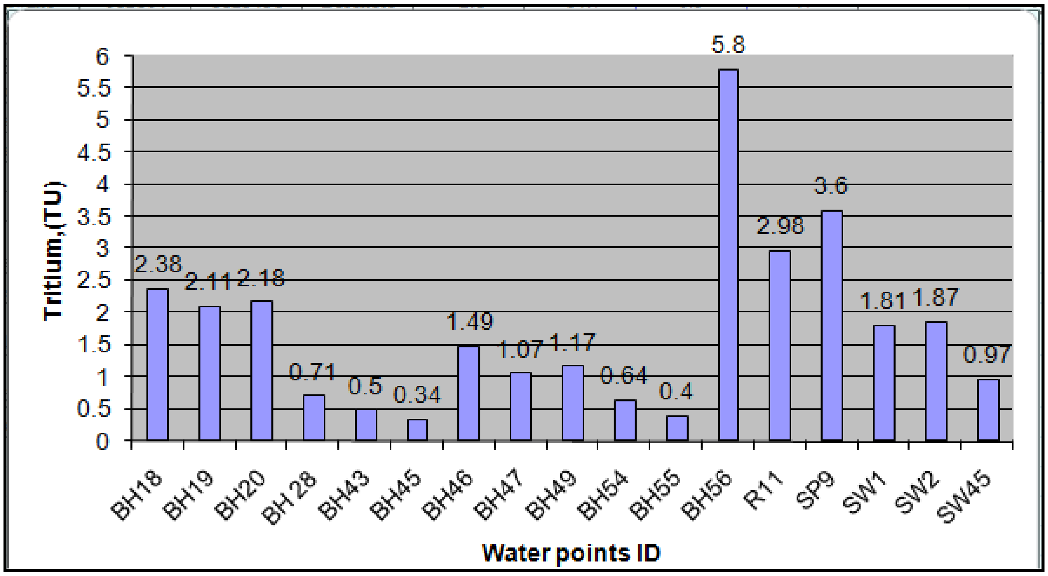

Figure 5.12: Tritium value of the water points

Groundwater age estimation using tritium only provides semi-quantitative, which is based on Mazor (1991) groundwater age classification;

- Water with <0.8 TU indicates a pre-1952 age
- Water with significant tritium concentration in practice >10 TU is of a post -1952 age
- Water with little, but measureable, tritium(0.8-10TU) indicates a mixture of pre-1952 age and post-1952 age

Among the water samples: BH56, SP9 and R11 have higher concentration (Figure 5.12) of tritium which could be most likely due to fast selective recharge through fractures. It is clearly indicates that high tritium value is indicated in isotope monitoring boreholes (BH20, SW1, BH20 and BH18) located in Allydegi plain depicts mixing of Awash river.

In general, most of water points located in Allydegi plain have tritium value in between 0.5 and 10 showing that they are recharged before and after 1952 which are also found under recharging system. According to Wakgari (2010), the lower value of tritium (<0.5TU) in boreholes (BH43, BH45 and BH55) which are located in active thermal field(WFB) of rift floor is most probably due to the ongoing decay of tritium associated with slow ground water flow through granular media.

6. Conclusions

The study area, which is located in the complex volcano-tectonic processes of the Main Ethiopian rift valley, is one of the areas marked by significant water supply Problems. Hydrogeochemistry and isotope tracers with conventional hydrological and hydrogeological methods were used in order to investigate the groundwater flow system and addressing questions like where water goes when it rains, what pathways it takes to the stream and how long water resides in the catchment. In order meet the objectives, collection of Chemical and isotope data of boreholes, springs, rivers and lakes were used and organization and interpretation were carried out by using statistical as well as geochemical methods.

The piper plot shows that most of the groundwater in the area is characterized by four major water types. These are: Ca-Na-HCO_3, Na-Ca-HCO_3, Na-HCO_3 and Na-HCO_3-Cl water types. Water group of Ca-Mg-HCO_3 is located in the highland areas characterized by recharge area waters as an early stage geochemical evolution. Na-HCO_3 type water is an evolved water types from highland and escarpments of Ca-Mg-HCO_3 and Na-Ca-HCO_3 water types located in the center of the study area along with active thermal fields of central rift which is most likely under active rock-water interaction phase. Na-HCO3-Cl and/or Na-HCO3-SO4 type waters are highly concentrated water types located in the northern sector which characterizes the discharge zone of the present study area. It reveals that the groundwater system of the area evolves from Ca-Mg-HCO_3 type to Na-HCO_3-Cl or Na-HCO_3-SO_4 water types, with progressive increasing of Residual Alkalinity and TDS.

The hierarchical cluster analysis classified the study area groundwater in to three and six identical major and minor clusters based on the eleven hydrochemical parameters(TDS,PH, Na^+, K^+, Ca^{2+}, Mg^{2+}, Cl^-, $HCO3^-$, $SO4^{2-}$, $NO3^-$ and F^-). The result of HCA shows that the groundwater flow direction is from Mieso, Bordede, Asebot and Fentale towards Gewane (Northern direction) through Allydegi plain and from northwestern plateau through Dulecha-Bahiri towards northern direction. It is strongly controlled by the existing geological structures (Faults) which are supported by the conventional geological, hydrogeological and hydrological approaches.

The result of inverse geochemical modeling depicts that processes such as dissolution of silicate, calcite, anhydrite and halite minerals, cation exchange of Ca^{2+} replaced in clay surfaces by Na^{+}, precipitation and/or weathering of clay minerals (Calcium-montimorilonite, k-mica, chalcedony, Allunite, illite) with a consumption of CO_2 (g) as a heat from deeper source through fractures control the groundwater chemistry of the area. Beside these, from the correlation of $\delta^{18}O$ as a function of chloride content of the groundwater implies that rigorous evaporation and dissolution can be discriminated as salinity sources without ignoring the impact of Beseka Lake after draining to Awash river.

Stable isotopes study of the present study area distinguishes the groundwater origin and recharge mechanism. The result illustrates that the ground water system is recharged from the combination of direct/diffuse recharge, from highlands that bounds the study area through fractures, faults or cavities and from Awash river. Waters of the study area depleted in heavy isotopes which indicate that the connectivity of modern rainfall with Aquifers of the area. Isotope monitoring result of Boreholes in Allydegi plain and Awash river also testifies the Awash river recharges the Allydegi plain and recharge of fractionated water in rift floor which testifies the strong rock water reaction along flow paths. The estimated groundwater recharge of the study area using CMB method is 98.11mm/yr. i.e. 15.12% of the annual rainfall amount (649.4mm/yr) and the roughly estimated ground water flow velocity using isotope monitoring results is about $5.6x10^{-3}$ m/sec. Most of water points located in Allydegi plain have tritium value in between 0.5 and 10 showing that they are recharged before and after 1952 which are also found under recharging system.

The relationship between δD and $\delta^{18}O$ for the waters involved at kesem dam reservoir, artesian well at dam axis, Toe drain and leakage at left abutment shows that the water of the leakage is the mixed water of groundwater and reservoir water. However, the monitoring (EC, temperature, water level of reservoir and piziometric well) results of such water points doesn’t agreed with the monitoring results that a combination of techniques in addition to the existing assessment work to discriminate the source of laekage and to find the most important measures for the remedial measures to prevent the excess seepage which create a serious problems related to the stability of dam.

7. References

Adane Bekele (1999).Surface water and ground water pollution problems in the upper Awash river basin, Ethiopia. Unpublished M.Sc. Thesis, Turun Yliopisto University of Turku.

Addisu Deresa (2012).Hydrogeochemical and Isotope hydrology in investigating groundwater recharge and flow processes, southern Afar,Eastern Ethiopia

Tamiru Alemayehu, Tenalem Ayenew and Seifu Kebede (2006). Environmental isotopes and hydrochemical study applied to surface water and groundwater interaction in the Awash river basin.

Asfaw Aymeku (2006). Hydrogeology of the Alleiydege Plain and its Environs Middle Awash valley, Afar Region).Unpublished M.sc.thesis, AAU.

Ashley R.P and Lloyd J.W. (1978). An example of the use of factor analysis and cluster analysis in groundwater chemistry interpretation. J. Hydrology 39, 355-364.

Bizuneh Bekele (2011). Hydrochemical and isotopic characteristics of the groundwater system of Allaydege plain. Unpublished M.sc.Thesis, AAU.

ChebotarevJ .I. (1955).``Metamorphism of natural waters in the crust of weathering.``Geochim.Cosmochim. Acta. 8,137-170.

Cook P. G. and Herczeg A. L. (2000). Environmental tracers in subsurface hydrology. Kluwer Academic Publishers, Boston.

Craig H. (1961). Standards for reporting concentrations of deuterium and oxygen-18 in natural waters. Science.133, 1833-1834.

Davis S. N., D. Cecil, M. Zreda and P. Sharma (1998). Chlorine-36 and the initial value problem Hydrogeology Journal. 6, 104-114.

De Vries J .J and Simmers I. (2002). Groundwater recharge: an overview of processes and challenges. Hydrogeol. Jo.10, 5-17.

D.T.Currey (1973). Earth Resources Technology Satellite-I usage and additional ground water studies in the Awash valley. Hydrogeological consultant, FAO.

D.T. Currey (1973). Geomorphic, geologic and groundwater studies in the awash valley hydrogeological consultant, FAO.

Edmunds W.M. and Smedley P. (2000). Residence time indicators in groundwater: the east midlands triassic sandstone aquifer. Appl. Geochem. 15, 737–752.

Eggleton R.A., Foudoulis Chris and Varkevisser Dane (1987).Weathering of Basalt Changes in Rock Chemistry and Mineralogy: Clays and Clay Minerals. 35, 161-169.

Evdsa H. (1989). Master Plan for the Development of Surface Water Resources in the Awash Basin, Final report.

FAO (1998). Crop Evapotranspiration: Guidelines for Computing Crop Water Requirements. Irrigation and Drainage Paper 56. Rome, Italy.

Fetter C.W.(1994). Applied hydrogeology, Prentice hall, university of Wisconsin-oshkosh,Fourth edition.

Freeze R.A. and Cherry J.A. (1979). Groundwater. Prentice-Hall, Englewood Cliffs. N.J USA. 603pp.

Fritz P. and Fontes J. (1980). Handbook of Environmental Isotope Geochemistry Elsevier Pub.Co.NY.

Güler C. and Thyne G.D. (2003). Hydrologic and geologic factors controlling surface and ground water chemistry in Indian Wells-Owens valley area, south eastern California USA. J. Hydrology. 285, 177-198.

Guler C., Thyne G. D., Mccray J. E. and Turner A. K. (2002). Evaluation of the graphical and multivariate statistical methods used for classification of water chemistry data.Hydrogeology Journal. 10, 455–474.

Handa B. K. (1975). Geochemistry and genesis of fluoride-containing ground waters in India. Groundwater. 13, 275–281.

Hem J.D. (1989). Study and Interpretation of the Chemical Characteristics of Natural Water.Water Supply Paper 2254, 3rd edition, US Geological Survey, 263 pp.

IAEA (1998). Water and environment, Issue number-4.

Kazmin V. (1972). Geological map of Ethiopia, 1:2,000,000scale. Geological Survey of Ethiopia.

Kazmin V.and Berhe S.M. (1978). Geology and development of Nazreth area, Northern Ethiopia. Ethiopian Institute of Geological Surveys.

Seifu Kebede (2004). Environmental isotope and geochemistry in groundwater and hydrology lake cases from Blue Nile basin, main Ethiopian rift and Afar, Ethiopia, PhD.Thesis,University of Avignon.

Seifu Kebede, Travi Y., Tamiru Alemayehu and Tenalem Ayenew (2005). Groundwater Recharge Circulation and geochemical Evolution in the source region of the Blue Nile river Ethiopia. Appl. Geochem. 20, 1658-1676.

Kendall C. and McDonell J. J. (1998). Isotope tracers in catchment hydrology Elsevier Amsterdam.

Ketema Tadesse and Heroic Ferdinand (1983). Groundwater Resource of the Allaidege plain.

Lerner D.A., Issar A. S .and Simmers I.(1990). Ground water recharge. A guide to understanding and estimating natural recharge. International Contributions to Hydrogeology Verlag Heinz Heise. 8, 245.

Mezemure Hailemeskale (1983). Hydrogeology of Southern Afar and adjacent areas (Ethiopia) supported by interpretation of Landsat imagery, unpublished Msc. thesis, International Institute for Aereal survey and Earth Sciences (ITC) Enschede ,the Netherlands.

Parkhurst D. L. and Appelo C. A. J. (1999). User's Guide to PHREEQC (Version 2): A Computer Program for Speciation, Batch-reaction, One-dimensional Transport and Inverse Geochemical Calculations, U.S. Geological Survey Water Resources Investigations Report .99-4259, 286 p.

Plummer L. N., Busby J.F., Lee R.W. and Hanshaw B.B. (1990). Geochemical modeling of Madison aquifer in parts of Montana, Wyoming, and South Dakota. Water Resource Research 26, 9, 1981–2014.

Plummer L.N., Parkhurst D.L. and Thorstenson D.C.(1983). Development of reaction models for ground-water systems. Geochim. Cosmochim. Acta. 47, 665–686.

Plummer M. A. (1996). Secular vabriation of cosmogenic nuclide production from chlorine-36 in fossil pack rat middens, M.sc.Thesis, N. M. Inst. of Mining and Techno. Socorro.

Pradeep K. Aggrawal (2007). Environmental isotopes in ground water studies. Groundwater.

Seifu kebede, Yves Travi and Susanne Stadler (2010). Ground waters of the central Ethiopian rift: diagnostic trends in trace elements, $\delta^{18}O$ and trace elements. Hydrogeology Journl.

Simmers I. (Ed) (1997). Recharge of phreatic aquifers in (semi-) arid areas. International Association of Hydrogeologists (IAH) 19. A.A. Belkema, Rotterdam. 277 pp.

Sophocleous M. (2004). Groundwater recharge, in Groundwater, [Eds. Luis Silveira, Stefan Wohnlich, and Eduardo J. Usunoff], in Encyclopedia of Life Support Systems.

Stephen E. Grasby, Ian Hutcheon and H.R. Krouse (2000). The influence of rock water interaction on the chemistry of thermal springs in western Canada. Applied geochemistry. 15, 439- 454.

Tenalem Ayenew (2007). The distribution and hydrogeological controls of fluoride in the ground water of central Ethiopian rift and adjacent highlands. Hydrogeology Journal.

Tenalem Ayenew and Tamiru Alemyahu (2001). Principle of Hydrogeology, AAU press.

Tenalem Ayenew, Seifu Kebede and Tamiru Alemyahu (2008). Environmental isotopes and hydrochemical study applied to surface water and groundwater interaction in the Awash River basin. Hydrol. Process. 22, 1548–1563.

Tewodros Mulugeta Chichaybelu (2011). Geophysical investigation for ground water potential assessment and mapping structures at Allidege plain, south Afar, Ethiopia. M.sc.Thesis Addis Ababa University.

Tilahun Azagegn (2008). Hydrogeochemical characterization of aquifer systems in upper awash basin and adjacent Abay plateau using geochemical modeling and isotope hydrology. Unpublished M.Sc. Thesis. University of Addis Ababa, Addis Ababa, Ethiopia.

Wakgari Furi (2010). Fluoride enrichment mechanism and geospatial distribution in the volcanic aquifer of Middle Awash, Northern MER, Journal, France.

WHO (1993). Guidelines for drinking water quality. Geneva.

WoldeGabriel G., Aronson J.L. and Walter R.C. (1990). Geology, geochronology, and rift basin development in the central sector of the Main Ethiopian Rift. Geological Society of America Bulletin. 102, 439–458.Ground water resource evaluation hydrogeological report.

Annex- I: Mean monthly climate data from different stations of the study area
(Data from Ethiopian Metrological agency)

Stations	UTM,E	UTM,N	Elevn, msasl	Recorded Period	Jan	Feb	Mar	Apr	May	Jun	Jul	Aug	Sep	Oct	Nov	Dec	Annual
Rainfall, mm																	
Asebe teferi	703345	1002751	1773	1980-2010	15	28	93.2	107	101	58	147	151.5	126	73	18	12	805.3
Awara Melka	608565	1012691	784	1971-2010	17	49	58.8	44	27.8	16	89.5	109.5	35.9	24	14	17	501.3
Awash-7	628052	993844	927	1985-2010	17	33	59.5	71	42.5	25	120.5	133.1	60.6	30	13	15	620.7
Bedesa	694755	985197	1713	1957-2010	11	21	79.1	145	132	80	142.2	151.3	154	70	32	9.6	1025
Debre Birhan	556351	1067959	2800	1978-2010	10	21	49	52	38.3	53	288.7	265.9	85.1	19	4.8	3.7	896.1
Methara	617065	987125	1047	1984-2010	12	27	48.3	48	34.4	25	122	116	42.1	24	6.1	8.3	493.9
Gewane	681663	1123060	622	1980-2010	13	35	67.4	52	26.7	8.6	94	106.3	32.7	26	7.2	8.6	477.1
Mieso	692944	1020713	1330	1962-2010	22	34	91.2	112	52.6	47	129.5	149.8	88.9	42	22	10	800.8
Melka worer	629750	1032343	741	1974-2001	3.1	49	67.9	58	38.5	25	115.9	123.5	59	25	8.2	2	574.4
Temperature, ^{0}C																	
Asebe teferi	703345	1002751	1773	1980-2010	19	20	20.6	21	21.4	22	20.8	20.6	20.6	21	20	19	20.4
Awash-7	628052	993844	927	1985-2010	24	26	27.4	28	29.4	31	27.9	27	27.8	27	25	24	27
Bedesa	694755	985197	1713	1968-2010	19	20	20.1	20	20	20	20.1	19.8	19.6	19	18	18	19.4
Methara	617065	987125	1047	1985-2010	23	25	26.3	27	28	29	26.8	26	26.9	25	23	22	25.7
Gewane	681663	1123060	622	1980-2010	25	27	28.4	30	31.1	33	30.8	29.6	30.2	28	27	26	28.8
Mieso	692944	1020713	1330	1989-2010	20	21	22.9	24	25.2	26	24.4	23.8	23.5	23	20	19	22.7
Melka Werer	629750	1032343	741	1984-2010	22	24	26.3	27	28.2	29	28.4	27.1	27.5	25	23	22	25.7
Evaporation, mm																	
Gewane	681663	1123060	622	200-2003	203	263	276.2	321	341	382	307	225	206	197	238	170	2867
Metehara	617065	987125	1047	1985-2002	259	244	276.8	245	288	311	239	189	201	276	279	259	3073
Wind speed, m/s																	

Stations	UTM,E	UTM,N	Elevn, msasl	Recorded Period	Jan	Feb	Mar	Apr	May	Jun	Jul	Aug	Sep	Oct	Nov	Dec	Annual
Asebe Teferi	703345	1002751	1773	1980-1993	0.5	0.6	0.6	0.7		1.1	0.9	1	0.9	0.7	0.6	0.6	0.8
Gewane	681663	1123060	622	1979-2003	1.4	1.5	1.8	2.1		3.4	3.5	4.4	2.4	1.8	1.6	1.4	2.2
Methara	617065	987125	1047	1984-2003	1.8	1.9	1.9	1.7		2.3	2.4	2	1.5	1.5	1.7	1.7	1.8
								Humidity, %									
Asebe Teferi	703345	1002751	1773	1980-1993	74	76	74.9	75		73	74.6	75.7	75.3	75	74	73	73.3
Melka Werer	629750	1032343	741	1973-2000	53	52	50.9	50		39	51.5	57.9	53.7	49	49	52	50
Methara	617065	987125	1047	1986-2003	58	58	58.7	61		50	59.9	63.6	62.7	55	54	55	57.5
Mieso	692944	1020713	1330	1979-2000	53	53	53.1	59		50	58.3	59.1	57.8	51	50	50	54.1
							Sun shine duration, hrs										
Gewane	681663	1123060	622	1980-2007	8.9	8.2	7.7	8.6		9	7.9	8.3	8.8	9.6	9.9	9.8	8.6
Melka Werer	629750	1032343	741	1980-2007	8.7	8.5	8.5	8.3		8.5	7.1	7.2	7.9	9.1	9.6	9.2	8.5
Methara	617065	987125	1047	1973-2004	8.7	8.4	8.3	8.3		8.7	7.3	7.3	7.5	8.4	9.4	9.4	8.3
							Rainfall coefficient										
Asebe teferi	703345	1002751	1773	1980-2010	0.2	0.4	1.39	1.6		0.9	2.19	2.26	1.88	1.1	0.3	0.2	
Awara Melka	608565	1012691	784	1971-2010	0.4	1.2	1.41	1.1		0.4	2.14	2.62	0.86	0.6	0.3	0.4	
Awash-7	628052	993844	927	1985-2010	0.4	0.8	1.42	1.7		0.6	2.88	3.19	1.45	0.7	0.3	0.4	
Bedesa	694755	985197	1713	1957-2010	0.3	0.5	1.89	3.5		1.9	3.4	3.62	3.68	1.7	0.8	0.2	
Debre Birhan	556351	1067959	2800	1978-2010	0.3	0.5	1.17	1.2		1.3	6.91	6.37	2.04	0.5	0.1	0.1	
Methara	617065	987125	1047	1984-2010	0.3	0.7	1.16	1.2		0.6	2.92	2.78	1.01	0.6	0.1	0.2	
Gewane	681663	1123060	622	1980-2010	0.3	0.8	1.61	1.2		0.2	2.25	2.55	0.78	0.6	0.2	0.2	
Mieso	692944	1020713	1330	1962-2010	0.5	0.8	2.18	2.7		1.1	3.1	3.59	2.13	1	0.5	0.2	
Melka worer	629750	1032343	741	1974-2001	0.1	1.2	1.63	1.4		0.6	2.77	2.96	1.41	0.6	0.2	0.1	

Annex- II: Average Monthly River discharge Data (MCM) (Data from EMA, 1975-to-2009 G.C)

Stations	UTM,E	UTM,N	Area, Km^2	Jan	Feb	Mar	Apr	May	June	July	Aug	Sep	Oct	Nov	Dec	Annual
Awash Arba	629057	1008191	72	0	0.15	2.21	2.78	3.14	2.91	31.92	57.82	47.46	5.1	0.04	0	153.53
Awash @ Awash-7	629697	994554	19111	95.05	88.95	103.56	111.97	107.8	100.38	189.04	317.31	347.53	156.34	92.61	87.55	1798.1
Awash @ Melka Sedi	623213	1017163	21520	92.92	79.74	95.07	111.11	101.19	87.47	174.3	303.27	281.31	143.3	87.8	79.87	1637.35
Awash @ Melka werer	629097	1030148	31183	91.16	86.94	111.04	115.87	100.72	78.16	232.28	453.93	361.39	146.61	92.3	86.37	1956.8
Awash @ Methara	620856	981414	16417	61.03	56.27	61.31	63.3	67.77	60.2	105.27	195.4	220.91	83.58	54.78	56.59	1086.4

Annex- III: Existing wells data

Well ID	Local Name	UTME	UTMN	Elevation, masl	Water Strike,m	well depth, m	SWL, m	yield, l/s	Draw down, m	Specific capacity, l/s/m	Transimissivity, m^2/d
BH14	School	652507	996029	1118	65	350	62.27	6	56.06	0.11city	17
BH13	Awash shisht	633633	995225	962	200	252	101.17	20	37.64	0.53	83.4
BH12	Molalita	627464	1015684	823	78	192	75.66	50	1.12	44.6	7180
BH11	Arage	636415	1039961	733	6	262.5	3.6	50	26.61	1.88	306
BH57	Arategna	626003	1025081	745	4	196	0				
BH58	Sisalabur	641424	1007510	892	160	257	72.95				
BH59	Elfora	635543	1021775	817	94	236	68	34	26.41	1.29	325
BH29	Andido-2	647560	1040111	820	82	120	81	5.6			
SW13	Bilen	644586	1047321	735		42		0.5			
SW54	Tsebay Maremia	628562	1038760	734		50	6	5.6	1.61	3.48	587
SW55	Degakoma	630277	1042299	735	11	48	8				
SW56	Melka Worer	629045	1030474	742		84	5.3	5.6	3.56	1.57	230
SW15	Kerensa/Deyilu	624546	1017845	782		81	39	2.95			
SW16	Eiei-1	632337	1031448	741		84	12	2			
HDW10	Eiei-2/Inside Ginnery	632988	1031094	749		76	13	6.3	10.7	0.59	161
SW17	Berta	633107	1027266	776		82	34	5			
SW48	Alaydege	643277	1025555	814	90	120	75	2.6			
SW25	Gelsa	638732	1072353	721		140	108	4.2			
BH31	Awash Arba Town	628683	1008918	827		126	55	2.1			
BH34	Defence/Wuha Netib/	628311	1007852	817		118	39	6.2	3.81	1.63	513
BH30	Lalibela Const.	632471	1008252	833	160	194	65.78	5			
SW18	Hasoba Bilen	638824	1043036	738		100	18	4.8			
SW17	Hasoba	638824	1043036	738			18				
BH60	Gonita Birka	637070	1017179	829		140	85.72	3.5			
BH61	BurkaMisra	696722	1018866	1382	66	123	67	8	0.85	11.43	1400
BH62	Entiaso/Andido-2	647560	1040111	820	82	120	81	5.6			
SW42	Mieso Town	693001	1021056	1316			21	4.4			
SW20	Fayo	691053	1020494	1346	65	95	53	6			
BH9	Uda Keneni	685353	1017107	1414		129		5.1			
BH35	Tutuftu	685854	1009743	1535	175	196	87	5.6	84.02	0.07	4.06
SW47	Daga dhaba	681409	1009313	1400		151	53	5.6	4.95	1.13	150
BH63	Sabaka	676209	1005803	1353		150	67		20.7		50
BH64	Ufe/Negib farm/	681160	1014332	1469		118	81	1.5			
BH65	Kurfa Jarti	676671	1014620	1380		267	157				
BH37	Hayo	668814	1001716	1333		228	61	1	148.8	0.01	0.11
SW21	Kora	669172	1006483	1235		37	6	5.2			
BH66	Fugnan Ajo	668234	1011339	1327		272	162	0.4	93.65	0	0.59

Well ID	Local Name	UTME	UTMN	Elevation, masl	Water Strike,m	well depth, m	SWL, m	yield, l/s	Draw down, m	Specific capacity, l/s/m	Transimissivity, m^2/d
BH67	Lias	680061	1120521	595		113	9	4.2			
BH25	Military Camp	632412	998041	891	180	242	121	4	10.035	0.4	30.3
BH30	Defence/Arba Wonz/	628898	1007914	796		148	93	2.5			
BH31	Awash arba St. Michael	628543	1009148	830		160	60	5	5.06	0.99	122
SW35	Elfora	643300	1025542	815		162	77	5.5	7	0.79	96
SW27	Andido	646034	1038429	817		130	80	5.5	6.5	0.85	60.4
BH15	Bilen dora	643798	1019148	835		287	86	16	42.6	0.38	34.3
BH16	Hardim	645334	996709	1007		310	150	4	23.26	0.17	10.1
BH17	Medene	645424	996570	824		300	72	12	89.64	0.13	7.92

Annex- IV: Selected Borehole lithological log in Allydegi plain and Awash Valley

(I) BH23(Allydegi plain)

No.	Lithological Description	Depth (m)	
		Form	To
1	Top soil	0	1
2	Massive Basalt	1	10
3	Moderately weathered and fractured basalt	10	40
4	Reddish clay	40	66
5	Slightly weathered Ignimbrite	66	112
6	Rhyolite	112	200
7	Moderately welded tuff	200	256
8	Moderately altered and fractured Ignimbrite	256	314
9	Tuff	314	338
10	Scoraceous Basalt	338	500

(II)BH57(Allydegi plain)

No.	Lithological Description	Depth interval (m)	
		From	To
1	Top soil	0	4
2	Clay dominated boulder	4	18
3	Sand	18	24
4	Weathered Ignimbrite	24	76
5	Moderately welded tuff	76	86
6	Fractured and weathered ignimbrite	86	108
7	Highly fractured basalt	108	142
8	Reddish clay	142	146
9	Tuff	146	150
10	Moderately altered and fractured Ignimbrite	150	184
11	Moderately to highly fractured and altered basalt	184	340
12	Iron rich basalt	340	348
13	Moderately fractured and altered basalt	348	420
14	Slightly fractured basalt	420	440
15	Moderately fractured and altered basalt	440	492
16	Gravel	492	504
17	Moderately to highly fractured and altered basalt	504	510

(III) BH58(Allydegi plain)

No.	Lithological Description	Depth (m)	
		Form	To
1	Top soil	0	4
2	Gravel outwash	4	18
3	Massive Basalt	18	42
4	Unwelded Tuff	42	84
5	Moderately weathered & fractured basalt	84	100
6	Unwelded Tuff	100	168
8	Massive basalt	168	182
9	Paleosol	182	184
10	Welded Tuff	184	204
11	Moderately fractured basalt	204	210
12	Welded Tuff	210	224
13	Massive basalt	224	234
14	Ignimbrite	234	264
15	Moderately altered and fractured basalt	264	278
16	Scoraceous Basalt	278	504

(IV) BH59(Allydegi plain)

No	Lithological Description	Depth (m)	
		Form	To
1	Top soil	0	24
2	Weathered Rhyolite	24	70
3	Coarse gravel with clay	70	122
4	Welded tuff	122	150
5	Massive basalt	150	176
6	Slightly fractured basalt	176	208
7	Moderately-to-highly fractured and altered basalt	208	404
8	Highly altered and fractured basalt	404	444
9	Slightly to moderately fractured basalt	444	462
10	Moderately to highly altered and fractured basalt	462	504

(V) BH11(Awash Valley)

No.	Depth	Depth(m)	
		From	To
1	Clay	0	20
2	Clay plus gravel intercalation	20	48
3	Boulders	48	58
4	Silty clay	58	68
5	Circulation loss	68	78
6	Sandy gravel	78	196

Annex- V: Hydrochemical data of water points in the study area, units (all in mg/l). Except EC,µs/cm, T-Temprature,°C
ND-Not determined TH-Total Hardness Alk-Alkalinity

No.	ID	Data Source	UTME	UTMN	Elevn, masl	Depth, m	EC	TDS	T	PH	Na^+	K^+	Ca^{2+}	Mg^{2+}	Cl^-	$NO3^-$	F^-	$HCO3^-$	$SO4^{2-}$	TH	AlK	WATER_TYPE
1	BH1	Primary data	626352	999668	829	100	827	530		7.8	122	69	16	4.8	49.14	0.31	1.25	253.8	74.23	60	290	Na-K-HCO3-SO4
2	BH6	Primary data	643091	1027968	809	505	837	534		8.1	178	8.5	8	3.84	60.07	2.5	0.66	329.4	72.56	36	270	Na-HCO3
3	BH7	Primary data	643091	1027968	809	505	1481	1022		7.7	250	6.3	71.2	23.04	210.3	32.2	1.44	268.4	221.43	274	220	Na-Ca-Cl-SO4-HCO3
4	BH11	WWDSE	636415	1039961	1535	262.5	2840	1704		8.1	565	7	18.48	5.1	434.2	3	2.6	507.28	384.5	67.2	415.8	Na-Cl-HCO3-SO4
5	BH12	WWDSE	627464	1015684	1400	192	885	534	34	7.5	123	19	34.96	8.96	68.16	7.37	1.52	281.31	47.08	124.2	230.58	Na-Ca-HCO3-Cl
6	BH13	WWDSE	633633	995225	1353	252	632	364	37	7.8	28	8.9	55.2	22.4	39.36	7.2	1.13	221.36	39.3	230	181.44	Ca-Mg-Na-HCO3
7	BH14	WWDSE	652507	996029	1469	350	1189	771	37	7.5	115	25	101.4	28.08	116.16	1.85	0.87	401.14	130.8	367.4	328.8	Ca-Na-HCO3-Cl-SO4
8	BH15	WWDSE	643798	1019148	1320	287	711	483	44	8.1	150	7.7	24.4	16.56	40	1.056	4	245	60	130	300	Na-HCO3-CO3
9	BH16	WWDSE	645334	996709	1333	310	964	623	38	7.4	188	7.8	36.12	8.16	91	1.2	1.2	359	107	124	294	Na-HCO3-Cl-SO4
10	BH17	WWDSE	645424	996570	1235	300	468	306	49	7.7	80	5.6	22.68	6.63	25.75	8	0.47	210	24	84	172	Na-Ca-HCO3
11	BH18	WWDSE	637189	1016763	831.29	220	677	436		7.6	123	11.7	24.8	4.32	40.95	0.49	0.68	305	76.51	80	250	Na-HCO3-SO4
12	BH19	WWDSE	643290	1025519	814.82	150	866	564		7.2	147	16.5	24.8	8.64	60.07	1.86	1.38	326.96	109.48	98	268	Na-HCO3-SO4
13	BH21	WWDSE	636265	1011528	829	420	819	470		7.5	122	13.7	28	6.72	53.7	2.67	2.04	317.2	68.29	98	260	Na-HCO3
14	BH22	WWDSE	653300	998623	1077	419	710	440	35	7.2	86	4.3	47.2	12	39.13	0.38	0.67	341.6	56.55	168	280	Na-Ca-HCO3
15	BH23	WWDSE	639707	1028668	805	495	819	470	43	7.5	122	13.7	28	6.72	53.7	2.67	2.04	317.2	68.29	98	260	Na-HCO3
16	BH24	AAU	645330	996699	1007	310	893	580	32	7.8	118	10.7	37.24	19.15	41.86	13.74	0.89	435.54	54.45	172.9	357	Na-Ca-HCO3
17	BH25	AAU	632421	998837	894	210	660	460		7.4	82	8.7	50.16	12.77	21.84	5.55	0.66	336	17.9	178.6	409.92	Na-Ca-HCO3
18	BH26	AAU	653235	998628	1083	194	873	572	36	7.4	93	17.5	54.72	9.12	73.72	1.69	0.73	307.44	78.06	174.8	252	Na-Ca-HCO3-Cl
19	BH27	AAU	632418	998037	891	242	705	480	36	7.4	96	13	36.48	11.86	36.4	4.73	1.06	333.06	56.36	140.6	273	Na-Ca-HCO3
20	BH28	AAU	628683	1008918	827	126	692	464	34	7.3	62	9.3	76	5.93	39.13	10.48	0.72	353.56	39.51	214.7	289.8	Ca-Na-HCO3
21	BH29	AAU	647560	1040111	820	120	732	514		7.6	120	12	26.6	10.03	41.86	5.22	0.92	294	44.65	108.3	358.68	Na-HCO3
22	BH30	AAU	632421	998837	894	210	666	446	38	7.6	98	11.4	44	9.6	38.8	4.39	0.5	308.29	87.35	150	252.7	Na-Ca-HCO3-SO4
23	BH31	AAU	628683	1008918	827	126	699	500	32	7.4	110	8.6	74.4	0.96	43.54	4.73	0.68	373.32	34.57	190	306	Na-Ca-HCO3
24	BH32	AAU	632471	1008252	833	194	579	378	36	7.4	90	9.1	51.2	5.76	19.88	0.6	0.6	348.92	19.08	152	286	Na-Ca-HCO3
25	BH33	WWDSE	628683	1008918	740	126	683	440	26	7.4	56	8.5	72.8	16.5	41.3	10	0.8	338.2	37.13	249.7	277.2	Ca-Na-HCO3
26	BH34	WWDSE	628311	1007852	782	118	689	478	28	7.2	74	9.1	61.9	13.2	38.4	8	1	353.6	33	208.8	289.9	Na-Ca-HCO3

No.	ID	Data Source	UTME	UTMN	Elevn, masl	Depth, m	EC	TDS	T	PH	Na^+	K^+	Ca^{2+}	Mg^{2+}	Cl^-	$NO3^-$	F^-	$HCO3^-$	$SO4^{2-}$	TH	AlK	WATER_TYPE
27	BH35	WWDSE	685854	1009743	827	196	748	468	33	7.5	69	21	63.7	17.6	31.7	10	0	397.1	50.88	231.5	325.5	Ca-Na-HCO3
28	BH36	WWDSE	681409	1009313	817	151	775	505	32	7.7	53	3.6	111.9	18.7	24.96	13.5	0	486.8	12.1	356.4	399	Ca-Na-HCO3
29	BH37	WWDSE	668814	1001716	860	228	765	486	31	7.7	43	8.4	104.7	20.9	37.4	17.5	0.5	407.4	17.3	347.3	333.9	Ca-Na-HCO3
30	SW1	WWDSE	633279	1027937	774.05	90	981	600		7.4	190	17.5	15.2	9.6	63.71	1.81	3.79	441.64	77.85	78	362	Na-HCO3
31	SW2	WWDSE	646032	1038432	816.78	80	714	444		7.5	116	13	28	12.96	40.95	2.85	1	334.28	53.87	124	274	Na-HCO3
32	SW3	AAU	652583	992169	1125	100	926	622	36	7.6	85	13.5	60.8	27.36	58.25	15.43	0.81	435.54	59.02	266	357	Na-Ca-Mg-HCO3
33	SW4	AAU	639505	1028953	806	60	866	566	40	8.1	158	15.5	19	11.4	54.61	3.52	2.45	430.42	48.17	95	352.8	Na-HCO3
34	SW5	AAU	624546	1017845	782	81	1191	704	29	8.2	198	12	19	16.87	105.57	8.63	2.31	471.41	61.4	117.8	386.4	Na-HCO3-Cl
35	SW6	AAU	695877	1015842	1386	51	454	296		7.5	35	2.8	45.6	14.14	10.01	4.82	0.67	294.63	2	172.9	241.5	Ca-Na-Mg-HCO3
36	SW7	AAU	633107	1027266	776	82	992	666	35	8	194	17	11.4	9.12	63.71	3.17	10.24	461.16	56.74	66.5	378	Na-HCO3
37	SW8	AAU	633278	1027936	771	90	983	640	37	7.9	190	13.8	16	9.12	67.2	2.77	3.24	452.1	65.42	78	370.5	Na-HCO3
38	SW9	AAU	633107	1027266	776	82	999	650	38	7.9	184	15	16	14	66.25	3.41	2.88	488	64.88	100	400	Na-HCO3
39	SW10	AAU	639505	1028953	770	60	846	550	38	7.7	168	13.6	28	1.44	55.84	2.74	6.12	402.6	31.72	76	330	Na-HCO3
40	SW11	AAU	652583	992169	1350	100	916	598	36	7	76	17	90	12	58	10	1	424	64	272	348	Ca-Na-HCO3
41	SW12	AAU	597136	1011337	918	70	1845	1288	50	8.3	500	26.2	4.8	0.96	149.54	4.93	2.91	776.53	193.84	16	674.5	Na-HCO3
42	SW13	WWDSE	644586	1047321	821	42	906	608	38	7.7	174	11.7	22.3	8.1	57.6	1.5	2.2	440.7	35.6	88.8	361.2	Na-HCO3
43	SW14	WWDSE	629045	1030474	815	84	3010	1840		7.7	585	6.9	37.3	23.7	358.1	17.5	4	940.3	80	190.7	770.7	Na-HCO3-Cl
44	SW15	WWDSE	624546	1017845	752	81	1095	672	37	8	204	10.5	20.5	17.3	92.2	7	2.7	499.6	47.5	122.1	409.5	Na-HCO3-Cl
45	SW16	WWDSE	632337	1031448	751	84	1888	1212	30	7.6	355	19.5	31.9	15.4	239	10	3.68	602.1	41.25	143	493.5	Na-HCO3-Cl
46	SW17	WWDSE	633107	1027266	753	82	1004	630	28	7.8	186	16	18.2	11	65.3	8	4.4	463.7	57.75	90.8	380.1	Na-HCO3
47	SW18	WWDSE	638824	1043036	803	100	949	600	28	7.9	190	3.9	15.5	4.4	77.8	10	1.24	399.7	68.75	56.8	327.6	Na-HCO3-Cl
48	SW19	WWDSE	695877	1015842	803	51	662	424	30	7.7	44	5.6	84.6	19.2	20.2	10.5	1	399.7	6.6	290.6	327.6	Ca-Na-Mg-HCO3
49	SW20	WWDSE	691053	1020494	727	95	726	446	30	7.6	70	9.1	80.1	14.8	16.3	7	0.8	468.8	14.3	261.1	384.3	Ca-Na-HCO3
50	SW21	WWDSE	669172	1006483	885	37	865	562	31	7.5	60	4.6	209.3	45.1	188.2	29	0.15	491.9	68.75	708.2	403.2	Ca-Mg-HCO3-Cl
53	SW22	WWDSE	611700	1011072	773	ND	1760	1210	37	8.8	410	####	2.52	2.04	198.58	0.75	14	675.1	55.39	14.7	601.4	Na-HCO3-Cl
54	SW23	WWDSE	615346	1012359	765	ND	1825	1270	33	8.6	425	9.7	3.36	0.5	213.04	0.75	12.4	713.2	59.34	10.5	628.6	Na-HCO3-Cl
56	SW24	WWDSE	633818	1034813	751	ND	830	540	38	8.5	180	3.7	8.4	1.53	61.7	3.2	4	375.4	20	27.3	331.7	Na-HCO3
57	SW25	WWDSE	663997	1092189	605	ND	1030	626	31	8.3	196	12.3	15.1	3.8	114.2	10	1.84	267.2	89.8	53.3	231	Na-HCO3-Cl

No.	ID	Data Source	UTME	UTMN	Elevn, masl	Depth, m	EC	TDS	T	PH	Na^+	K^+	Ca^{2+}	Mg^{2+}	Cl^-	$NO3^-$	F^-	$HCO3^-$	$SO4^{2-}$	TH	AlK	WATER_TYPE
58	SW26	WWDSE	681441	1126215	596	ND	2060	1304	32	8.5	425	18.5	28.5	7	303.4	20	1.84	447	211.2	99.9	386.4	Na-Cl-HCO3-SO4
59	SW27	WWDSE	646837	1039522	746	ND	734	508	37	7.5	116	12.4	30.3	15.7	39.4	5	1.84	366.4	46.2	139.9	300	Na-HCO3
60	SW28	WWDSE	629485	1031634	820	ND	2970	1936	28	7.8	660	7.6	40.1	18.9	364.8	10	3.3	922.3	303.6	177.6	756	Na-HCO3-Cl
61	SW29	WWDSE	629784	1027212	735	ND	1060	686	31	8.5	248	2.3	4.5	2.2	68.2	1.25	3.66	454.9	72.6	19.98	396.9	Na-HCO3
62	SW30	WWDSE	624705	1021649	735	ND	1008	626	38	8.1	208	13.3	13.4	7	71	4.8	2.7	456	60.7	62	373.8	Na-HCO3
63	SW31	WWDSE	623270	1023044	733	ND	1302	800	36	7.9	276	10.2	12.5	3.2	119	1.25	2.31	517	76.6	44.4	424.2	Na-HCO3-Cl
64	SW32	WWDSE	623396	1027152	742	ND	1464	926	31	8.3	335	4.5	4.5	2.2	120.9	5	4	572.8	75.2	20	493.5	Na-HCO3-Cl
65	SW33	WWDSE	633726	1034606	754	ND	894	584	37	8.2	190	4.1	9.1	2.75	57.6	7	3.2	415.3	49.5	34	344.4	Na-HCO3
66	SW34	WWDSE	639503	1028955	748	ND	846	592	38	7.8	135	14.3	24.6	12.6	52.8	8	2.2	409.9	44	113.5	336	Na-HCO3
67	SW35	WWDSE	642486	1025611	750	ND	797	516	25	7.7	144	12.6	20.9	7.7	49.9	8	2.48	381	49.5	83.99		Na-HCO3
68	SW36	WWDSE	641074	1068549	748	ND	640	386	31	8	72	6.6	47.3	17	29.8	19.5	1.6	320	26.4	199.4	262.5	Na-Ca-HCO3
69	SW37	WWDSE	632047	999422	749	ND	1500	975	34	7.7	81	8.8	49.1	11.6	29.8	7.5	0.9	350.99	21.75	170.3	287.7	Na-Ca-HCO3
70	SW38	WWDSE	692622	1057124	740	ND	519	324	28	7.4	33	4.4	55.5	20.9	19.2	10	0	281.8	12.1	224.7	231	Ca-Mg-Na-HCO3
71	SW39	WWDSE	660074	1077852	741	ND	1792	1058	25	7.3	290	11.2	45.5	9.4	312.96	22.5	0.9	166.5	167.75	152.1	136.5	Na-Cl-SO4
72	SW40	WWDSE	626351	999671	776	ND	1523	960	34	7.4	220	25	86.5	24.8	236.2	20	0.9	269.01	176	317.8	220.5	Na-Ca-Cl-HCO3-SO4
73	SW41	WWDSE	694136	1019853	814	ND	576	404	29	7.5	50	8.2	57.3	15.95	15.4	16.25	0.8	333.1	7.43	208.8	273	Ca-Na-Mg-HCO3
74	SW42	WWDSE	693001	1021056	817	ND	572	362	31	7.3	54	8.2	59.2	13.8	10.6	17.5	1.1	327.9	4.4	204.3	268.8	Ca-Na-HCO3
75	SW43	WWDSE	687371	1018850	721	ND	812	526	31	8.5	152	2.8	12.7	1.1	120.9	67.5	0	54.3	123.7	36.3	52.5	Na-Cl-SO4
76	SW44	WWDSE	677651	1014913	798	ND	889	546	32	7.9	184	5.5	18.2	4.4	104.6	8.5	0	366.4	1.65	63.6	300	Na-HCO3-Cl
77	SW45	WWDSE	652583	996169	833	ND	893	588		7.3	82	21	81.9	24.2	55.7	11.5	0.5	422.7	56.38	304.2	346.5	Ca-Na-HCO3
78	SW46	AAU	598836	1005342	1020	ND	533	345	24	7.3	47	3.9	53.1	14.8	22.6	8	0.8	320	42.7	212		Ca-Na-HCO3
79	SW47	AAU	652655	995894	1018	ND	538	348	36	7.8												
81	SW48	AAU	642540	1025602	809	ND	1167	757			91		40	15	57	10		309		279		Na-Ca-HCO3-Cl
82	SW49	AAU	682104	1123461	584	ND	1677	1088			268		4	1	87	5	2.5	433				Na-HCO3-Cl
83	SW50	AAU	682104	1123451	580	ND	2560	1662	47	8.2	541	29.4	8.3	6.3	506.2	24.7	2.4	473	485.2			Na-Cl-SO4-HCO3
84	SW51	AAU	700322	1005380	1648	ND	693	449		8.1	12		144		124		0.5	154	55.5			Ca-Cl-HCO3
85	SW52	AAU	591851	994111	1050	ND	1792	1112	44	8.5	425	28.5	6.4	3.36	123.6	3.5	2.45	727.12	136.05	30	636	Na-HCO3
87	SW53	AAU	592742	986659	981	ND	1964	1174	37	8.7	437	37.4	0	0.4	129	2.8	4.8	250	93			Na-HCO3-Cl

No.	ID	Data Source	UTME	UTMN	Elevn, masl	Depth, m	EC	TDS	T	PH	Na^+	K^+	Ca^{2+}	Mg^{2+}	Cl^-	$NO3^-$	F^-	$HCO3^-$	$SO4^{2-}$	TH	AlK	WATER_TYPE
88	HDW1	Primary data	616633	1027149	746	18	996	658	47	7.3	210	12.1	20	3.36	73.72	1.03	3.23	451.4	83.54	64	370	Na-HCO3
89	HDW2	AAU	639406	1048416	723	5	2060	1356	32	8.2	540	2.7	8	2.4	109.79	0.4	11.29	950.38	110.86	30	836	Na-HCO3
90	HDW3	AAU	605024	1012199	821	3	366	220	23	8.4	43	4	37.8	3.57	16.39	3.2	0.075	203.2	8.44	109.2	174.6	Ca-Na-HCO3
91	HDW4	AAU	608884	1011449	786	11.1	1563	1120	31	8.7	395	5.5	5.9	0.51	108.48	27.75	7	712.6	40	16.8	644.1	Na-HCO3
92	HDW5	AAU	607452	1008792	786	12	2900	2070	33	8.6	800	####	5.04	2.04	331.6	8.5	14	958.3	221.54	21	857.5	Na-HCO3-Cl
93	HDW6	AAU	608430	1009677	787	12	1476	1080	33	8.8	380	5	3.32	0.51	92.54	12.5	8	681	56.7	10.5	638.3	Na-HCO3
94	HDW7	WWDSE	677693	1114533	792	ND	3240	2004	36	8.2	790	20.5	7.1	1.6	437.8	4.8	6.2	979.7	234.9	24.4	819	Na-HCO3-Cl
95	HDW8	WWDSE	677533	1114397	871	ND	3280	1990	36	8.7	810	20.5	4.45	1.6	474.2	5	8	800	208.6	17.8	756	Na-Cl-HCO3
96	HDW9	WWDSE	693732	1072401	738	ND	1724	1126	32	8	345	1	20.9	6.1	112.3	25	1.68	358.7	400	77.2	294	Na-SO4-HCO3
97	HDW10	WWDSE	674028	1119302	1418	ND	1577	956	32	7.2	206	9.7	121	37.8	167	10.5	1.84	758.4	13.2	457.3	621.6	Na-Ca-HCO3-Cl
98	HDW11	WWDSE	693630	1072192	1407	ND	818	542	36	7.5	61	3.9	109.2	14.3	17.3	14.25	0.5	271.6	170	331.4	222.6	Ca-Na-HCO3-SO4
99	HDW12	WWDSE	693790	1072232	738	ND	981	650	31	8	200	0.3	15.5	4.95	24.9	17.5	1.92	461	57.75	59	378	Na-HCO3
100	HDW13	WWDSE	639409	1048416	829	ND	4410	2956	31	7.8	1020	6.1	30	14.8	425.3	8.5	18	1685.8	143	136.2	1381.8	Na-HCO3-Cl
102	HDW14	WWDSE	693627	1072312	1329	ND	1250	820	31	7.5	71	1.4	151.1	24.2	49.9	29	0	240.8	330	476.7	197.4	Ca-Na-SO4-HCO3
103	L1	Primary data	644249	1046847	761	0	918	542	42	7.2	158	18	16	9.6	55.52	2.61	1.73	341.6	76.17	80	280	Na-HCO3
105	SP1	AAU	644235	1046853	731	0	924	582	43	8.1	164	16	15.2	9.12	55.52	2.65	4.21	412.48	51.03	76	338.1	Na-HCO3
106	SP2	WWDSE	668821	1102656	820	0	1164	682	43	8.2	248	11.5	6.2	1.6	111.4	7	2	397.6	87.1	22.2	39.9	Na-HCO3-Cl
107	SP3	WWDSE	669108	1103908	1316	0	1201	730	34	8.7	266	8.3	2.7	1.1	109.4	5	1.9	373.9	83.2	11.1	352.8	Na-HCO3-Cl
108	SP4	WWDSE	674163	1025893	1346	0	80	54	25	7	1.3	1	15.5	1.1	1	4.8	0	48.7	1.1	43.1	237.3	Ca-HCO3
109	SP7	AAU	580166	1088759	3010	0	109	69	18	6.9	5.2	1	13.4	2.4	1.3	5.8	0.1	60	1.1			Ca-Na-HCO3
111	SP8	AAU	580555	1088521	3137	0	109	69	18	6.9	5.2	1	13.4	2.4	1.3	5.8	0.1	60	1.1		62	Ca-Na-HCO3
112	SP9	AAU	582739	1091179	3016	0	110	70	17	7.4	5.2	1	15	3.8	0.9	2.7	0.1	85.4	0.9		88	Ca-Mg-HCO3
113	SP10	WWDSE	612163	1007102	879	0	1740	1110	44	8.5	415	20	6.4	1.92	144.84	5.08	3.41	653.68	150.42	24	577.6	Na-HCO3-Cl
114	SP11	AAU	564889	1028218	2688	0	110	87	17	7.4	5.2	3.1	15.3	3.8	0.9	2.7	0.1	85.5	0.9		89	Ca-Mg-HCO3
115	SP12	AAU	580996	1053990	3260	0	109	85	15	6.8	5.2	1	13.4	2.4	1.3	5.8	0.1	60	1.1		58	Ca-Na-HCO3
116	R2	Primary data	590626	984632	1013	0	429	266	23	7.4	32	7.2	35.2	18.24	9.1	1.03	0.59	248.88	21.13	164	204	Ca-Mg-Na-HCO3
117	R3	Primary data	629816	995323	823	0	922	544	22	7.3	106	12.4	28	5.76	57.34	2.92	2.62	390.4	127.88	94	320	Na-HCO3-SO4
118	R4	Primary data	629087	1031083	762	0	1480	882	26	7.6	256	20	28	9.12	108.3	0.98	2.51	536.8	127.46	108	440	Na-HCO3-Cl

No.	ID	Data Source	UTME	UTMN	Elevn, masl	Depth, m	EC	TDS	T	PH	Na^+	K^+	Ca^{2+}	Mg^{2+}	Cl^-	$NO3^-$	F^-	$HCO3^-$	$SO4^{2-}$	TH	AlK	WATER_TYPE
119	R5	Primary data	656736	1101336	575	0	1308	836	26	7.9	250	13.5	26.4	8.16	96.47	1.2	3.51	488	152.48	100	400	Na-HCO3-SO4
120	R6	Primary data	604977	1012010	767	0	643	404	25	7.8	100	8.7	24	6.72	41.86	4.75	1.38	219.6	85.9	88	180	Na-HCO3-SO4
121	R7	Primary data	604387	1056001	1030	0	353	202	29	7.3	15	17.5	42.4	6.24	8.19	0.51	0.51	195.2	12.65	132	160	Ca-HCO3
122	R10	AAU	589368	1029172	950	0	385	250		8.5	8	2	30	5	3		0.7	132	3			Ca-HCO3
123	R11	WWDSE	622893	1017591	755	0	1462	900	29	8.1	280	17.5	40	4.8	103.75	2.64	4.07	512.4	164.28	120	420	Na-HCO3-SO4
124	BH20	WWDSE	628683	1008918	826.56	126	720	452		7.1	67	9.3	68	7.2	48.23	8.2	0.7	317.2	54.94	200	260	Na-Ca-HCO3-SO4
125	R1	Primary data	417558	988965	2085	0	369	242		6.9	45	7.6	28	4.8	15.47	3.84	0.9	173.24	43.79	90	142	Na-Ca-HCO_3-SO_4
126	R14	AAU	522507	936524		0	380	287	25	8.3	71	11	32.7	6.3	25.3	1.2	2.5	300	15.3			Na-Ca-HCO_3
127	SW54	AAU	546408	971443	1674		547	329	35	7.3	110	12.7	52.7	9.5	11.6	2.8	1.5	305	15.2			Na-Ca-HCO_3
128	SW55	AAU	591729	938934	1544		402	243	32	6.9	49.2	7.8	69.2	9.5	7.4	3.3	0.8	604	4.8			Ca-Na-HCO3
129	L2	AAU	599267	983752		0	6170	4652	26	9.4	1960	68	1.3	17	525.3	35	31.4	3218	525.8			Na-K-HCO3-Cl-SO4
130	R15	AAU	766812	1276796			812		37	8.8	141	9.2	20.3	6.7	71.1	8.8	2.4	351	3			Na-HCO3-Cl

Annex- VI: Environmental Isotope Data

No.	ID	Sampling time	Data Source	UTME	UTMN	SOURCE	$\delta^{18}O$ (‰)	δD(‰)	^{3}H(TU)	Temp.°C
1	BH1	Feb, 2013	Primary data	626352	999668	Bore hole	-2.3	-17.03		
2	BH2	Feb, 2013	Primary data	605661	1055260	Bore hole	-1.97	0.05		
3	BH3	Feb, 2013	Primary data	620256	1040033	Bore hole	-3.99	-19.33		
4	BH5	Feb, 2013	Primary data	657056	1065134	Borehole	-4.61	-18.73		
5	BH6	Feb, 2013	Primary data	643091	1027968	Borehole	-3.79	-15.14		
6	BH7	Feb, 2013	Primary data	643091	1027968	Borehole	-5.14	-17.5		
7	BH9	Feb, 2013	Primary data	685050	1016620	Bore hole	-2.39	-6.13		
8	BH10	Feb, 2013	Primary data	645334	996709	Bore hole	-4.34	-14.13		
9	BH18	Feb,2013	Primary data	637189	1016763	Borehole	-4.8	-23.45	2.38	
10	BH19	Feb,2013	Primary data	643290	1025519	Bore hole	-4.13	-17.12	2.11	
11	BH20	Feb,2013	Primary data	628683	1008918	Bore hole	-1.75	-1.46	2.18	
12	BH23	Feb,2013	WWDSE	639707	1028668	Borehole	-3.82	-13.4		43
13	BH24	Sep,2010	AAU	645330	996699	Spring	-2.62	-7.84		32.3
14	BH25	Sep,2010	AAU	632421	998837	Borehole	-3.41	-5.48		
15	BH26	Sep,2010	AAU	653235	998628	Borehole	-0.49	13.24		35.5
16	BH27	Sep,2010	AAU	632418	998037	Borehole	-3.44	-11.61		36.2
17	BH 28	Jan,2011	AAU	628683	1008918	Borehole	-1.69	-8.42	0.71	31.6
18	BH29	Sep,2010	AAU	647560	1040111	Borehole	-0.20	11.68		
19	BH 30	Jan,2011	AAU	632421	998837	Borehole	-4.85	-19.80		37.8
20	BH 32	Sep,2010	AAU	632471	1008252	Borehole	-2.68	-5.59		
21	BH38		AAU	598836	1005342	Borehole	-1.57	-0.6		24
22	BH39		AAU	652655	995894	Borehole	-2.39	-9.8		36.2
23	BH40		AAU	642769	1025743	Borehole	-2.88	-12.3		43.1
24	BH41		AAU	599267	983752	Borehole	-0.1	6.3		29.4
25	BH42		AAU	628684	1008910	Borehole	-1.9	-2.9		33
26	BH43		AAU	682104	1123451	Borehole	-2.8	-14.7	0.5	47
27	BH44	Feb,2013	WWDSE	641201	1027418	Bore hole	-3.69	-15.85		
28	BH44	Feb,2013	WWDSE	641201	1027418	Bore hole	-3.95	-14.17		
29	BH44	Feb,2013	WWDSE	641201	1027418	Borehole	-4.38	-16.19		
30	BH44	Feb,2013	WWDSE	641201	1027418	Bore hole	-4.23	-13.31		
31	BH44	Feb,2013	WWDSE	641201	1027418	Bore hole	-3.75	-12.19		
32	BH45		WWDSE	560362	969076	Bore hole	-3.68	-10.88	0.34	36.6
33	BH46		WWDSE	591729	938934	Bore hole	-3.1	-9.59	1.49	32
34	BH47		WWDSE	591942	994317	Bore hole	-2.23	-9.78	1.07	44.3
35	BH48		WWDSE	592742	986659	Bore hole	-2.36	-9.38		37.1
36	BH49		WWDSE	546408	971443	Borehole	-3.7	-12.97	1.17	34.6
37	BH50		WWDSE	506902	1016138	Bore hole	-4.15	-12.85		19
38	BH51	Jan,2011	WWDSE	625836	1021173	Borehole	-1.71	1.91		
39	BH52	Sep,2010	WWDSE	625836	1021173	Borehole	-3.86	-11.09		35.9
40	BH52	Jan,2011	WWDSE	629045	1030474	Borehole	-2.17	-2.57		
41	BH53	Jan,2011	WWDSE	641424	1007510	Borehole	-1.43	-0.14		28
42	BH54		WWDSE	632509	998046	Borehole			0.64	
43	BH55		WWDSE	652655	995894	Borehole			0.4	
44	BH56		WWDSE	598836	1005342	Borehole			5.8	
45	HDW1	Feb, 2013	Primary data	616633	1027149	Hand dug well	-3.18	-13.97		
46	HDW0	Feb, 2013	Primary data	605000	1011993	Hand dug well	-3.28	-7.22		

No.	ID	Sampling time	Data Source	UTME	UTMN	SOURCE	$\delta^{18}O$ (‰)	δD(‰)	^{3}H(TU)	Temp.°C
47	HDW2	Jan,2011	WWDSE	639406	1048416	Borehole	-4.52	-13.99		32
48	HDW15		AAU	601450	978322	Hand dug well	-0.4	3.3		
49	KDLA1	April,2014	Primary data	598557	1011161	Left Abutment	-2.02	-8.11		
50	KDR	April,2013	Primary data	596844	1010793	Reservoir	-0.44	-0.04		
51	KDTd	April,2015	Primary data	598557	1011152	Toe drain	-1.67	-3.34		
52	KDW	April,2016	Primary data	598579	1011118	Well	-2.31	-10.46		54
53	L1	Feb, 2013	Primary data	644249	1046847	Small lake (Blen)	-3.93	-14.32		
54	L2	Feb, 2013	AAU	599267	983752	Lake	6.9	41.9		25.9
55	R1	Feb, 2013	Primary data	417558	988965	River	-0.84	3.6		
56	R2	Feb, 2013	Primary data	590626	984632	River	1.36	14.31		
57	R3	Feb, 2013	Primary data	629816	995323	Awash river	-0.14	6.58		
58	R4	Feb, 2013	Primary data	629087	1031083	Awash river	-0.39	3.39		
59	R5	Feb, 2013	Primary data	656736	1101336	Awash river at gewane	-0.4	3.85		
60	R6	Feb, 2013	Primary data	604977	1012010	River	-3.57	-4.73		
61	R7	Feb, 2013	Primary data	604387	1056001	River	-1.56	5.92		
62	R8		AAU	522507	963524	River	-0.2	4.9		
63	R9	Feb, 2013	Primary data	618753	1013701	River	-3.7	-13.18		
64	R11	Feb,2018	Primary data	622893	1017591	River	-0.88	7.09	2.98	
65	R12	Jan,2011	AAU	622962	1017702	River	-1.94	2.30		
66	R13	Feb,2013	WWDSE	433783	960032	River	-0.76	-0.76		
67	R14		AAU	766812	1276796	River	6	37.7		37.4
68	SP1	Feb, 2013	Primary data	645204	1048781	Blen spring	-4.36	-16.04		
69	SP5		AAU	617507	1030165	Thermal spring	-1.2	-7.1		
70	SP6		AAU	580166	1088759	Spring cold	-4.19	-13.7		18
71	SP8		AAU	580555	1088521	Spring	-4.2	-13.7		18
72	SP9		AAU	582739	1091179	Spring	-4.3	-14.3	3.6	17
73	SP11		AAU	564889	1028218	Spring	-4.33	-14.31		17
74	SP12		AAU	580996	1053990	Spring	-4.2	-13.7		15
75	SW1	Feb,2013	Primary data	633279	1027937	Borehole	-3.29	-14.32	1.81	
76	SW2	Feb,2013	Primary data	646032	1038432	Borehole	-5.87	-26.21	1.87	
77	SW4	Jan,2011	WWDSE	639505	1028953	Borehole	-3.77	-13.48		38
78	SW6	Sep,2010	WWDSE	695877	1015842	Borehole	-2.28	4.75		
79	SW7	Jan,2011	WWDSE	633107	1027266	Borehole	-1.08	2.50		38
80	SW8	Jan,2011	WWDSE	633278	1027936	Borehole	-4.37	-17.20		37
81	SW12	Jan,2011	WWDSE	597136	1011337	Borehole	-0.46	-1.78		50
82	SW13	Jan,2011	WWDSE	644582	1047320	Borehole	-2.02	-5.36		
83	SW14	Sep,2010	WWDSE	633726	1034606	Borehole	-1.61	3.24		
84	SW18	Jan,2011	WWDSE	638824	1043036	Borehole	-0.09	5.47		
85	SW30	Jan,2011	WWDSE	632471	1008252	Borehole	-0.19	0.80		35.50
86	SW31	Jan,2011	WWDSE	623270	1023044	Borehole	-0.87	-1.57		
87	SW35	Jan,2011	WWDSE	643300	1025542	Borehole	-3.12	-10.86		43
88	SW45	Jan,2011	WWDSE	652583	992169	Borehole	-0.82	-4.26	0.97	35.60

Annex- VII: Selected Water points for Estimation of Recharge using CMB

(Clgw and Clp is Chloride concentration in groundwater and Precipitation respectively in (mg/l), Pav is Average Annual precipitation (mm/year) and Rgw-Groundwater recharge (mm/year))

S.No	EpID	Locality	UTME	UTMN	Elevation, masl	Pav (mm/year)	Clp (mg/l)	Clgw(mg/l)	Rgw(mm/yr) =(Pav*Clp)/Clgw
1	BH1	Dudub	626352	999668	829	649.4	0.91	49.14	12.03
2	BH13	Awash vally	633633	995225	1353	649.4	0.91	39.36	15.01
3	BH15	Allydegi plain	643798	1019148	1320	649.4	0.91	40	14.77
4	BH17	Allydegi plain	645424	996570	1235	649.4	0.91	25.75	22.95
5	BH18	Allydegi plain	637189	1016763	831.287	649.4	0.91	40.95	14.43
6	BH20	Allydegi plain	628683	1008918	826.555	649.4	0.91	48.23	12.25
7	BH22	Allydegi plain	653300	998623	1077	649.4	0.91	39.13	15.10
8	BH24	Hardem	645330	996699	1007	649.4	0.91	41.86	14.12
9	BH25	Defence	632421	998837	894	649.4	0.91	21.84	27.06
10	BH27	Defence	632418	998037	891	649.4	0.91	36.4	16.24
11	BH28	Awash Arba	628683	1008918	827	649.4	0.91	39.13	15.10
12	BH29	Andido -Intiaso	647560	1040111	820	649.4	0.91	41.86	14.12
13	BH30	Defence	632421	998837	894	649.4	0.91	38.8	15.23
14	BH31	Awash Arba	628683	1008918	827	649.4	0.91	43.54	13.57
15	BH32	Lalibela	632471	1008252	833	649.4	0.91	19.88	29.73
16	BH33	Awash Arba	628683	1008918	740	649.4	0.91	41.3	14.31
17	BH34	Defence	628311	1007852	782	649.4	0.91	38.4	15.39
18	BH35	Tutuftu	685854	1009743	827	649.4	0.91	31.7	18.64
19	BH36	Daga dhaba	681409	1009313	817	649.4	0.91	24.96	23.68
20	BH37	Hayo	668814	1001716	860	649.4	0.91	37.4	15.80
21	HDW11	Afasse	693630	1072192	1407	649.4	0.91	17.3	34.16
22	HDW12	Afasse	693790	1072232	738	649.4	0.91	24.9	23.73
23	HDW14	Afasse	693627	1072312	1329	649.4	0.91	49.9	11.84
24	R10	Kebena river	589368	1029172	950	649.4	0.91	3	196.98
25	R6	Kesem at sabure	604977	1012010	767	649.4	0.91	41.86	14.12
26	R7	Dulecha river	604387	1056001	1030	649.4	0.91	8.19	72.16
27	SP11	Sheno	564889	1028218	2688	649.4	0.91	0.9	656.62
28	SP12	Ankober	580996	1053990	3260	649.4	0.91	1.3	454.58
29	SP4	Trinity Monastery	674163	1025893	1346	649.4	0.91	1	590.95
30	SP7		580166	1088759	3010	649.4	0.91	1.3	454.58
31	SP8	Tarmaber	580555	1088521	3137	649.4	0.91	1.3	454.58
32	SP9	Debresina	582739	1091179	3016	649.4	0.91	0.9	656.62
33	SW19	Huse Sodoma	695877	1015842	803	649.4	0.91	20.2	29.26
34	SW2	Allydegi plain	646032	1038432	816.782	649.4	0.91	40.95	14.43
35	SW20	Fayo	691053	1020494	727	649.4	0.91	16.3	36.25
36	SW27	Andido -1	646837	1039522	746	649.4	0.91	39.4	15.00
37	SW35	Elfora	642486	1025611	750	649.4	0.91	49.9	11.84
38	SW36	Halidebi	641074	1068549	748	649.4	0.91	29.8	19.83
39	SW37	Kurkura	632047	999422	749	649.4	0.91	29.8	19.83
40	SW38	Butiji	692622	1057124	740	649.4	0.91	19.2	30.78
41	SW41	Gende Aliware	694136	1019853	814	649.4	0.91	15.4	38.37
42	SW42	Mieso Town	693001	1021056	817	649.4	0.91	10.6	55.75
43	SW46		598836	1005342	1020	649.4	0.91	22.6	26.15
44	SW6	Huse Sodoma	695877	1015842	1386	649.4	0.91	10.01	59.04

Annex- VIII: Environmental Isotope monitoring Data of Awash River and Allydegi plain wells

Month	ID	SW2	BH20	BH19	BH18	SW1	R11
	Locality	Andido	Awash Arba	Allydegi plain	Gonita Birka	Adebtole	Sidafage
	UTME	646032	628683	643290	637189	633279	622893
	UTMN	1038432	1008918	1025519	1016763	1027937	1017591
	Source	Borehole	Borehole	Borehole	Borehole	Borehole	River
	Well depth(m)	90	150	126	220	80	0
	Yield(l/s)	19	6	2	20	8	0
Aug,2012	δD(‰)	-9.29	-2.84	-12.97	-10.86	-14	-9.82
	δ^{18}O(‰)	-3.13	-2.18	-3	-2.44	-2.41	-2.63
	^{3}H(TU)	1.97	2.31	2.01	2.52	1.78	3.28
Sep,2012	δD(‰)	-11.72	-5	-13.2	-9.04	-11.32	-2.54
	δ^{18}O(‰)	-2.74	-1.73	-2.63	-2.12	-2.7	-1.76
	^{3}H(TU)	1.89	2.22	1.98	2.44	1.73	3.16
Oct,2012	δD(‰)	-9.17	-3.37	-11.82	-10.22	-11.3	9.47
	δ^{18}O(‰)	-2.24	-1.52	-2.71	-2.66	-3.05	0.25
	^{3}H(TU)	1.91	2.27	2.09	2.46	1.74	3.21
Nov,2012	δD(‰)	-13.94	-4.97	-12.66	-4.57	-11.1	-0.87
	δ^{18}O(‰)	-3.42	-2.43	-3.29	-2.17	-3.25	-0.99
	^{3}H(TU)	1.9	2.25	2.06	2.42	1.77	3.1
Dec,2012	δD(‰)	-17.5	-14.71	-10.56	-15.39	-4.03	1.25
	δ^{18}O(‰)	-3.49	-3.42	-2.99	-3.64	-2.34	-1.21
	^{3}H(TU)	1.87	2.18	2.11	2.38	1.81	2.98
Jan,2013	δD(‰)	-9.63	-5.05	-15.54	-9.84	-13.7	8.83
	δ^{18}O(‰)	-3.81	-2.73	-3.87	-3.67	-4.12	-0.39
	^{3}H(TU)						
Feb,2013	δD(‰)	-26.21	-1.46	-17.12	-23.45	-14.32	7.09
	δ^{18}O(‰)	-5.87	-1.75	-4.13	-4.8	-3.29	-0.88
	^{3}H(TU)						
Mar,2013	δD(‰)	-15.89	-12.05	-19.76	-14.93	-8.22	-0.52
	δ^{18}O(‰)	-4.26	-3.99	-4.74	-3.74	-2.55	-2.09
	^{3}H(TU)						
Apr,2013	δD(‰)	-12.88	-2.26	-14.6	_	-9.04	13.56
	δ^{18}O(‰)	-3.14	-2	-3.61	_	-3.02	0.93
	^{3}H(TU)						

Annex- IX: Monitoring of Water level, Water Quality of reservoir and other water bodies around Kesem Dam

Monitoring date		Reservoir Water			Piezometer Well	Artesian Wells		Toe drian Water		Leakage water at left Abutment	
Date	Time	Level, masl	EC, µs/cm	Temp, °C	Water level, masl	EC, µs/cm	Temp, °C	EC, µs/cm	Temp, °C	EC, µs/cm	Temp, °C
13/11/2012	5:30	905.94	365.4	27		1942	52	2181	35	1741	40
14/11/2012	11:00	905.9	278.4	26		1935	52	2170	35	1733	40
15/11/2012	10:45	905.86	276.3	26		1852	52	2134	35	1658	40
16/11/2012	11:00	905.82	315.3	25		1925	52	2091	35	1660	40
17/11/2012	11:15	905.78	279.2	26		1869	52	2007	35	1653	40
18/11/2012	10:45	905.74	275.6	24	881.192	1907	52	1988	35	1640	40
19/11/2012	10:09	905.74	342.8	24	881.192	1965	52	2020	35	1679	40
20/11/2012	10:00	905.65	346.8	25	881.252	1940	52	1977	34	1652	39
21/11/2012	11:05	905.62	314.2	25	881.252	1908	52	1941	35	1626	39
22/11/2012	11:00	905.58	275.8	25	881.322	1891	52	1904	35	1629	40
23/11/2012	11:00	905.54	283	26	881.322	1889	52	1880	35	1604	40
24/11/2012	10:30	905.51	272.1	25	881.378	1912	52	1872	34	1610	40
25/11/2012	10:45	905.48	273	25	881.436	1908	52	1856	34	1607	39
26/11/2012	11:15	905.46	268.9	27	881.436	1900	52	1877	35	1606	40
27/11/2012	11:00	905.41	265.8	26	881.494	1901	52	1821	34	1575	39
28/11/2012	11:00	905.37	265.5	26	881.494	1910	52	1818	34	1565	39
29/11/2012	9:32	905.34	266.5	25	881.521	1904	52	1773	34	1557	39
30/11/2012	10:00	905.31	265.1	21	881.521	1891	52	1763	33	1526	38
1/12/2012	10:20	905.27	272.6	25	881.542	1876	52	1750	34	1522	39
2/12/2012	10:00	905.24	270	26	881.542	1881	52	1523	32	1518	39
3/12/2012	11:00	905.2	274.2	26	881.542	1869	52	1501	32	1522	39
4/12/2012	11:15	905.14	270.8	27	881.587	1888	52	1779	34	1525	39
5/12/2012	10:05	905.09	271.7	27	881.587	1892	52	1503	32	1523	39
6/12/2012	10:00	905.05	270	25	881.587	1877	52	1765	34	1525	39
7/12/2012	11:00	905	273	26	881.626	1873	52	1753	34	1529	39
8/12/2012	10:30	904.96	276.2	27	881.626	1892	52	1850	35	1513	39
9/12/2012	11:00	904.92	281.7	26	881.673	1885	52	1719	34	1511	39
10/12/2012	11:00	904.88	297.1	27	881.673	1904	52	1733	34	1524	39
11/12/2012	11:00	904.84	296.8	26	881.727	1897	52	1729	34	1501	39
12/12/2012	10:00	904.8	296.2	25	881.727	1898	52	1707	33	1493	39
13/12/2012	10:00	904.78	301.1	26	881.78	1873	52	1709	33	1478	39
14/12/2012	10:30	904.71	308.0	25	881.78	1892	52	1724	32	1497	38
15/12/2012	10:30	904.68	314.2	25	881.78	1910	52	1708	34	1486	38
16/12/2012	10:20	904.64	283.7	25	881.78	1881	51	1680	34	1456	38
17/12/2012	10:30	904.57	282.8	25	881.78	1903	52	1676	34	1465	38
18/12/2012	10:30	904.54	282.6	26	881.78	1880	52	1659	35	1422	39
19/12/2012	10:40	904.54	276.3	24	881.78	1892	52	1618	33	1433	36
20/12/2012	10:20	904.5	274.2	24	881.78	1830	52	1605	33	1431	37
21/12/2012	10:20	904.46	279.5	24	881.78	1874	52	1615	34	1430	37
22/12/2012	10:00	904.42	277.8	24	881.78	1919	52	1609	33	1440	36
23/12/2012	10:15	904.4	278.2	24	881.78	1855	52	1598	33	1403	36
24/12/2012	11:30	904.355	281.2	25	881.78	1899	52	1632	35	1406	38
25/12/2012	11:00	904.31	281.6	26	881.78	1827	52	1595	35	1392	38
26/12/2012	11:30	904.27	276.6	26	881.78	1877	52	1585	35	1430	38
27/12/2012	10:45	904.23	273.4	26	881.78	1842	52	1595	35	1397	38
28/12/2012	10:30	904.2	285.3	26	881.78	1848	52	1585	35	1394	38
29/12/2012	10:30	904.16	286.4	26	881.78	1840	52	1555	35	1393	38
30/12/2012	10:45	904.12	278.6	26	881.78	1936	52	1588	35	1430	38
31/12/2012	10:45	904.08	282.4	25	881.78	1852	52	1561	34	1384	38
1/1/2013	10:40	904.04	285.4	26	881.78	1885	52	1540	34	1396	38
2/1/2013	10:00	903.99	281.4	25	881.78	1865	52	1540	34	1394	38
3/1/2013	10:30	903.95	281.4	25	881.78	1865	52	1538	34	1385	37
4/1/2013	10:30	903.91	285.3	25	881.78	1862	52	1525	34	1375	38
5/1/2013	10:45	903.88	286.4	25	881.78	1850	52	1510	35	1385	38
6/1/2013	10:20	903.84	275.3	25	881.78	1845	52	1525	35	1392	37
7/1/2013	10:35	903.79	272.4	25	881.78	1875	51	1540	34	1395	38
8/1/2013	10:40	903.75	273.6	25	881.78	1865	52	1555	35	1385	37
9/1/2013	10:20	903.71	285.4	26	881.78	1862	52	1525	34	1345	38
10/1/2013	10:45	903.68	282.2	26	881.78	1845	52	1545	34	1390	38
11/1/2013	10:40	903.64	287.3	26	881.78	1869	52	1595	34	1345	38
12/1/2013	10:30	903.64	289.3	24	881.78	1834	51	1485	32	1331	38
13/1/2013	10:15	903.59	296.8	24	881.78	1834	51	1472	32	1324	38
14/1/2013	10:30	903.56	290.6	25	881.78	1833	51	1470	33	1322	38
15/1/2013	9:50	903.51	296.5	24	881.78	1860	52	1463	33	1326	38
16/1/2013	10:30	903.48	292.4	24	881.78	1839	52	1452	32	1325	38
17/1/2013	10:30	903.43	291.1	23	881.78	1847	52	1445	32	1313	38

Monitoring date		Reservoir Water			Piezometer Well	Artesian Wells		Toe drian Water		Leakage water at left Abutment	
18/1/2013	10:10	903.4	290.7	24	881.78	1849	52	1440	33	1315	38
19/1/2013	10:30	903.36	292	23	881.78	1817	52	1432	32	1311	38
20/1/2013	10:00	903.34	294.9	24	881.78	1861	52	1425	32	1311	38
21/1/2013	10:30	903.3	296.2	23	881.78	1836	52	1404	33	1312	38
22/1/2013	9:21	903.26	293.2	24	881.78	1880	52	1404	32	1306	38
23/1/2013	9:13	903.21	293.6	23	881.78	1847	52	1407	32	1302	38
24/1/2013	10:20	903.15	282.9	24	881.78	1900	52	1453	32	1313	38
25/1/2013	10:30	903.11	295.2	24	881.78	1939	52	1405	32	1329	38
26/1/2013	10:20	903.08	282.4	25	881.78	1935	52	1410	33	1340	38
27/1/2013	10:00	903.04	310.2	25	881.78	1931	52	1482	33	1534	38
28/1/2013	10:40	903	305.2	25	881.78	1945	52	1495	33	1540	38
29/1/2013	10:30	902.96	301.1	25	881.78	1822	52	1440	33	1535	38
30/1/2013	10:00	902.93	307.2	26	881.78	1890	52	1448	33	1311	38
31/1/2013	10:40	902.9	299.8	25	881.78	1925	52	1229	33	1285	37
1/2/2013	10:30	902.85	289.7	25	881.78	1910	52	1232	33	1246	37
2/2/2013	10:20	902.8	275.3	25	881.78	1935	52	1345	33	1252	37
3/2/2013	10:40	902.75	291.5	25	881.78	1867	52	1275	33	1237	37
4/2/2013	10:15	902.71	287.4	25	881.78	1840	52	1256	33	1358	37
5/2/2013	10:30	902.71	303.1	25	881.78	1833	52	1236	33	1255	37
6/2/2013	10:05	902.63	302.8	25	881.78	1870	52	1236	31	1266	38
7/2/2013	10:30	902.59	300.8	25	881.78	1861	52	1271	32	1260	38
8/2/2013	10:15	902.56	300.6	24	881.79	1853	52	1240	32	1251	38
9/2/2013	11:15	902.52	305.7	25	881.79	1841	52	1250	32	1253	38
10/2/2013	10:25	902.47	302.9	25	881.79	1843	52	1238	32	1255	38
11/2/2013	10:30	902.45	304.7	25	881.79	1844	52	1229	32	1251	38
12/2/2013	10:30	902.41	305.8	25	881.79	1853	52	1222	32	1255	38
13/2/2013	10:00	902.37	302.6	25	881.79	1865	52	1203	32	1252	38
14/2/2013	10:19	902.33	305.9	25	881.79	1867	52	1180	31	1244	38
15/2/2013	10:50	902.27	309.9	25	881.79	1855	52	1172	31	1244	38
16/2/2013	9:50	902.23	304.6	25	881.79	1865	52	1158	31	1246	38
17/2/2013	11:00	902.21	306.8	25	881.79	1842	52	1148	30	1239	38
18/2/2013	10:30	902.15	306.8	25	881.79	1854	52	1147	31	1239	38
19/2/2013	11:00	902.11	305.8	26	881.79	1861	52	1158	31	1241	38
20/2/2013	10:00	902.07	308.7	25	881.79	1868	52	1200	32	1236	38
21/2/2013	10:00	902.03	309.7	24	881.79	1852	52	1166	32	1228	38
22/2/2013	10:00	901.99	309.6	25	881.79	1858	52	1147	31	1231	38
23/2/2013	10:00	901.95	310.7	25	881.79	1806	52	1149	31	1226	38
24/2/2013	10:00	901.91	309	25	881.79	1853	52	1152	31	1225	38
25/2/2013	10:30	901.87	336	25	881.79	1824	52	1141	31	1214	38
26/2/2013	10:30	901.82	310.5	26	881.79	1845	52	1136	31	1220	38
27/2/2013	10:30	901.76	319.5	25	881.79	1855	52	1132	31	1222	38
28/2/2013	10:00	901.72	311.8	25	881.79	1851	52	1098	31	1217	37
1/3/2013	10:30	901.69	314	26	881.79	1837	52	1132	31	1210	37
2/3/2013	10:30	901.65	316.4	25	881.79	1839	52	1124	31	1216	37
3/3/2013	10:20	901.6	311.3	26	881.79	1852	52	1118	31	1213	37
4/3/2013	10:45	901.56	309.5	26	881.79	1848	52	1110	31	1198	37
5/3/2013	10:10	901.51	311.4	26	881.79	1838	52	1120	31	1203	37
6/3/2013	10:30	901.47	313.8	26	881.79	1813	52	1117	31	1208	37
7/3/2013	10:30	901.42	314.7	26	881.79	1848	52	1103	31	1207	37
8/3/2013	10:30	901.38	321.6	26	881.79	1818	52	1089	31	1197	37
9/3/2013	11:00	901.34	314.1	25	881.79	1828	52	1099	31	1192	38
10/3/2013	10:00	901.3	313	25	881.79	1835	52	1095	31	1199	38
11/3/2013	10:30	901.24	317.1	25	881.79	1842	52	1093	31	1198	38
12/3/2013	10:20	901.19	318.2	25	881.79	1842	52	1094	31	1198	38
13/3/2013	10:40	901.14	318.4	25	881.79	1840	52	1045	31	1198	37
14/3/2013	10:35	901.09	316.2	25	881.79	1820	52	1018	31	1198	37
15/3/2013	10:45	901.04	313.4	25	881.79	1816	52	1018	31	1172	37
16/3/2013	10:45	900.99	312.4	25	881.79	1815	52	1020	31	1170	37
17/3/2013	10:30	900.95	314.2	25	881.79	1817	52	1015	31	1175	37
18/3/2013	10:20	901.03	311.4	25	881.79	1820	52	1020	32	1165	37
19/3/2013	10:15	900.98	320.7	25	881.79	1815	52	1022	31	1170	37
20/3/2013	10:40	900.93	321.2	25	881.79	1813	52	1021	32	1174	37
21/3/2013	10:50	900.88	316.7	25	881.79	1847	52	1065	32	1191	37
22/3/2013	9:40	900.83	316.2	26	881.79	1845	52	1047	31	1194	37
23/3/2013	9:30	900.81	314.6	26	881.79	1810	52	1047	31	1174	37
24/3/2013	9:30	900.81	320.8	26	881.79	1818	52	1042	31	1184	37
25/3/2013	10:00	900.8	315.2	26	881.79	1822	52	1043	31	1178	37
26/3/2013	10:00	900.8	320.5	27	881.79	1839	52	1012	31	1181	37
27/3/2013	10:50	900.8	323.5	27	881.79	1835	52	1040	31	1179	37
28/3/2013	9:15	900.79	316.7	26	881.79	1832	52	1010	31	1169	37
29/3/2013	9:30	900.76	342.8	27	881.79	1825	52	1022	31	1171	37
30/3/2013	9:30	900.75	324.2	26	881.69	1812	52	1004	31	1168	37
31/3/2013	9:20	900.74	320	26	881.69	1818	52	1013	31	1168	37

Monitoring date		Reservoir Water			Piezometer Well	Artesian Wells		Toe drian Water		Leakage water at left Abutment	
1/4/2013	10:15	900.75	323.4	26	881.69	1842	52	1022	31	1170	37
2/4/2013	10:30	900.74	323.1	27	881.69	1833	52	997	31	1166	37
3/4/2013	10:30	900.73	323.1	29	881.69	1821	52	1004	31	1159	37
4/4/2013	10:30	900.69	342.9	27	881.69	1809	52	1001	31	1159	37
5/4/2013	10:30	900.67	323.7	30	881.69	1834	52	1007	31	1167	37
6/4/2013	10:30	900.65	325.7	29	881.69	1815	52	997	31	1162	37
7/4/2013	10:30	900.62	328.2	28	881.69	1819	52	973	31	1160	37
8/4/2013	11:00	900.58	329.2	27	881.69	1820	52	994	31	1154	37
9/4/2013	10:45	900.56	325	28	881.69	1834	52	989	31	1149	37
10/4/2013	10:30	900.53	325.3	29	881.69	1833	52	982	31	1152	37
11/4/2013	10:30	900.5	325.8	29	881.69	1836	52	969.3	31	1146	37
12/4/2013	10:45	900.48	326.3	29	881.69	1838	52	986	31	1143	37
13/4/2013	10:30	900.45	324.3	28	881.69	1817	52	989	31	1148	37
14/4/2013	10:45	900.41	329.7	28	881.69	1814	52	963	31	1135	37
15/4/2013	10:45	900.37	329.4	29	881.69	1822	52	970.2	31	1139	37
16/4/2013	10:30	900.34	329	28	881.69	1834	52	984.4	31	1140	37
17/4/2013	10:45	900.3	324	28	881.69	1818	52	974	32	1144	37
18/4/2013	10:30	900.29	330.8	28	881.69	1824	52	984	32	1139	37
19/4/2013	10:30	900.28	331.6	28	881.69	1840	52	964.5	31	1134	37
20/4/2013	10:45	900.275	356.6	28	881.69	1796	52	990.1	31	1116	37
21/4/2013	10:30	900.26	356	28	881.69	1839	52	980	31	1128	37
22/4/2013	10:15	900.23	340	28	881.69	1835	52	986.1	31	1130	37
23/4/2013	10:45	900.21	330.2	28	881.69	1816	52	975.8	31	1129	37
24/4/2013	10:55	900.205	338.6	28	881.69	1809	52	992	31	1129	37
25/4/2013	11:00	900.1	345.5	28	881.69	1809	52	994.4	31	1131	37
26/4/2013	3:30	900	347.3	27	881.69	1813	52	1008	32	1137	37
27/4/2013	10:55	862.63	343.4	27	881.69	1815	52	978	32	1119	37
28/4/2013	10:15	862.64	333.7	27	881.69	1845	52	986	32	1115	37
29/4/2013	11:00	862.64	334.8	27	881.69	1857	52	957.7	32	1130	37
30/4/2013	10:30	862.64	347.5	28	881.69	1802	52	982	31	1109	37
1/5/2013	10:15	862.65	334.6	28	881.69	1826	52	960	32	1043	37
8/5/2013	10:55	862.69	336	28	881.69	1822	52	978	32	1107	37
9/5/2013	10:45	862.69	337	28	881.69	1828	52	978	32	1118	37
10/5/2013	10:30	862.69	339	28	881.69	1810	52	975	32	1112	37
11/5/2013	11:30	862.69	333.4	28	881.69	1815	52	920.1	32	1098	37
12/5/2013	11:15	862.69	333.2	28	881.69	1805	52	941	32	1101	37
13/5/2013	11	862.69	339.3	28	881.69	1808	52	943.7	32	1099	37
14/5/2013	10:50	862.69	327.2	28	881.69	1866	51	918.1	32	1096	37
15/5/2013	10:15	862.69	336.1	27	881.69	1823	51	915.4	32	1091	37
16/5/2013	10:30	862.69	367.4	27	881.69	1785	51	920.6	32	1076	37
17/5/2013	10:00	862.69	343.8	27	881.69	1804	51	923	32	1085	37
18/5/2013	10:15	862.69	333.2	27	881.69	1831	51	926.3	32	1096	37
19/5/2013	10:15	900.71	345.6	27	881.69	1821	51	924.7	32	1093	37
20/5/2013	11:15	900.71	341	27	881.69	1814	51	912.5	32	1091	37
21/5/2013	10:30	900.67	343.6	27	881.69	1804	51	931	32	1090	37
22/5/2013	10:45	900.64	337.2	27	881.69	1810	51	913.1	32	1081	37
23/5/2013	10:00	900.59	339.2	27	881.69	1808	51	936.4	32	1092	37
24/5/2013	9:30	900.56	336.2	27	881.69	1799	51	922.5	32	1077	37
25/5/2013	10:15	900.53	346.2	27	881.69	1786	51	913.6	32	1072	37
26/5/2013	10:45	900.17	336.7	27	881.7	1795	51	911.7	32	1072	37
27/5/2013	10:30	900.44	331	27	881.7	1819	51	900.5	32	1079	37
28/5/2013	11:15	900.4	339.4	27	881.7	1802	51	899	32	1073	37
29/5/2013	10:00	900.38	332.3	29	881.7	1862	51	907	32	1072	37
30/5/2013	10:30	900.4	331	29	881.7	1824	51	903.4	32	1084	37
31/5/2013	10:45	900.36	337.5	29	881.7	1831	51	896	32	1081	37
1/6/2013	10:50	900.32	326	29	881.7	1819	51	902	32	1075	37
2/6/2013	10:00	900.29	331.8	29	881.7	1815	51	882.9	32	1073	37

DECLARATION

I the undersigned declare that this thesis is my original work and has not been presented for a degree in any other university. All sources of material used for the thesis have been duly acknowledged.

Name: Ephrem Tadesse Tagegne

Signature: ____________________

The thesis has been submitted for examination with our approval as university:

Advisor

Name: Seifu Kebede (Ph.D)

Signature: ____________________

Co-advisor

Name: Engida Zemedagegnehu (M.Sc)

Signature: ____________________

Place: Addis Ababa University, College of Natural Sciences, School of Planetary and Earth Sciences.

Date of Submission: June, 2013